Anaerobic Benzene Degradation in Albertan Sediments

by

Korris Lee

A thesis submitted in partial requirement for the degree of

Doctor of Philosophy

in

Environmental Science

Department of Civil and Environmental Engineering

University of Alberta

ABSTRACT

Benzene is a priority contaminant that is commonly coincident with fossil fuel entities, whether natural or anthropogenic, and is characterized by high mobility and toxicity. In Alberta, Canada, where oil and gas production comprises much of the provincial industrial output, benzene contamination presents an omnipresent environmental risk to health and safety, necessitating economical methods that can minimize such threats. In this study, bioremediation is investigated as a benzene removal option for contaminated sites. Bioremediation can involve the use of microorganisms to metabolize benzene, and typically requires either the potentiation of available microbes (i.e. biostimulation) or the introduction of external microbes (i.e. bioaugmentation) *in situ*. Remediators can benefit greatly in using indigenous cultures that have been developed to maximize degradative capabilities and minimize time burden. This project, therefore, is focused on the generation of anaerobic benzene degrading cultures (under methanogenic, sulfate-reducing, iron-reducing, and nitrate-reducing conditions) derived from indigenous Albertan sediments and analysis of their community properties and primary degrader populations, while investigating different strategies to enhance their metabolic performance. These include the implementation of iron-dissolution protocols with external chelators such as acetohydroxamic acid and oxalic acid to expand ferric iron pools, and the addition of conductive magnetite at nano and micrometer scales to enhance the conductivity of microbial morphologies that can ease the transfer of electrons for metabolism. Lastly, an attempt was made to produce the putative benzene carboxylase AbcDA *in vitro* and subvert the difficulties of culture creation and maintenance entirely.

The research in this thesis demonstrated robust degradation of benzene in cultures sourced from Albertan sediments in a multitude of redox conditions, including nitrate-reducing, iron-reducing, sulfate-reducing, and methanogenic contexts, with iron and nitrate-reducers exhibiting the highest levels of benzene degradation (11-12 uM/d). Primary benzene degraders were

identified in nitrate-reducing and iron-reducing cultures, namely *Peptococcaceae* and *Geobacter*, respectively. *Geobacter metallireducens* was also identified at a species taxonomic level in iron-reducing cultures. While the isolation of *Geobacter* from iron-reducing cultures was unsuccessful, and putative benzene hydroxylases *gmet 0231-0232* were not found within these consortia, the potential of certain chelator combinations such as acetohydroxamic acid (aHA) and oxalic acid in enhancing the benzene degrading performance of iron-reducing cultures was demonstrated, although their specific functions within these cultures could not be elucidated.

PREFACE

This thesis is an original work by Korris Lee. Special thanks to supervisors Ania Ulrich and Tariq Siddique, as well as committee members Elizabeth Edwards and Tong Yu. Thanks also to the Edwards Lab and Siddique Lab, namely Courtney Toth, Shen Guo, and Alsu Kuznetsova, as well as the lab manager and post-doctoral researcher of Ulrich Lab, Petr Kuznetsov and Nabeel Mian.

ACKNOWLEDGEMENTS

Thank you to my supervisors, Dr. Ulrich at first and then Dr. Siddique, as well as my mentors Dr. Edwards and Dr. Yu for their support, including the assistance of Edwards Lab, particularly from Courtney Toth and Shen Guo, as well as Siddique Lab, particularly from Alsu Kuznetsova.

Thank you to my labmates, in no particular order, Xiaoxuan Yu, Kelvin Chan, Amy-Lynne Balaberda, Luke Gjini, Heidi Cossey, Huixin Zhang, Sarah Miles, Evelyn Asiedu, Stanley Poon, Anya Batycky, Erika Strytveen, Nabeel Mian, Chelsea Benally, Kai Wei, and Petr Kuznetsov.

TABLE OF CONTENTS

LIST OF TABLES

LIST OF FIGURES

ABBREVIATIONS

aHA – acetohydroxamic acid

BTEX – benzene, toluene, ethylene, xylene

DGG-B – Dunja Grbic-Galic Benzene

GC – gas chromatography

ICP-MS – inductively coupled plasma mass spectrometry

Koc – soil adsorption coefficient

Kow – octanol:water coefficient

LMWOA – low molecular weight organic acid

NTA – nitrilotriacetic acid

OXA – oxalic acid

PCR – polymerase chain reaction

qPCR – quantitative polymerase chain reaction

SI – Shannon index

TEA – terminal electron acceptor

WGS – whole genome sequencing

Bi-letter Culture Nomenclature:

1. M/S/I/N – methanogenic, sulfate-reducing, iron-reducing, nitrate-reducing
2. C/S/M – clay, sand, mixed.

LIST OF EQUATIONS

1 Introduction

Benzene is a non-threshold mutagen, capable of causing cancer at any concentration of exposure (Government of Canada : Environment Canada : Health Canada 1993). It is notable for its high water solubility (825 mg L^{-1} at 25℃), volatility (10.1 kPa at 25℃), and low octanol:water coefficients ($LogK_{OW}$ = 1.56) (Government of Canada, Environment Canada, & Health Canada, 1993) as well as a soil adsorption coefficient of $LogK_{oc}$ = 1.8 (CDC, 2008). It typically enters the body through inhalation or ingestion routes, and distributed throughout the circulatory system with partial accumulation in adipose tissue and bone marrow, where its metabolism produces benzoquinone and muconaldehyde byproducts. These themselves stimulate the production of reactive oxygen intermediates that aggravate oxidative stress and cause genetic instability, ultimately resulting in disorders such as acute myeloid leukemia (Austin, Delzelli, & Cole, 1989). Benzene is naturally occurring in fossil fuel deposits, is a common chemical solvent used in industrial processes, and is key to the production of multiple organic chemicals and the exploitation, refinement, and transport of petroleum assets (Figure 1-1-1).

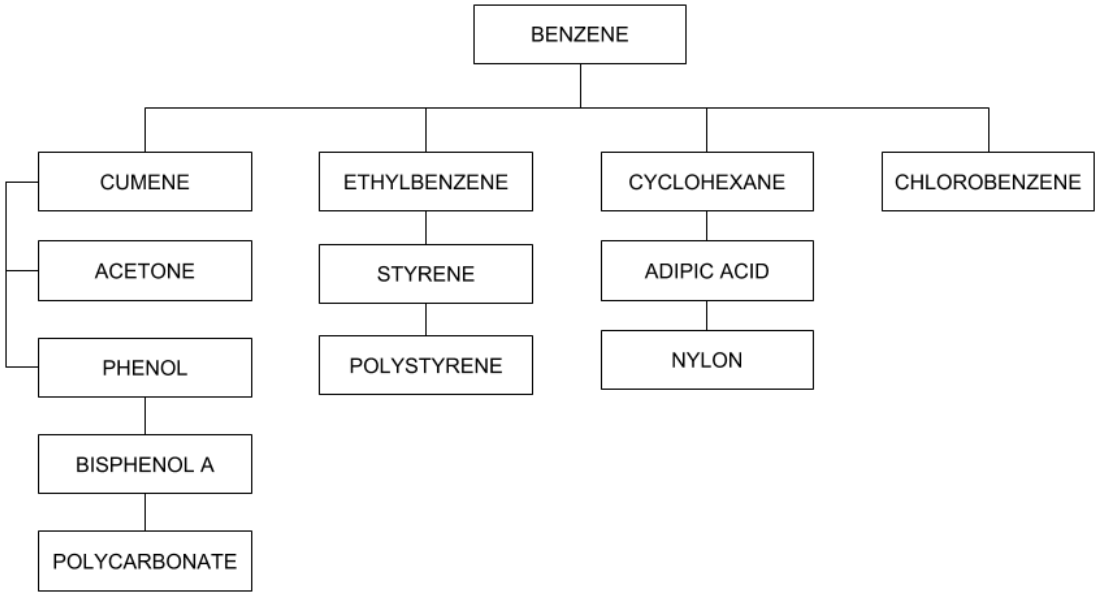

Figure 1-1. Benzene as an Industrial Precursor for Solvents and Plastics

Benzene is a chemical precursor for myriad plastic, solvent, and polymer production protocols (United States International Trade Commission & United States Tariff Commission, 1984) and is a ubiquitous entity in industrial processes.

In particular, the province of Alberta, Canada, is economically dependent on the oil and gas industry (Economic Dashboard - Oil Production, 2019), and of the 1265 major BTEX (benzene, toluene, ethylbenzene, xylene) contaminated sites present in Canadian federal inventories (Government of Canada, 1994), 430 of them are resident in Alberta (Economic Dashboard - Oil Production, 2019), apportioned primarily among leaking pipelines and underground storage tanks of compromised integrity (Government of Canada P. S., 2019). Meanwhile, the Albertan catalogue of over 10000 provincial orphan oil wells (that is, those lacking a liable owner) lists 3321 sites in need of decommissioning (Dachis, Shaffer, & Thivierge; Orphan Inventory, 2021), all of which are an imminent benzene contamination risk. Altogether, these amount to more than 30 billion CAD worth of governmental financial responsibility (Singh, 2020), and necessitates the

development of effective remediation strategies capable of neutralizing benzene with minimal economic investment.

Bioremediation is ideally suitable for benzene removal in Alberta, due to its cost effectiveness and low environmental invasiveness relative to more overt physicochemical methods (Azubuike, Chikere, & Okpokwasili, 2016). Bioremediation can involve the addition of degradative microbes *in situ* (bioaugmentation), as well as the potentiation of existing microbes by providing amendments that promote metabolism (biostimulation). The optimization of these techniques requires the *de novo* generation of benzene-degrading mixed cultures, and an intimate understanding of native sediments and the microbial populations therein (Adams, Fufeyin, Okoro, & Ehinomen, 2020). The available anaerobic benzene-degradation literature is scarcely invested in the benzene-degrading capabilities of microbial populations indigenous to Alberta, where benzene contamination risks are most relevant. This study will therefore focus on anaerobic benzene degradation as it pertains to Alberta and its native microbial communities, with a view towards future remediation strategies for this notoriously persistent contaminant.

Benzene is a fully conjugated annulene comprising six carbons and six hydrogens, arranged in a planar hexagonal ring. This specific geometry is the principal chemical basis for its recalcitrance, as it allows the ring to exhibit the emergent phenomenon of resonance, where the π electrons perpendicular to the hexagon disperse freely about the ring structure, lowering the basal energy level of the entire compound as well as the energetic ceiling at which degradative reactions are possible. Furthermore, contamination sites often polarize to anaerobic conditions (Weelink, van Eekert, & Stams, 2010), and necessitate respiration with alternative terminal electron acceptors such as nitrate, iron, sulfate, and carbon dioxide, which results in a reduction of reaction kinetics, as these terminal electron acceptors have redox values lower than oxygen (Abbasian, Lockington, Mallavarapu, & Naidu, 2015), and therefore yield comparatively less

energy for cellular metabolism. The stability of benzene, combined with the tendency for contamination sites to exhaust any sources of available oxygen, lays a heavy tax on the time requirements of benzene bioremediation and the manhour commitments of *ex situ* culturing attempts (Vogt, Kleinsteuber, & Richnow, 2011).

This study focuses exclusively on anaerobic culturing conditions to maximize relevance to remediators. To lay a foundation for further scholarship, it was imperative to establish that microorganisms resident in Alberta sediments had innate benzene biodegradative capabilities under methanogenic, sulfate-reducing, iron-reducing, and nitrate-reducing conditions. Generating these cultures not only supports the possibility that Alberta microbes could accomplish natural attenuation or biostimulated removal in extant contamination sites, but also provides a research foothold for *ex situ* laboratory enrichment, verification, and in the far future, field application through bioaugmentation with laboratory-cultivated material. Further aims of this study include the biostimulation of these cultures, particularly iron-reducing cultures singular to Albertan degraders, first through the promotion of iron dissolution, and second through magnetite amendments expected to promote biofilm formation and electroconductivity. Lastly, an attempt was made to divorce researchers from the need to perform anaerobic cultivation completely by creating recombinant enzymes capable of degrading benzene *in vitro*.

The four main research questions presented in this thesis are as follows:

1. Can microbes native to Albertan sediments support anaerobic benzene degradation under methanogenic, sulfate-reducing, iron-reducing, and nitrate-reducing conditions?
2. What are the taxonomical details and genetic characteristics of Albertan iron-reducing benzene-degrading cultures?
3. Can Albertan iron-reducing benzene-degrading cultures be biostimulated with external chelators and magnetite subtypes?

4. What are the functional characteristics of the putative benzene carboxylase AbcDA?

1.1 Can Microbes Native to Albertan Sediments Support Anaerobic Benzene Degradation?

The need to establish indigenous Alberta-based cultures capable of degrading benzene is the central theme and fundamental basis for all experiments in this study, as this addresses an immediate concern for remediators who require inexpensive removal tools applicable to the challenges that face Alberta's multi-billion dollar energy industry, whose harvesting, manufacture, transport, and storage assets permeate the landscape of the province, and are imminently poised to be major benzene contamination risk factors (Economic Dashboard - Oil Production, 2019; Government of Canada, Environment Canada, & Health Canada, 1993). Any cultures generated from this work would be relevant to remediation efforts, as their pristine Albertan origins imply innate benzene degrading capacity in certain Albertan microbial populations. Furthermore, their indigenous nature precludes concerns about the introduction of foreign organisms into the ecosystem if a bioaugmentation approach is to be developed and adopted for future use.

The study at hand therefore proposes to generate benzene-degrading cultures from Albertan sediments, cultivated under various anaerobic redox conditions, specifically methanogenic, sulfate-reducing, iron-reducing, and nitrate-reducing respiratory groups (Figure 1-2).

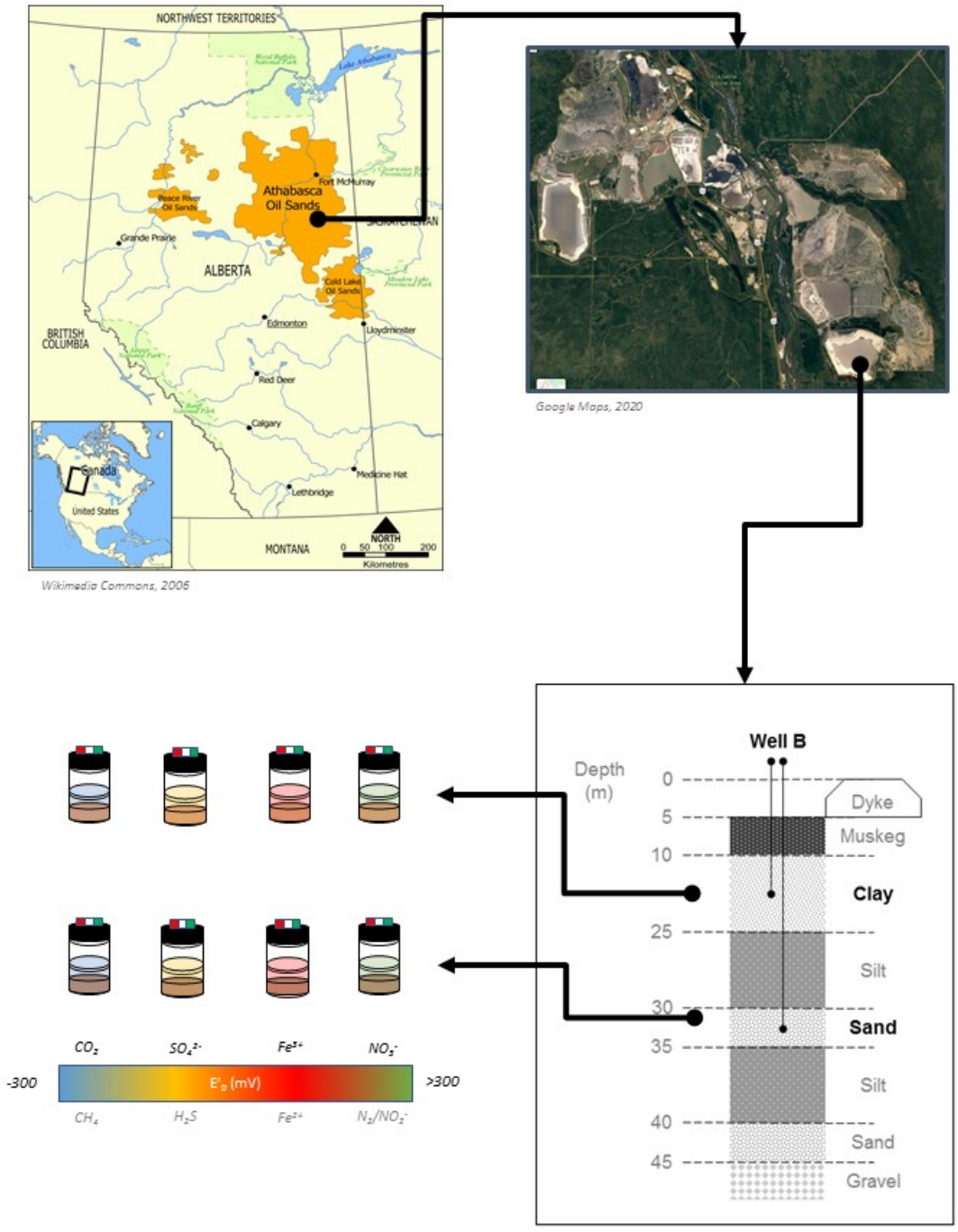

Figure 1-2. Graphical Representation of Culture Origin and Creation

The massive scale of Alberta fossil fuel deposits and accompanying oil and gas industry, and their importance in the Albertan economy vis a vis their contamination risk, are visible through

geographical mapping and satellite imagery of the refinery and associated tailings storage site from which the sediments used in this study were originally sourced, prior to operations. These clay and sand inocula came from Well B of the South Tailings Pond in Northern Alberta, where the Athabasca McMurray formation is situated (Holden, Donahue, & Ulrich, 2011), as pristine samples that had never been previously exposed to anthropogenic petroleum products. The sediments were then cultured anaerobically with benzene as a sole carbon source under methanogenic, sulfate-reducing, iron-reducing, and nitrate-reducing conditions with appropriate terminal electron acceptor amendments.

Table 1-1. Redox reactions pursued in Sediment Cultivation

	Terminal Electron Acceptor	Reaction
Methanogenic	$CO_2 \rightarrow CH_4$	$C_6H_6 + 10.5H_2O + 3.75CO_2 \rightarrow 6HCO_3^- + 3.75CH_4 + 6H^+$
Sulfate-Reducing	$SO_4^{2-} \rightarrow H_2S$	$C_6H_6 + 3H_2O + 3.75SO_4^{2-} \rightarrow 6HCO_3^- + 1.875H_2S + 1.875HS^- + 0.375H^+$
Iron-reducing	$Fe^{3+} \rightarrow Fe^{2+}$	$C_6H_6 + 18H_2O + 30Fe^{3+} \rightarrow 6HCO_3^- + 30Fe^{2+} + 36H^+$
Nitrate-reducing (incomplete)	$NO_3^- \rightarrow NO_2^-$	$C_6H_6 + 15NO_3^- \rightarrow 6HCO_3^- + 15NO_2^- + 6H^+$
Nitrate-reducing (complete)	$NO_3^- \rightarrow N_2$	$C_6H_6 + 6NO_3^- \rightarrow 6HCO_3^- + 3N_2$

A variety of anaerobic redox conditions representing increasing order of redox potentials and energy yields (Vogt, Kleinsteuber, & Richnow, 2011).

Although not a comprehensive suite of all possible anaerobic conditions, the experimental array to be tested spanned a wide range of redox potentials (Table 1-1), provided a useful starting point for further laboratory investigation, and could be readily compared with previous scholarship regarding microbial profiles and primary benzene degraders (Noguchi, Kurisu, Kasuga, & Furumai, 2014; Alfreider & Vogt, 2007; Sakai, Kurisu, Yagi, Nakajima, & Yamamoto, 2009; Luo, Devine, & Edwards, 2016; Musat, Wilkes, Behrends, Woebken, & Widdel, 2010; Oka, et al., 2008; Zhang, Bain, Nevin, Barlett, & Lovley, 2012; Abu Laban, Selesi, Jobelius, & Meckenstock, 2009; Bedard, Ritalahti, & Loffler, 2007; Zaan, et al., 2012).

The stability and recalcitrance of benzene, the propensity of contamination sites to become anaerobic (Anderson & Lovley, 1997; Lovley D. R., 1997), and the low energy kinetics available in anaerobic respiration (Vogt, Kleinsteuber, & Richnow, 2011), complicate the generation of benzene-degrading anaerobic cultures, where even successful attempts only yielded substantial

volumes of active culture only after hundreds if not thousands of days of careful, fastidious, and deliberate cultivation, where benzene and terminal electron acceptor availability, strict anaerobicity, and low toxic byproduct concentrations were steadfastly monitored and/or maintained. Among these are the cultures from the Meckenstock group in Europe (Abu Laban, Selesi, Jobelius, & Meckenstock, 2009; Abu Laban, Selesi, Rattei, Tischler, & Meckenstock, 2010; Rabus, et al., 2016; Meckenstock, et al., 2016; Winderl, Anneser, Griebler, Meckenstock, & Lueders, 2008; Kunapuli, Lueders, & Meckenstock, 2007; Meckenstock, et al., 2015; Meckenstock & Mouttaki, 2011; Dong, et al., 2017), notable for iron and sulfate reduction in particular, and the iron-reducing cultures from Lovley lab, developed over decades, yielding one of the few reported pure culture isolates in anaerobic benzene degradation scholarship, *Geobacter metallireducens* (Zhang, Bain, Nevin, Barlett, & Lovley, 2012; Lovley, et al., 1989). Nitrate-reducing cultures include those of the Gerritse group, which at the time of publication had been cultivated in a chemostat for 8 years (Zaan, et al., 2012), the *Dechloromonas* RCB and JJ isolates of the Achenbach group (Coates, et al., 2001), the *Azoarcus* isolates of the Watanabe group, derived from contamination sites in the Japanese archipelago (Kasai, Takahata, Manefield, & Watanabe, 2006), and the Cartwright cultures of Edwards group (Burland & Edwards, 1999), continuously maintained under careful upkeep since the 1990's (Luo, et al., 2014). Edwards group is also the keeper of the DGG-B methanogenic cultures (Toth, et al., 2021), named in honour of Dunja Grbic-Galic and cultivated for over twenty years (Nales, Butler, & Edwards, 1998; Ulrich & Edwards, 2003).

Therefore, due to the empirical precedent of generating benzene-degrading cultures, it is expected that Albertan sediments would also be capable of sustaining benzene degradation, though even in ideal laboratory environments, this cultivation has always been fraught with difficulty, requiring copious amounts of time and effort to establish, describe, and sustain. Any microcosms created from these sediments would also be expected, on account of the

previously-observed worldwide distribution of primary degraders, to host the same taxa seen in those consortia, in accordance to their respective redox conditions, namely: *Deltaproteobacterium ORM2a* in methanogenic cultures (Luo, Devine, & Edwards, 2016), *Clostridiales* and *Cryptanaerobacter/Pelotomaculum* in sulfate-reducing cultures (Kleinsteuber, et al., 2008; Taubert, et al., 2012), *Geobacter metallireducens* in iron-reducing cultures (Zhang, Bain, Nevin, Barlett, & Lovley, 2012; Abu Laban, Selesi, Rattei, Tischler, & Meckenstock, 2010), and *Peptococcaceae*, *Dechloromonas*, or *Azoarcus* in nitrate-reducing cultures (Zaan, et al., 2012; Coates, et al., 2001; Kasai, Takahata, Manefield, & Watanabe, 2006).

The findings from this experiment will serve as a foundation for a more comprehensive survey of Alberta sediments, establish the possibility of said sediments to degrade benzene intrinsically, and provide a body of knowledge for downstream laboratory studies. Results were published in Water Environmental Research (2020) http://dx.doi.org/10.1002/wer.1454.

1.2 What are the Taxonomical Details and Genetic Characteristics of Iron-reducing Cultures?

Among the established anaerobic benzene-degrading cultures derived from Albertan sediments, it was the iron-reducing cultures that were the most novel, with only one other laboratory, the Lovley group, describing such cultures in detail (Lovley D. R., et al., 1993). It was therefore pertinent to investigate these cultures more thoroughly to build on the scant scholarship available on the subject and establish reproducibility of empirical results.

The available literature describes the Lovley group iron-reducing cultures as pure isolates of *Geobacter metallireducens* (Lovley D. R., et al., 1993; Lovley, et al., 1989), derived from enriched mixed cultures with benzene as a sole carbon source and iron from ferric citrate as a terminal electron acceptor. To the author's knowledge, no other mesophilic iron-reducing benzene-degrading cultures exist in the scholarship, although a thermophilic archaeon, *Ferroglobus placidus*, has been reported to degrade benzene (Holmes, Risso, Smith, & Lovley, 2012). Isolated *Geobacter metallireducens* has also been observed to differentially express the gene transcripts *gmet 0231* and *gmet 0232*, which are thought to be benzene hydroxylases, on account of the association of *Geobacter metallireducens* with benzene-phenol degradation pathways (Zhang T. , et al., 2013; Zhang T. , et al., 2014). Therefore, any iron-reducing microcosms generated from the Alberta sediments would be expected to not only host *Geobacter metallireducens*, but also the putative hydroxylases *gmet 0231* and *gmet 0232*.

The primacy of *Geobacter metallireducens* in iron-reducing benzene-degrading cultures may also be demonstrated outright by the isolation of the bacterium into pure culture. This was accomplished by the Lovley group in the 1980s and 1990s from their mixed culture enrichments (Lovley D. R., et al., 1993; Lovley, et al., 1989), and the procedures described in these experiments, namely the serial cultivation of the culture from nitrate to ferric iron terminal electron acceptors within sealed Hungate slant tubes, would be hypothesized to yield similar results in the Alberta cultures. A successful isolation would not only legitimize the role of *Geobacter metallireducens* in iron-reducing benzene degradation, but would also have decisive consequences for future experiments, as it would simplify cultivation and limit experimental variables in empirical analysis. Unfortunately, benzene-degrading isolates such as *Azoarcus* (Kasai, Takahata, Manefield, & Watanabe, 2006) and *Geobacter* (Lovley D. R., et al., 1993; Lovley, et al., 1989) are comparatively rare, and the relative lack of replication from other

research groups suggests a fastidiousness in *Geobacter* that would complicate isolation attempts.

1.3 Can Albertan iron-reducing benzene-degrading cultures be biostimulated with external chelators and magnetite subtypes?

1.3.1 Chelator Amendments and Iron Availability

The third of the study foci came from an unexpected finding in the culture establishment experiments, that is, the incongruence between empirical and theoretical stoichiometries in the iron-reducing cultures (Lee & Ulrich, 2021). Because ferric iron was provided as insoluble ferrihydrite in non-limiting amounts, it was reasoned that this stoichiometric disconnect was a result of a lack of bioavailable soluble iron, and that the remainder of benzene degradation was being accomplished by methanogenic processes. This was a non-ideal situation in a remediation context, as the redox potential of ferric iron is much higher than that of carbon dioxide (Vogt, Kleinsteuber, & Richnow, 2011), and energy yields and metabolic activity would be much greater if benzene was shunted to iron reduction pathways rather than methanogenesis (Silva, Ruiz-Aguilar, & Alvarez, 2005; Lueders, 2017). This could potentially be done by amending the cultures with external iron chelators that would extract ferric iron from ferrihydrite deposits via dissolution.

The importance of iron and iron chelators is evident in the scarcity and essentiality of iron for microbial life (Sandy & Butler, 2009). Prokaryotic metabolisms require iron for coenzymatic function and also for iron-reducing respiration (Hider & Kong, 2010), but ferric iron Fe(III) is limited in the biosphere due to its low solubility at neutral pH (Johnstone & Nolan, 2015). To overcome this disparity between supply and demand, bacteria synthesize small molecules called siderophores, which can be highly specific to ferric iron and capable of drawing it from the environment, even in competition with powerful sequestration molecules such as transferrin (Crichton & Charloteaux-Wauters, 1987; Holden & Bachman, 2015). This broadcast of siderophores is then recaptured by the producing bacteria and reintroduced into the bacterial cytoplasm for its metabolic needs (Neilands, 1995) (Figure 1-3).

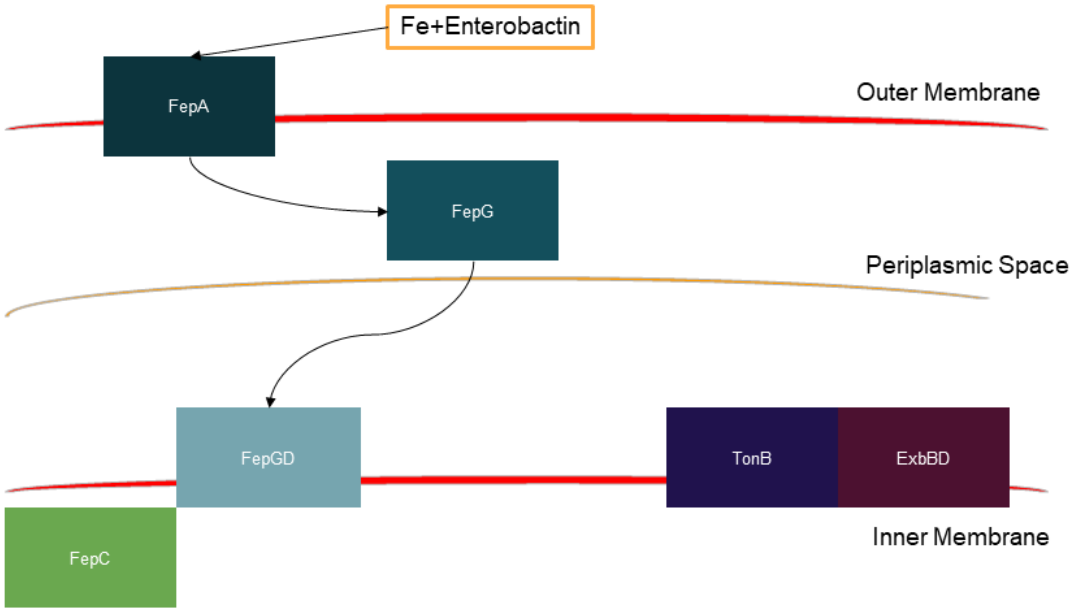

Figure 1-3. Interception of Fe(III)-Enterobactin by Escherichia coli.

Perhaps the best-characterized siderophore is enterobactin (Crichton & Charloteaux-Wauters, 1987; Neilands, 1995), of the catecholate subclass. The enterobactin gene is located on the entCDEBAH operon which is regulated by Fur, a ferrous iron-binding repressor, and synthesis begins with a trilactone precursor, to which catechol structures are added (Peralta, et al., 2016; Hider & Kong, 2010). Following coordination of catechols with Fe(III), the bound enterobactin is intercepted by FepA on the outer membrane, transported into the periplasm, and shuttled to the inner membrane FepGD via periplasmic binding protein FepG. Proton motive force generated by TonB and ExbBD then provides energy along with FepC ATPase to transport enterobactin into the cytoplasm, where the iron is released through enzymatic cleavage of the siderophore by ferrienterobacin esterase (Hider & Kong, 2010).

The evolution of such complex iron capture mechanics is indicative of the importance of iron regulation in microbial metabolism, to the point where siderophore synthesis can be essential to bacterial life (Khan, Singh, & Srivastava, 2018). However, siderophores can also perform other

duties besides chelating iron; for example, their long range and concentration-dependent effects make them well-suited for quorum sensing (Guan, Kanoh, & Kamino, 2001; Guan, Onuki, & Kamino, 2000), implicating siderophores in emergent roles such as intercellular signaling. Another role of siderophores is their protective quality against reactive oxygen species, which can irreversibly deactivate essential enzymes in strictly anaerobic cultures (Martins, et al., 2019). This protection can occur both through the oxygen-scavenging abilities of the molecules themselves as well as the reducing abilities of the iron that the molecules provide (Cornelis, Wei, Andrews, & Vinckx, 2011; Peralta, et al., 2016), suggesting that siderophores can be an essential component of the oxidative stress response in anaerobic cultures.

To facilitate the provisioning of iron to benzene-degrading iron-reducing cultures, different amendments were considered that could promote the dissolution of ferrihydrite, including low molecular weight organic acids and siderophore analogues. These chelators were also used in conjunction to exploit a potential synergistic phenomenon between the two (Lin, et al., 2018), a characteristic previously reported in abiotic settings which has not yet been explored in regards to contaminant-degrading microbial cultures. Previous experiments that explored the effect of chelators on benzene degradation in iron-reducing cultures were successful in enhancing their activity, most notably with substances such as nitrilotriacetic acid (NTA) (Lovley & Woodward, 1996), and the synergy of low molecular weight organic acids and siderophores, known to be effective at the dissolution of ferric materials (Lin, et al., 2018), would be expected to have a similar effect, but without the known toxicity of NTA. Three types of chelators were tested, including nitrilotriacetic acid (a triskelion polydentate chelator), acetohydroxamic acid (an analogue for hydroxamate siderophores such as desferrioxamine B), and oxalic acid (a representative low molecular weight organic acid) (Figure 1-4). The findings in this experiment could potentially improve the efficiency of benzene degradation in iron-reducing cultures by improving exploitation of existing ferric iron assets and polarizing metabolism towards iron

reduction, a process that is advantageous due to its relatively high energy yields and low byproduct toxicity.

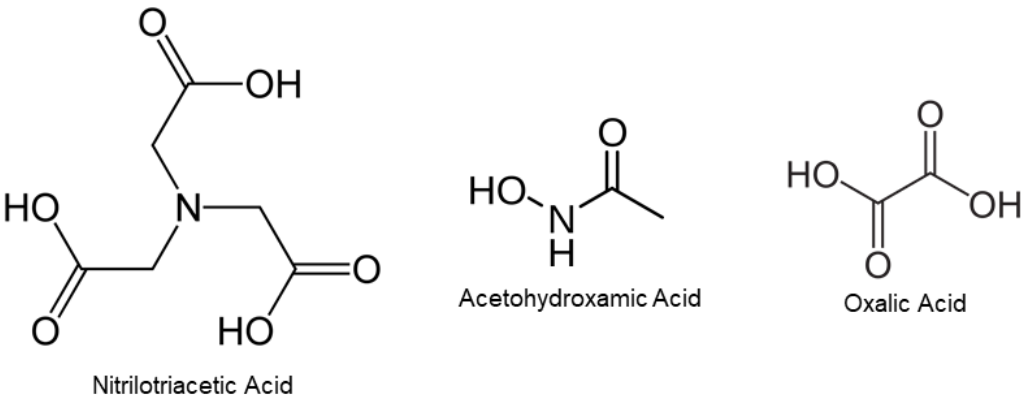

Figure 1-4. Representative Chelator Subgroups.

1.3.2 Magnetite Amendments, Biofilm Formation, and Electroconductance

Magnetite amendments were another avenue that would be explored for the purpose of enhancing iron-reducing benzene degradation, related to the importance of promoting attached growth as well as the potential for improving electroconductivity in *Geobacter* nanowires (Lovley & Walker). As *Geobacter metallireducens* is thought to be the primary degrader in iron-reducing benzene cultures (Lovley D. R., et al., 1993), it was expected that magnetite would be capable of enhancing metabolic activity in these microcosms. Overall, sessile growth in biofilms has the potential to confer survivability and metabolic advantage in consortium microorganisms. Those biofilm-specific aspects that have been characterized in pathogens (Vestby, Gronseth, Simm, &

Nesse, 2020; Costerton, et al., 1987) may have corollaries in benzene bioremediation contexts, including but not limited to: the biofilm-induced activation of benzene-activating enzymes, spatial and functional organization of primary degraders and syntrophic microbes into metabolic and respiratory niches, or biofilm-specific generation of attachment structures that enhance growth on substrata.

The introduction of growth substrates, particularly those that can double as respiratory sources and/or conductors for electron transfer i.e. certain iron oxides such as magnetite, therefore appears promising as an initiative to promote the growth and metabolism of characteristically lethargic anaerobic microorganisms. Ferric iron oxides such as magnetite have hexa O^{-}/OH^{-} constituents in an octahedral structure (Cornell & Schwerfmann, 2003), as hexagonal (eg. goethite) or cubic packed (eg. lepidocrocite) forms, and the arrangement of which determines their classifications. Magnetite ($Fe(II)Fe(III)_2O_4$), for example, shares structural similarities with maghemite. It is cubic in structure, with interstices coordinated in an octahedral and tetrahedral manner with oxygen (Cornell & Schwerfmann, 2003). The mineral itself is black, ferrimagnetic and can be integrated into certain microorganisms for magnetotaxis (Fassbinder, Staniek, & Vali, 1990), and magnetite, one of many iron oxides, is likely to be a formative mineral in primordial life on earth (Vargas, Kashefi, Blunt-Harris, & Lovley, 1998). Comprising both ferrous and ferric iron, this mineral has interesting electrochemical properties (White, Peterson, & Hochella, 1994) that can facilitate a diversity of redox reactions (Gorski, Nurmi, Tratnyek, Hofstetter, & Scherer, 2010). Some systems even act as batteries do (Byrne, et al., 2015), with photosynthetic *Rhodopseudomonas palustris* TIE-1 oxidizing ferrous iron, and *Geobacter* reducing ferric iron in a redox cycle, suggesting a complex syntrophic profile in contamination remediation contexts with highly diverse mixed cultures (Zhou, Xu, Yang, & Zhuang, 2014; Zhuang, Tang, Wang, Hu, & Zhou, 2015; Li, et al., 2015; Zhang & Lu, 2016; Cruz Viggi, et al.,

2014; Yang, et al., 2016; Yamada, Kato, Ueno, Ishii, & Igarashi, 2015; Baek, Jung, Kim, & Lee, 2017).

Magnetite is also associated with DIET (direct interspecies electron transfer) processes, which has been documented with *Geobacter* organisms (Ueki, et al., 2018; Lovley & Walker), particularly in coculture with other *Geobacter* (Summers, et al., 2010) or methanogens such as *Methanosaeta* (Rotaru A.-E. , et al., 2014) and *Methanosarcineae* (Holmes, et al., 2018; Rotaru A. , et al., 2014). *Geobacter* is proposed to have an electron transfer pathway consisting of quinol on the cytoplasmic face of the inner membrane (Levar, Chan, Mehta-Kolte, & Bond, 2014; Zacharoff, Chan, & Bond, 2016), which transfers electrons to periplasmic and trans-outer membrane porin-cytochrome systems (Lloyd, et al., 2003; Liu Y. , et al., 2014), that eventually relays the electrons to the extracellular face of the outer membrane in order to reduce ferric iron (Shi, et al., 2016). Since *Geobacter* does not synthesize soluble electron shuttles, and requires direct physical contact with electron transfer materials (Nevin & Lovley, 2000), DIET between *Geobacter* and partner organisms appears to be mediated by nanowires, which are conductive proteinaceous filaments rooted in the plasma membrane (Reguera, et al., 2005). The conductance of e-pili is inversely correlated with temperature and pH (Malvankar, et al., 2015), in a manner similar to aforementioned conductive polymers. Researcher conclusions differ on their properties, but they are either formed from OmcS polymers (Wang, Schenkeveld, Kraemer, & Giammar, 2015) or assembled from PilA subunits (Liu X. , et al., 2019).

Historically, the search for the mediator of DIET in *Geobacter* organisms first centered upon the cytochrome OmcS (outer membrane cytochrome S), which is a multihaem c-type cytochrome (Lovley D. R., et al., 1993; Summers, et al., 2010). OmcS is differentially expressed in *Geobacter* grown with insoluble ferric iron versus soluble ferric iron (Mehta, Coppi, Childers, & Lovley, 2005), and was therefore thought to be involved in iron dissolution and electron transfer.

High resolution cryo-electron microscopy, in conjunction with mass spectrometry, appears to support the position that nanowires are composed of polymeric type-c cytochromes (Wang, et al., 2019) arranged in hexahaemic patterns that are packed proximal enough to mediate conductance. The PilA protein in these model systems is nonfilamentous and appears to have an extracellular export role for OmcS, to which expression is positively correlated (Liu, Zhuo, Rensing, & Zhou, 2018; Leang, Malvankar, Franks, Nevin, & Lovley, 2013), although this relation is contentious within the scholarship (Shrestha, et al., 2013).

However, the presence of OmcS is not necessary for conductance in e-pili, as demonstrated in heterologous PilA expression studies (Liu X. , et al., 2019) as well as the existence of cytochrome-absent e-pili in *Syntrophus aciditrophicus* (Walker, et al., 2020). *Geobacter* and *Syntrophus* studies that advocate for a central role of PilA observed the necessity of ~10% abundance of aromatic amino acids in the e-pili monomer protein for capacitating conductance in DIET type-IV pili nanowires (Walker, et al., 2020); these residues are conserved among *Geobacter* species (Feliciano, da Silva, Reguera, & Artacho, 2012), and non-conductive pili in other microbes do not host these aromatic amino acids in their variable regions (Reardon & Mueller, 2013), although some models support a multistep hopping electron transfer system over one based on metal-like systems (Feliciano, Steidl, & Reguera, 2015). For advocates of the centrality of PilA to nanowire composition, OmcS appears to serve as a mediator of iron oxide reduction and dissolution (Qian, et al., 2011), and only in conjunction with the presence of e-pili; intriguingly, this ability can be substituted by the addition of magnetite (Liu F. , et al., 2015), in that magnetite both repressed OmcS production in wild-type *Geobacter* and reconstituted conductance in *omcS*- mutants.

Magnetite, being highly conductive, is therefore thought to substitute for OmcS in *Geobacter* nanowires, and the DIET mediation-capabilities of magnetite have been observed to facilitate

methanogenesis by *Methanosarcina* (Kato, Hashimoto, & Watanabe, 2012) and *Methanosaeta* (Cruz Viggi, et al., 2014). Magnetite also promotes DIET between *Geobacter sulfurreducens* and *Thiobacillus denitrificans* (Kato, Hashimoto, & Watanabe, 2012). In comparison, GAC (granulated activated carbon) (Liu F. , et al., 2012), biochar (Chen, et al., 2014), and carbon cloth (Chen, et al., 2014) are also semi-conductive and can promote syntrophic electron transfer thereby. Importantly, these materials are in the mm scale, while magnetite studies used nanoscale minerals (Liu F. , et al., 2015), so the mechanisms of action may differ between them.

Regardless of the school of thought on the matter (that is, the prominence of PilA or OmcS in nanowire composition), it appears that DIET between *Geobacter* and methanogens requires, firstly, conductive e-pili, and secondly, OmcS. *Geobacter* is a motile bacterium that uses conductive nanowires to facilitate physical contact with ferric iron in order to pass electrons to the iron surface (Levar, Chan, Mehta-Kolte, & Bond, 2014; Zacharoff, Chan, & Bond, 2016; Lloyd, et al., 2003; Rotaru A.-E. , et al., 2014; Liu Y. , et al., 2014; Shi, et al., 2016), suggesting that colonization of these surfaces could be a limiting factor in ferric iron exploitation and metabolic activity in iron-reducing benzene-degrading cultures. These nanowires are made conductive by OmcS (outer membrane cytochrome S), but because *omcS*- mutants could restore nanowire conductivity with the addition of nanoscale magnetite (Liu F. , et al., 2015), magnetite has the potential to replace OmcS functionality, and aid in the colonization of *Geobacter* on ferrihydrite surfaces, which can eliminate the energetic burden of *Geobacter* needing to generate OmcS *de novo*. Therefore, the evidence suggests that conductive iron oxide minerals such as magnetite could enhance the process of DIET between *Geobacter* and partner organisms. Findings from this experiment could provide a simple and effective method for minimizing lag times in iron-reducing cultures, and ease expansion of limited culture volumes for laboratory manipulations.

1.4 What are the functional characteristics of the putative benzene carboxylase AbcDA?

The final component of this study involves an attempt to liberate benzene degradation from anaerobic cultivation of mixed culture altogether, and was focused on AbcA, a putative benzene carboxylase discovered in the genome of primary benzene degrader *Peptococcaceae* (Abu Laban, Selesi, Rattei, Tischler, & Meckenstock, 2010; Luo, et al., 2014). The *abcA* (anaerobic benzene carboxylase A) gene shows promising experimental support for its purported function (Abu Laban, Selesi, Rattei, Tischler, & Meckenstock, 2010), and is thought to catalyze the carboxylation reaction that converts toxic benzene into non-toxic benzoate, making it a prime candidate for recombinant expression and cell-free enzymatic assays. If the proposed function of AbcA could be verified through heterologous expression in an easily manipulated laboratory bacterium such as *E. coli*, it could absolve experimenters from needing to maintain slow-growing anaerobic cultures completely, and transpose benzene degradation onto a system that could be scaled simply and efficiently for remediation purposes.

1.5 Statement of Purpose

Overall, the fundamental objective of these studies is to generate and investigate the properties of anaerobic benzene-degrading cultures relevant to Alberta and to Alberta-based remediators, who must address imminent and ubiquitous benzene contamination risks for a province in which

the fossil fuel energy sector is omnipresent. These data can contribute to the scholarship of anaerobic benzene bioremediation and provide researchers a basis for further cultivation of laboratory materials to study and mitigate benzene contamination events.

2 Indigenous Microbial Communities in Albertan Sediments are Capable of Anaerobic Benzene Biodegradation Under Methanogenic, Sulfate-reducing, Nitrate-reducing, and Iron-Reducing Redox Conditions

Korris Lee[1]*, Ania Ulrich[1].

1 *Department of Civil and Environmental Engineering, University of Alberta, Alberta, Canada.

This chapter is a version of a published paper (Lee & Ulrich, 2021).

2.1 Abstract

Alberta is a major center for oil and gas production, and correspondingly harbors hundreds of unresolved contamination sites by environmental hazards such as benzene (C_6H_6). Due to its cost-effectiveness, bioremediation has become a promising strategy for C_6H_6 removal. Contamination sites typically take on an anaerobic context, which complicates the energetics of contamination sites and is a subject that is scarcely broached in studies of Albertan sediments. In this study, the innate potential for indigenous microbial communities in Albertan sediments to mineralize C_6H_6 in a multitude of reduced conditions is examined. Community profiles of these sediments were analyzed by 16S rRNA amplicon sequencing, and degradation rates and reaction stoichiometries were observed by gas chromatography and ion chromatography. Organisms belonging to known primary degrader taxa were identified, including

Deltaproteobacteria (methanogenic), *Clostridiales* (sulfate-reducing), *Geobacter* (iron-reducing), and *Peptococcaceae* (nitrate-reducing). Furthermore, degradation patterns of the cultures were similar to those observed in previously reported microcosms, with lag times between 70-168 days and degradation rates between 3.27-12.70 μM d^{-1}. Such information could support a survey of Albertan sediment consortia which may be utilized in informing future remediation efforts in the province.

Keywords: Benzene, Bioremediation, Anaerobic, Alberta, Canada.

Practitioner Points:

- Clay and sand sediments originating from Northern Alberta could oxidize benzene under methanogenic, sulfate-reducing, iron-reducing, and nitrate-reducing conditions.
- Degradation profiles were broadly comparable to those of reported cultures from other geographical locales.
- Key degrader taxa observed included: *Deltaproteobacteria* (methanogenic)*, Clostridiales* (SO_4^{2-}-reducing)*, Geobacter* (Fe^{3+}-reducing), and *Peptococcaceae* (NO_3^--reducing).
- Knowledge gained can be implemented in informing remediation strategies in soil and water matrices for priority contamination cases of Alberta such as leaking underground storage tanks and orphan wells.

2.2 Introduction

The province of Alberta in the Canadian Prairies is notable for the ubiquitous presence of the oil and gas energy sector (Economic Dashboard - Oil Production, 2019), which is a major revenue stream for the provincial economy (Government of Alberta, 2019). Consequently, Alberta is replete with petroleum storage units (Government of Canada, Federal Contaminated Sites Inventory, 1994), pipelines, and orphan wells (Dachis, Shaffer, & Thivierge) that pose an imminent environmental risk. These risks are especially elevated with oil-and-gas-related hydrocarbons such as benzene (C_6H_6), a priority contaminant (Canada Environment & Canada Health and Welfare, 1993) associated with both natural fossil fuel deposits and anthropogenic processes, and characterized by its singular stability, mobility, and toxicity (McHale, Zhang, & Smith, 2012), with long-standing links to acute myeloid leukemia (Fishbein, 1985). Currently, there are a total of 1265 BTEX (benzene, toluene, ethylbenzene, xylene)-contaminated sites in soil and/or groundwater in the Federal Canadian Contaminated Sites Inventory, 34% of which are active in Alberta (Government of Canada, Federal Contaminated Sites Inventory, 1994). C_6H_6 contamination events are therefore an immediate public health concern that will require effective engineering solutions to remedy.

Bioremediation shows promise as an unintrusive, cost-effective alternative to conventional physicochemical removal approaches (Azubuike, Chikere, & Okpokwasili, 2016), and previous scholarship has reported enrichment cultures capable of degrading C_6H_6 (Keller, Kleinsteuber, & Vogt, 2018; Rabus, et al., 2016; Fuchs, Boll, & Heider, 2011; Philipp & Schink, 2012). Importantly, although aerobic pathways have been characterized, field site conditions regularly demonstrate a tendency towards highly-reduced conditions (Weelink, van Eekert, & Stams, 2010), and it is therefore the anaerobic removal of C_6H_6 that deserves particular attention. In

contrast to the regular presence of C_6H_6 in Alberta's energy sector, little is known about the indigenous microbiota of Alberta and its ability to remediate C_6H_6. Obtaining natively-derived anaerobic cultures that can attenuate C_6H_6 contaminants has the potential to benefit remediation studies in a province of which C_6H_6 contamination is of critical importance.

Hydrocarbon degradation typically proceeds according to redox potential values in decreasing order and according to the availability of terminal electron acceptors (Abbasian, Lockington, Mallavarapu, & Naidu, 2015), which can have dramatic effects on microbe population profiles and degradation pathways.

Anaerobic benzene degradation has previously been demonstrated in various redox contexts (Rabus, et al., 2016; Philipp & Schink, 2012; Fuchs, Boll, & Heider, 2011), with evidence for multiple pathways of benzene ring activation, including: methylation into toluene, hydroxylation into phenol, and carboxylation into benzoate (Meckenstock, et al., 2016). NO_3^--reducing cultures have been reported, with the primary oxidizer being identified as a *Peptococcaceae* (Zaan, et al., 2012), a *Dechloromonas* (Coates, et al., 2001), or an *Azoarcus* (Kasai, Takahata, Manefield, & Watanabe, 2006), although the latter has not been seen to host any canonical degradation genes (Devanadera, et al., 2019). A *Peptococcaceae*-containing culture known as the Cartwright culture has previously been seen to have a consistent degradation rate of 5.00-10.00 μM d^{-1} (Luo, et al., 2014). Fe^{3+}-reducing cultures have also been reported, with the primary degrader being identified as *Geobacter metallireducens* (Zhang, Bain, Nevin, Barlett, & Lovley, 2012; Abu Laban, Selesi, Rattei, Tischler, & Meckenstock, 2010), with degradation rates of such cultures measured at 6.00 μM d^{-1} (Kunapuli, Lueders, & Meckenstock, 2007). SO_4^{2-}-reducing cultures exist as well, which have separately demonstrated degradation rates of 36.00 μM d^{-1} (Kleinsteuber, et al., 2008) and lag times of about 200 days post-benzene dispersion (Taubert, et al., 2012); these cultures have primary degraders of the *Clostridiales* (Kleinsteuber, et al., 2008) and *Cryptanaerobacter/Pelotomaculum* (Taubert, et al., 2012) taxa, respectively.

Methanogenic cultures have shown primary degraders from the *Deltaproteobacteria* (Luo, Devine, & Edwards, 2016) and the *Desulfobacterales* and *Coriobacteriaceae* (Luo, Devine, & Edwards, 2016; Noguchi, Kurisu, Kasuga, & Furumai, 2014), with demonstrated degradation rates of 1.40-25.00 μM d^{-1} (Luo, Devine, & Edwards, 2016). Although understanding of anaerobic benzene biodegradation continues to expand globally, information on benzene-degrading consortia native to Alberta remains limited, in contrast to the ubiquity of the province's oil and gas ventures and their associated contamination risk factors. Such knowledge of native benzene-degrading consortia can help inform engineering remediation strategies, by determining the viability of natural attenuation, predicting degradation rates, suggesting biostimulatory tactics, and allows the possibility of bioaugmentation with lab-cultivated material. The logistical and technical challenges in acquiring this body of knowledge are many, due to the general metabolic lethargy in anaerobic cultures and the fastidious syntrophy of benzene-degrading mixed cultures (Vogt, Kleinsteuber, & Richnow, 2011).

Therefore, the ability of intrinsic microbial communities in uncontaminated Albertan sediments to initiate C_6H_6 removal will be examined, the aim of which is to establish the challenges inherent to anaerobic benzene-degrading culture maintenance and show the history of these cultures as a contribution to the scholarship. This information is intended to initiate a more comprehensive study of Albertan sediments that will eventually allow remediation specialists to more effectively assess and monitor bioremediation of contaminated sites in the province, and to ultimately generate cultures capable of robust biodegradation for bioaugmentation efforts. The sediments under study were collected from a location near an oil-sands mine-lease site in the northeastern Athabasca region (56°58'40.1"N 111°28'56.3"W) in Alberta. Two sediment types were gathered from clay (10 mbgs) and sand (25 mbgs) horizons of this site and cultured anaerobically as previously described (Holden, Donahue, & Ulrich, 2011) with C_6H_6 enrichments and in the presence of CO_2, SO_4^{2-}, NO_3^-, or Fe^{3+} serving as TEAs (terminal electron acceptors). C_6H_6, CH_4,

SO_4^{2-}, NO_3^-, NO_2^-, and Fe^{2+} levels were monitored over the course of the study, and microbial consortia were analyzed by NGS (next generation sequencing). As described above, both *Peptococcaceae* and *Geobacter metallireducens* appear to be relatively common primary degraders, and should be expected in Albertan NO_3^- and Fe^{3+}-reducing cultures, respectively. Other redox conditions have more diverse primary degrading taxa, and methanogenic and SO_4^{2-}-reducing cultures are therefore less predictable in regards to metabolic activity and the identity of their primary degrading organisms, although their removal rates should be expected to follow redox potential patterns (Silva, Ruiz-Aguilar, & Alvarez, 2005; Vogt, Kleinsteuber, & Richnow, 2011).

2.3 Methodology

2.3.1 Culture Source and Enrichment

Microcosm inoculum material was collected at clay and sand horizons adjacent to the South Tailings Pond in Northern Alberta, at 10 and 25 mbgs, respectively (Holden, Donahue, & Ulrich, 2011). These sediments are predominantly composed of illite and kaolinite (Jansen, Sharma, Barbour, & Hendry; Holden, Donahue, & Ulrich, 2011), with aluminum, iron, manganese, silicon, and strontium detected as trace minerals in groundwater samples at transect monitoring wells on-site (Ulrich, Donahue, & Biggar, 2007). Clay sediments had a cation exchange capacity of 15.5 meq/100 g, a specific gravity of 2.643 at 20℃, and an organic content fraction of 0.986%. Sand sediments had a cation exchange capacity of 5.59 meq/100 g, and specific gravity of 2.733 at 20℃ (Holden, Donahue, & Ulrich, 2011). Sealed sediments were frozen at -20℃ for storage, thawed in an anaerobic chamber (Coy Laboratory Products, Madison, WI)

(atmosphere 5/5/90% v/v/v $H_2/CO_2/N_2$), transferred to sterile, anaerobically-acclimated 250 mL glass vials, and infused with 150 mL of previously-defined anaerobic mineral media (Edwards & Grbic-Galic, 1994). Microcosms were amended as appropriate to establish methanogenic (n/a), sulfate-reducing (15 mM SO_4^{2-}), iron-reducing (2% v/v insoluble Fh ($(Fe^{3+})_2O_3$•$0.5H_2O$, ferrihydrite)), and nitrate-reducing (3 mM NO_3^-) conditions. A suite of eight microcosms was established: MC, MS, SC, SS, IC, IS, NC, and NS, with bi-letter designations for, firstly, redox conditions (M = methanogenic, S = sulfate-reducing, I = iron-reducing, N = nitrate-reducing) and secondly, sediment type (C = clay, S = sand).

Bottles were sealed with Mininert™ caps and separately amended with neat C_6H_6 via a 10 µL glass syringe (Hamilton Company, USA) to an expected final liquid concentration of 280 µM (Edwards & Grbic-Galic, 1994). A dimensionless Henry's law constant of 0.183 was used to calculate liquid concentrations (Peng & Wan, 1997), and equilibrium (280±0.7 µM) was reached within 24 h of C_6H_6 dispersal (Supplemental 1). Concentrations of C_6H_6 and TEA were analyzed regularly and amendments were performed periodically to maintain metabolic activity. All manipulations were performed under anaerobic conditions, and all microcosms were stored in an anaerobic atmosphere with light-exclusion at 25℃. Microcosms were enriched for 260 days over the course of the study.

A separate 50 mL sample of culture, designated as a heat-sterilized control, was transferred to a 125 mL serum bottle, capped with a butyl stopper, and sealed with an aluminum crimp. The serum bottle then underwent heat-sterilization with three separate 90 min liquid autoclave cycles and was supplemented with neat C_6H_6 to a liquid concentration of 280 µM. Equilibrium (280±0.7 µM) was reached within 24 h of C_6H_6 dispersal (Supplemental 1). Over the course of 108 days there was a 5.87 nM d^{-1} change in C_6H_6 in the killed control sample (Table 1) (Supplemental 1). The biletter designation of HK denoted the heat-killed control.

2.3.2 C_6H_6 and CH_4 Analysis

C_6H_6 was quantified by headspace analysis using an Agilent™ 7890A equipped with a flame ionization detector and an HP-1 methylsiloxane (30 m x 320 µm x 0.25 µm) column. The injector was set to 17.735 psi with septum purge flow at 3 mL min^{-1}, the column was set at 350℃, 4.5 mL min^{-1}, the oven was set at 50℃, 4.5 min, and the detector was set at 250℃, 45 mL min^{-1} hydrogen, 450 mL min^{-1} air, and 25 mL min^{-1} helium.

CH_4 was quantified by headspace analysis using an Agilent™ 7890A equipped with a flame ionization detector and an HP-1 methylsiloxane (30 m x 320 µm x 0.25 µm) column. The injector was set to 17.735 psi with septum purge flow at 3 mL min^{-1}, the column was set at 350℃, 4.8 mL min^{-1}, the oven was set at 50℃, 8 min, and the detector was set at 250℃, 40 mL min^{-1} hydrogen, 450 mL min^{-1} air, and 23 mL min^{-1} helium.

Single injections were performed using a 500 µL manual injection volume extracted from the headspace under anaerobic conditions with gas-locking syringes (Sigma-Aldritch™ VICI Series A-2). The error for C_6H_6 concentration measurements was ±6.24%. Calibration was performed with external standards and the detection limit was 0.01 mM C_6H_6 and 0.2% CH_4. Daily removal rates (µM d^{-1}) were determined by calculation of overall removal over days 117-260 of culturing i.e. (total [C_6H_6] removed (µM)/(143 d). Total cumulative C_6H_6 removal was calculated by the summation of removal cycles (defined as the difference in concentrations immediately adjacent to feeding events, and excluding intervening data points). Statistical significance in the differences between removal cycles between experimental samples and controls were estimated with Student's t-test in Excel™ Analysis Toolpak, and deemed significant upon

presentation of p-values < 0.05. Sampling was performed approximately once every 30 d for methanogenic cultures and once every 7 d for SO_4^{2-}, Fe^{3+}, and NO_3^--reducing cultures.

2.3.3 TEA and Byproduct Analysis

SO_4^{2-}, NO_3^-, and NO_2^- concentrations were quantified by 100 µL injections of 0.2 µm-filtered, 50X-diluted liquid samples into a Dionex™ ICS-2100 ion chromatographer with an IonPac™ AS18 IC column. The eluent flowrate was 0.25 mL min^{-1} with 10-32 mM KOH, the suppressor was a 2 mm ASRS set at 20 mA, the conductivity detector was set at 35℃, and the background conductance was < 1 µS with a backpressure of ~ 2000 psi. Calibration was performed with external standards and the detection limit was 2.5 mg L^{-1} SO_4^{2-}, NO_3^-, or NO_2^-. Iron was quantified by the ferrozine assay as described previously (Lovley & Phillips, 1986), with a detection limit of 0.001 M. Rates and stoichiometries were calculated from overall degradation over days 117-260 of culturing i.e. (total [C_6H_6] degraded (µM)/(143 d) (Figure 1-4.) and compared to theoretical values (Vogt, Kleinsteuber, & Richnow, 2011). Theoretical ratios for NO_3^--reducing reactions are based on either complete ($NO_3^- \rightarrow N_2$, 6:1 mol:mol NO_3^-:C_6H_6) or incomplete ($NO_3^- \rightarrow NO_2^-$, 15:1 mol:mol NO_3^-:C_6H_6) denitrification (Vogt, Kleinsteuber, & Richnow, 2011). * = statistical significance (p-value < 0.05).

2.3.4 16S rRNA Community Analysis

Regular acquisition of 1 mL culture for TEA analysis coincided with harvesting for DNA extraction at 260 days. Samples were centrifuged at 8000 xg for 3 min, and DNA extraction on collected biomass was performed with FastDNA™ kits. Primary PCR of the V3-V4 region of the

16S rRNA gene was performed by Phusion™ polymerases using the following oligonucleotides, specific for *Archaea* and *Bacteria*: 16S rRNA V3-4 IL-F (TCG TCG GCA GCG TCA GAT GTG TAT AAG AGA CAG CCT ACG GGN GGC WGC AG) and 16S rRNA V3-4 IL-R (GTC TCG TGG GCT CGG AGA TGT GTA TAA GAG ACA GGA CTA CHV GGG TAT CTA ATC C). PCR cleanup was performed by QIAEX™ kits (Qiagen™), and prepared samples were delivered to the DNA core at the University of British Columbia for Illumina-MiSeq™ analysis. All kit-based techniques were performed as directed by the manufacturer. Raw fastq file reads were processed by the Mothur pipeline for 16S rRNA community analysis, with DNA library preparation and analytic workflows adapted from previously-developed toolkits and protocols (Schloss, et al., 2009). A cutoff threshold identity of 97% was used in analyses, and alpha diversity was calculated by Shannon indices. Raw sequence reads were submitted to the NCBI database, and the data are openly available at https://www.ncbi.nlm.nih.gov, Accession No. PRJNA608926. To generate a phylogenetic analytic of primary degraders, selected sequences (Noguchi, Kurisu, Kasuga, & Furumai, 2014; Alfreider & Vogt, 2007; Sakai, Kurisu, Yagi, Nakajima, & Yamamoto, 2009; Luo, Devine, & Edwards, 2016; Musat & Widdel, 2008; Oka, et al., 2008; Zhang, Bain, Nevin, Barlett, & Lovley, 2012; Bedard, Ritalahti, & Loffler, 2007; Abu Laban, Selesi, Jobelius, & Meckenstock, 2009; Zaan, et al., 2012) were imported into Mega7 (Kumar, Stecher, & Tamura, 2016; Gatesy, 2002), aligned via the default ClustalW algorithm parameters (Kumar, Stecher, & Tamura, 2016), and input into a maximum-likelihood tree construction tool using the Tamurai-Nei model (Kumar, Stecher, & Tamura, 2016; Page & Holmes, 2009; Swofford, Olsen, Waddell, & Hillis, 2021).

2.4 Results and Discussion

2.4.1 Removal rate and Stoichiometry

C_6H_6 removal under all redox conditions and sediment types was observed through multiple removal cycles (Table 2-1.), with the highest rates visible in the Fe^{3+}-reducing (IC/IS), and NO_3^--reducing (NC/NS) microcosms (11.20-12.70 μM d^{-1}), and the lowest rates visible in the methanogenic (MC/MS) and SO_4^{2-}-reducing (SC/SS) microcosms (3.27-8.14 μM d^{-1}). This is in agreement with energetics predicted by redox potentials (Silva, Ruiz-Aguilar, & Alvarez, 2005; Vogt, Kleinsteuber, & Richnow, 2011). The high removal rates of Fe^{3+}-reducing cultures may be due to the high redox energy potential of Fe^{3+} (ΔE^0 = +36 V) (Silva, Ruiz-Aguilar, & Alvarez, 2005; Lueders, 2017) as a terminal electron acceptor, as well as the low toxicity of Fe^{2+}, which would not interfere with further C_6H_6 removal in the closed system except at very high levels. This is in contrast with NO_3^--reducing and SO_4^{2-}-reducing cultures, which can generate NO_2^- and H_2S compounds that can interfere with culture activity (Silva, Ruiz-Aguilar, & Alvarez, 2005). Previous scholarship suggests a wide range of NO_2^- tolerance in various cultures, but significant inhibition of C_6H_6 metabolism has been reported at levels of 5-7 mM NO_2^- (Gitiafroz, 2012).

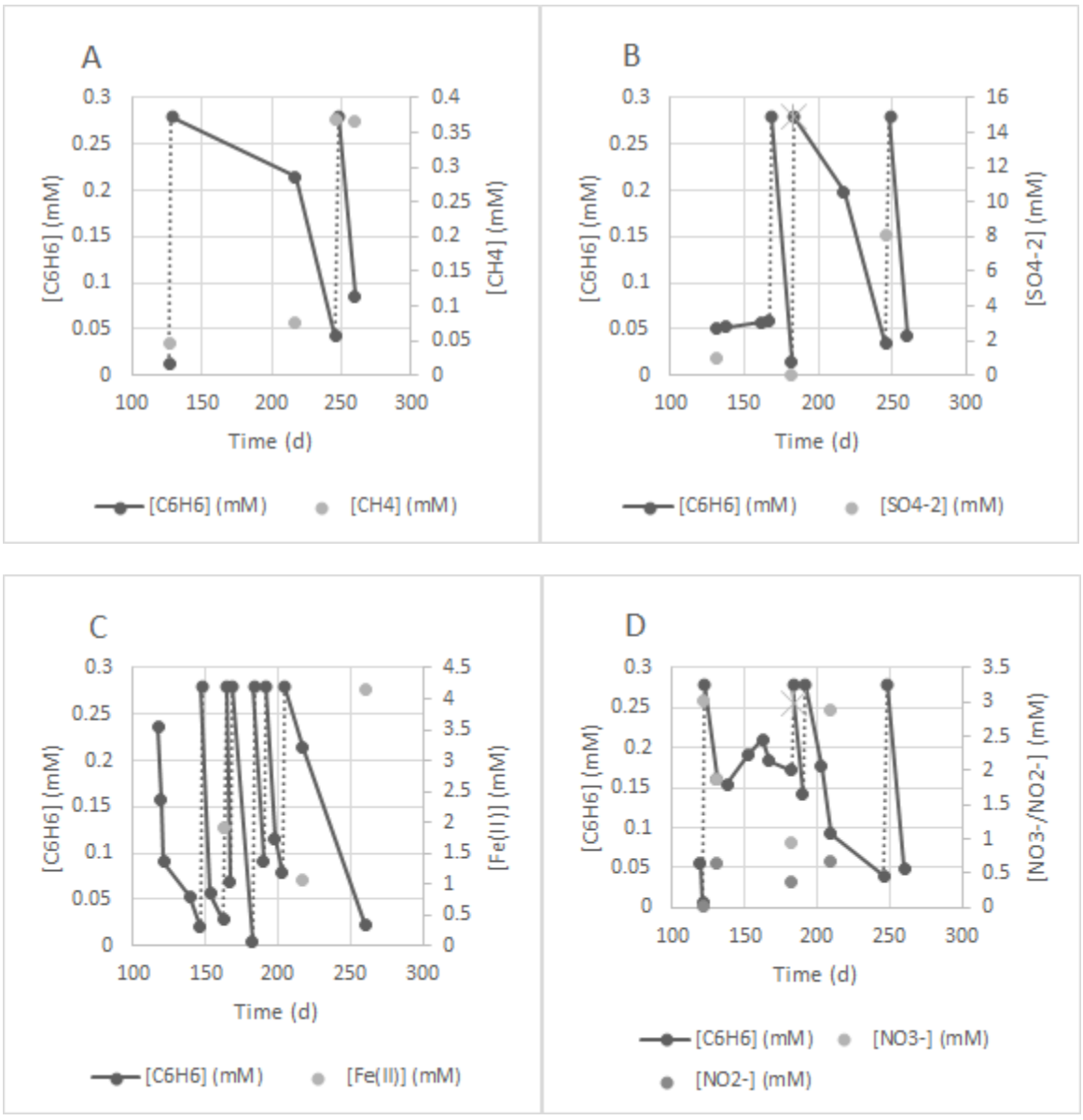

Figure 2-1. C6H6 Degradation and TEA Depletion/byproduct Generation of Clay-based cultures.

Enrichment cultures were maintained in anaerobic conditions, and C_6H_6 and CH_4 concentrations were monitored by headspace GC analysis. TEA depletion was measured by anion-exchange IC, and Fe^{2+} generation was measured by ferrozine assay. A = MC (methanogenic), B = SC (SO_4^{2-}-reducing), C = IC (Fe^{3+}-reducing), , D = NC (NO_3^--reducing). A 15% v/v dilution of anaerobic mineral media was performed at 183-200 days in all cultures except for MC. C_6H_6

feeding events are represented by dotted lines and TEA feeding events are represented by asterisks (*). Data points represent single measurements.

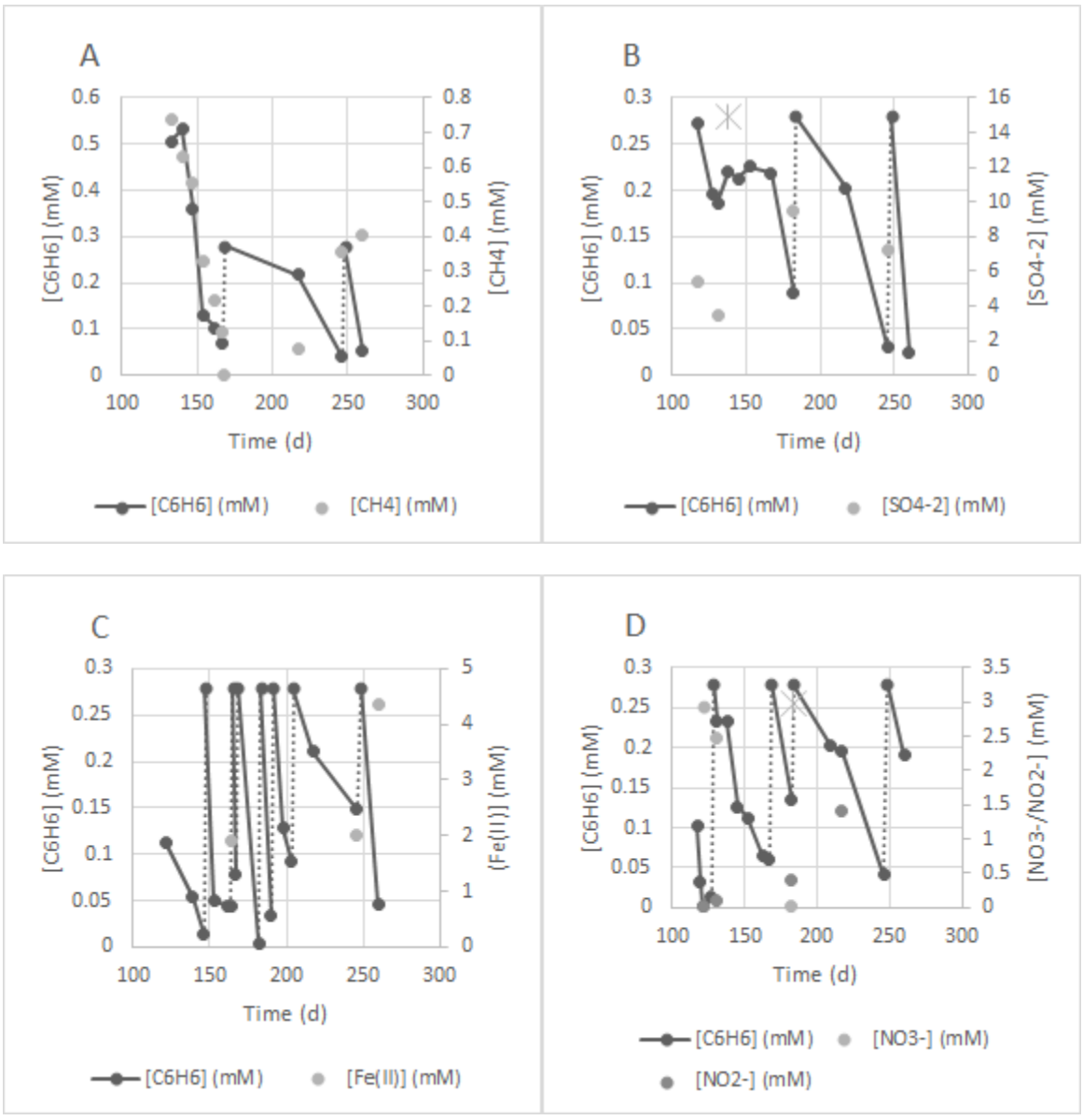

Figure 2-2. C6H6 Degradation and TEA Depletion/byproduct Generation of Sand-based Cultures.

Enrichment cultures were maintained in anaerobic conditions, and C_6H_6 and CH_4 concentrations were monitored by headspace GC analysis. TEA depletion was measured by anion-exchange IC, Fe^{2+} generation was measured by ferrozine assay. A = IS (Fe^{3+}-reducing), B = MS (methanogenic), C = NS (NO_3^--reducing), D = SS (SO_4^{2-}-reducing). A 15% v/v dilution of anaerobic mineral media was performed at 183-200 days in all cultures except for MS. C_6H_6

feeding events are represented by dotted lines and TEA feeding events are represented by asterisks (*). Data points represent single measurements.

Table 2-1. Degradation Rates and Stoichiometry of Enrichment Cultures.

Microcosm	Lag period (d)	Removal Rate (μM d^{-1})		Stoichiometry (mol:mol TEA consumed/byproduct generated:C_6H_6)	
		Literature	Empirical	Theoretical	Empirical
MC	128	1.40-25.00 (Luo, Devine, & Edwards, 2016)	3.27	3.75:1	1.35:1
MS	147		5.08		1.58:1
SC	168	36.00 (Taubert, et al., 2012)	8.14	3.75:1	3.85:1
SS	117		6.55		4.07:1
IC	80	6.00 (Kunapuli, Lueders, & Meckenstock, 2007)	11.20*	30:1	16.10:1
IS	89		12.70*		22.72:1
NC	80	10.00 (Luo, et al., 2014)	11.32*	6/15:1	9.63:1
NS	77		12.20*		7.66:1
HK	n/a	n/a	0.05	n/a	n/a

Compared to cultures elsewhere, the rates of NC and NS (11.32-12.20 μM d^{-1}) (Table 2-1.) were highly similar to previously reported values of 10.00 μM d^{-1} (Luo et al. 2014), whereas the rates of IC and IS (11.20-12.70 μM d^{-1}), were about twice as high as those of previously reported cultures (Kunapuli, Lueders, & Meckenstock, 2007). The IC and IS cultures, however, had been enriched for 260 days, while the microcosms described in previous studies had been enriched for only 120 days (Kunapuli, Lueders, & Meckenstock, 2007). Enrichment correlates with redox specialization (Winderl, Anneser, Griebler, Meckenstock, & Lueders, 2008) and enhanced removal, so the extra culturing time may account for the difference in activity. This may also explain the low rates of SC/SS when compared to well-studied cultures derived from a German aquifer (Taubert, et al., 2012) (Table 2-1.), which had been under continuous cultivation for multiple years. Both iron-reducing and nitrate-reducing microcosms exhibited removal cycles that were significantly different from the heat-killed control.

Stoichiometry ratios indicated that C_6H_6 oxidation occurred at varying degrees within tested redox conditions. Fe^{3+}-reducing microcosm (IC/IS) stoichiometric values only reached approximately 50-75% that of theoretical stoichiometric values (30:1 mol Fe(II):mol C_6H_6) (Vogt, Kleinsteuber, & Richnow, 2011) - this may be due to the low bioavailability of amorphous iron, resulting in concurrent degradation of C_6H_6 by methanogenesis, as well as precipitation of ferrous iron (Villatoro-Monzon, Morales-Ibarria, Velazquez, Ramirez-Saad, & Razo-Flores, 2008). Additionally, methanogenic cultures (MC/MS) demonstrated approximately 37% fidelity to theoretical (3.75:1 mol CH_4:mol C_6H_6) stoichiometries; the cause of this discrepancy is unknown. SO_4^{2-} and NO_3^--reducing redox conditions demonstrated similar stoichiometric comparisons to theoretical values (Table 2-1), suggesting that the appropriate TEA in NO_3^- and SO_4^{2-}-reducing microcosms was being consumed during the oxidation of C_6H_6. NO_3^- reduction stoichiometries are particularly notable because their values are intermediate between full and partial denitrification (Vogt, Kleinsteuber, & Richnow, 2011). Combined with the presence of low

quantities of NO_2^- (Figure 2-1C, 2-4C), these observations suggested that incomplete reduction of NO_3^- had taken place in the NC and NS cultures. The conformity of empirical stoichiometry ratios to theoretical values is a helpful indicator for the nature and energetics of reactions occurring both *in vitro* and *in situ*. These metrics can predict the generation of chemical byproducts, toxic (NO_2^-/H_2S) or otherwise, and can be used to track or alter the progression and kinetics of benzene degradation at a contamination site.

Lag periods were observed in all microcosms, in which no change in C_6H_6 concentrations occurred post-dispersal. This lag was most prominent in methanogenic and SO_4^{2-}-reducing cultures. This is consistent with the low redox potential of both TEAs, and with the long doubling times of previously-reported methanogenic key degraders like *Deltaproteobacteria* ORM2, estimated to be approximately 34±3.0 d (Luo, Devine, & Edwards, 2016). The lag period was also similar to previously-described SO_4^{2-}-reducing cultures that exhibited lag times of 200 d (Taubert, et al., 2012). The long lag time of these cultures was in contrast to Fe^{3+} and NO_3^--reducing microcosms, both of which have higher redox potentials and exhibited lag times similar to previous Fe^{3+}-reducing cultures, at 87-122 days (Lovley, Woodward, & Chapelle, 1994). Additionally, MS had a leak event between 117-163 days (Figure 2-2) which was not included in degradation and stoichiometry calculations. All microcosms other than the MC/MS cultures exhibited decreased removal rates at 183-203 days; this coincided with a dilution event of 15% v/v anaerobic mineral media that occurred at that time in the IC/IS, NC/NS, and SC/SS cultures, and demonstrated the importance of cell concentrations in maintaining robust C_6H_6 catabolism, and the potential negative consequences of diluting culturing volumes. Remediation doctrine for natural attenuation often assumes that the absence of contaminant removal is evidence for the absence of degradative microorganisms; however, a lack of activity may merely indicate that degrading population concentrations are too low to sustain removal (Meckenstock, et al., 2015).

2.4.2 Microbial Community Analysis and Quantification

Members of known anaerobic primary C_6H_6 degrader taxa were discovered in cultivated microcosms that reduced ferric iron and nitrate, with similar Shannon index metrics and coverage exceeding 99% in all samples (Figure 2-3, Figure 2-4, Figure 2-5). MC and MS microcosms hosted organisms of the *Deltaproteobacteria*, mainly of the *Desulfomicrobiaceae* (4.14%) and *Desulfuromonadaceae* (2.94%) family, respectively. However, these were not the same organisms as those found in previous scholarship (Luo, Devine, & Edwards, 2016). SC and SS cultures contained members of the *Clostridiales* (0.60 and 4.59% read instances, respectively), but again, these were not the same as those found in previous scholarship (Abu Laban et al. 2009). Another known primary degrader in SO_4^{2-}-reducing conditions is *Pelotomaculum* (Abu Laban, Selesi, Jobelius, & Meckenstock, 2009), thought to have decarboxylase activity, but this taxon was not present in the SC consortium. IC and IS cultures hosted members of the *Geobacteraceae* (6.61 and 2.02% read instances, respectively), while NC and NS cultures contained *Peptococcaceae* organisms (57.8% and 1.13% read instances, respectively). Those *Peptococcaceae* in NC cultures had identical 16S rRNA sequences as those found in previous scholarship (Luo, et al., 2014), although the *Peptococcaceae* in NS cultures did not. The presence of *Peptococcaceae* in multiple cultures described worldwide (Abu Laban, Selesi, Rattei, Tischler, & Meckenstock, 2010) illustrated the extent of the ubiquity of these organisms.

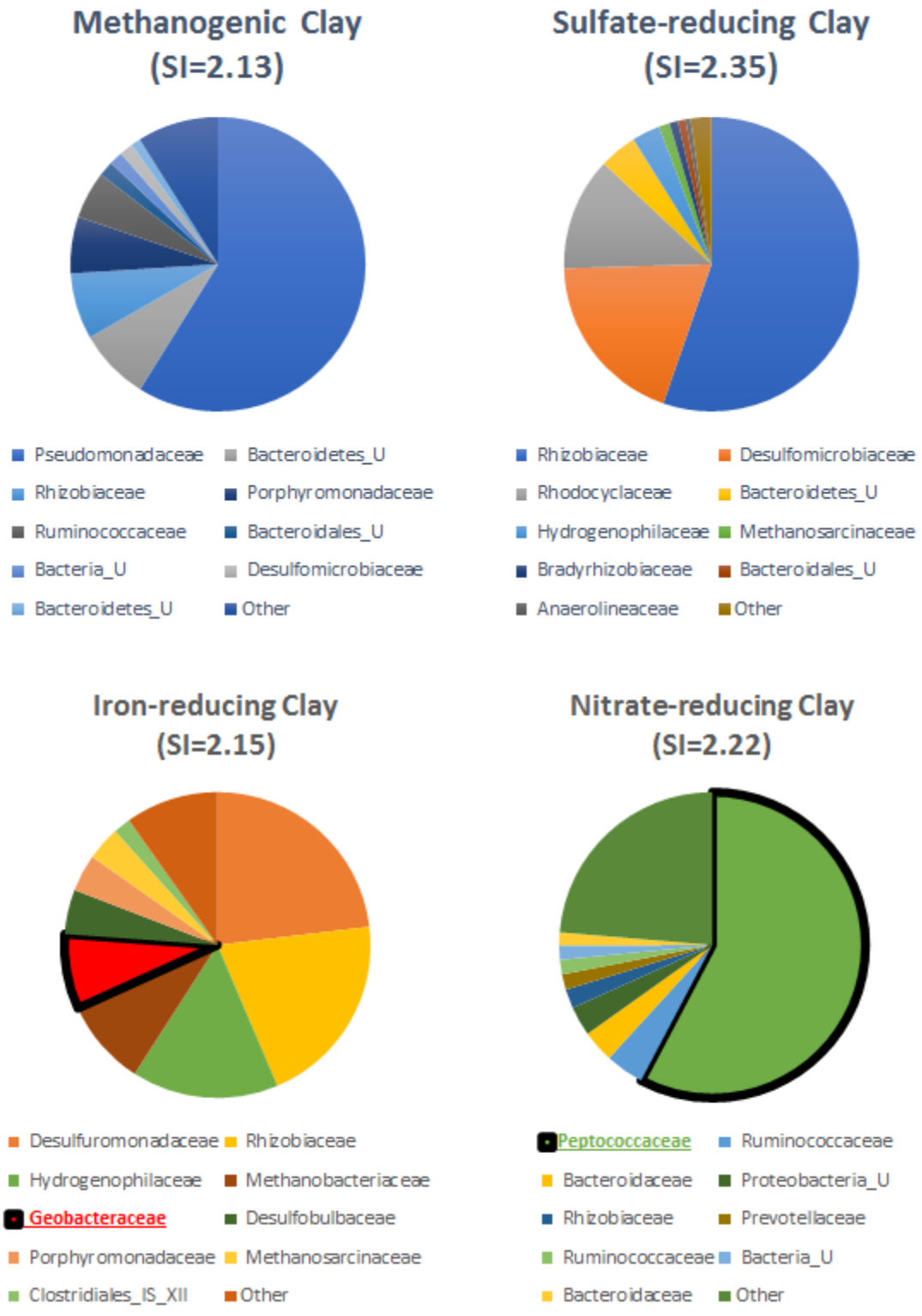

Figure 2-3. 16S rRNA Community of Clay-based Microcosms MC, SC, IC, NC.

The top 9 OTUs (operational taxonomic units) at day 260 are shown in community profile at the family taxon level, in order of abundance with 1° degraders in bold. U = unclassified, SI = Shannon Index.

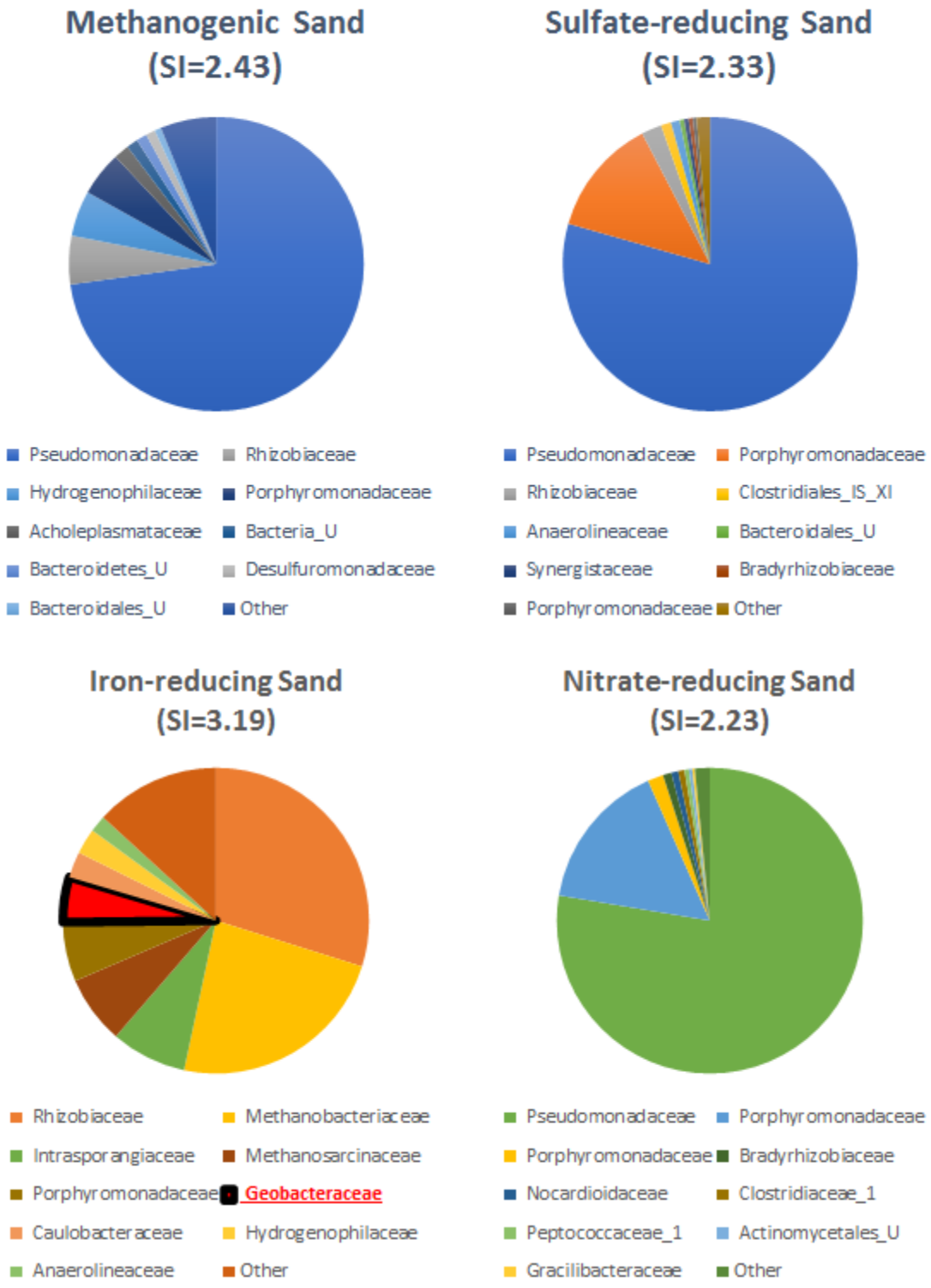

Figure 2-4. 16S rRNA Community of Sand-based Microcosms MS, SS, IS, NS.

The top 9 OTUs (operational taxonomic units) at day 260 are shown in community profile at the family taxon level, in order of abundance with 1° degraders in bold. U = unclassified, SI = Shannon Index.

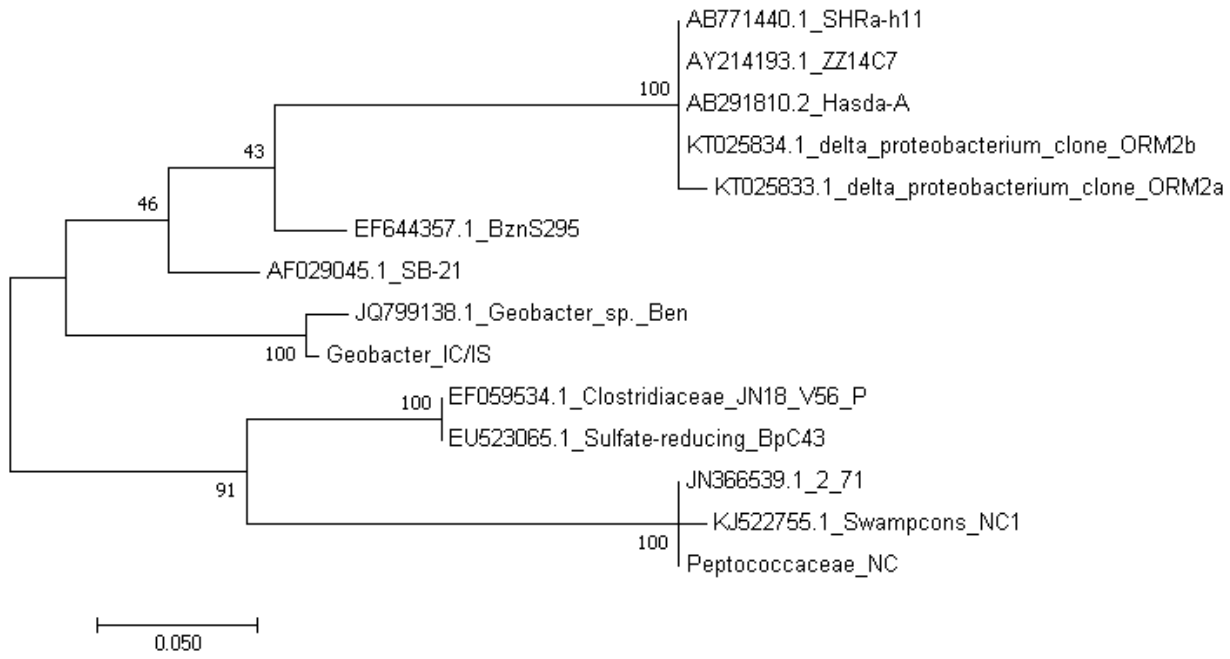

Figure 2-5. Identification of Primary Benzene Degraders by 16S rRNA Gene Homology

16S rRNA gene amplicon sequences of suspected primary benzene degraders were compared with those of known degraders from literature (Noguchi, Kurisu, Kasuga, & Furumai, 2014; Alfreider & Vogt, 2007; Sakai, Kurisu, Yagi, Nakajima, & Yamamoto, 2009; Luo, et al., 2014; Luo, Devine, & Edwards, 2016; Musat, Wilkes, Behrends, Woebken, & Widdel, 2010; Oka, et al., 2008; Zhang, Bain, Nevin, Barlett, & Lovley, 2012; Bedard, Ritalahti, & Loffler, 2007; Zaan, et al., 2012), to establish a minimum of 97% sequence homology. Maximum likelihood joining of said sequences was performed to generate a phylogenetic analysis, with branch lengths measured in number of substitutions per site (Page & Holmes, 2009; Kumar, Stecher, & Tamura, 2016; Swofford, Olsen, Waddell, & Hillis, 2021). Accession numbers for Genbank are included for reference. The two primary degraders identified in this study are listed as Geobacter_IC/IS and Peptococcaceae_NC, found in IC/IS and NC cultures, respectively.

Auxiliary taxa were identified as well. Fe^{3+}-reducing cultures contained known methanogens such as *Methanosarcinaceae* (1.76-5.64%) (Balch, Fox, Magrum, Woese, & Wolfe, 1979)

(Figure 2-3, Figure 2-4), perhaps indicative of methanogenesis occurring alongside Fe^{3+} reduction. The incongruence between empirical and theoretical stoichiometries (Table.1.) in these microcosms further suggests that methanogenesis may be taking place concurrently within the sediment microniches of these cultures. In addition, the presence of *Hydrogenophilaceae* (2.87-16.56%) in multiple cultures, including non-methanogenic ones, may be an artifact resulting from an infiltration of H_2 from the glovebox atmosphere into the sample bottles. The presence of H_2 in anaerobic chambers is a common practice necessary for the scavenging of micro-quantities of O_2 over a Pd catalyst, which maintains a strict anaerobic atmosphere. The sand-based cultures IS, NS and SS (Figure 2-4) also contained a notable population of another taxon present in previously-reported NO_3^-/SO_4^{2-}-reducing cultures, namely *Anaerolineae* (2.01-2.48%) (Keller, Kleinsteuber, & Vogt, 2018), suggesting a sand-specific habitat for this organism, but more analysis remains to be done in order to identify important syntrophic relationships between primary degraders and auxiliary organisms.

The identification of these taxa suggests a worldwide distribution of primary benzene degraders *Geobacter* and *Peptococcaceae* and hints that such organisms can be utilized as biomarker candidates for field sites that can indicate a positive prognosis for natural attenuation or advocate for biostimulatory introductions of certain TEAs like Fe(III) and NO_3^-. Although primary degraders were positively identified in iron-reducing (clay and sand) and nitrate-reducing (clay) cultures, more research has to be done in order to confirm primary degrader identities in other redox conditions and sediments. Furthermore, these data on candidate organisms can be used as a starting point for modeling reaction kinetics, and determining population threshold values and their correlation to removal rates.

2.5 Conclusions

Anaerobic culture enrichment was successful in establishing the ability of native Albertan sediments to remove C_6H_6 under methanogenic, SO_4^{2-}-reducing, Fe^{3+}-reducing, and NO_3^--reducing redox conditions, at rates (3.27-12.70 μM d^{-1}) comparable to known C_6H_6-degrading cultures from previously-reported systems (Aburto-Medina & Ball, 2015). Lag periods were also determined, ranging from 77-168 d, establishing broad temporal guidelines based on ideal conditions for laboratory cultivators to set timelines required to observe degradation in batch experiments and according to a variety of redox environments.

These redox reactions were confirmed stoichiometrically, particularly in SO_4^{2-}-reducing cultures, and revealed incomplete denitrification reactions in NO_3^--reducing cultures. Consequently, the expected accumulation of H_2S or NO_2^- in these environments may be deleterious for attenuations operating under these redox conditions, and the toxicity of these metabolites may require redress in engineered remediation programs, perhaps by the introduction of ferrous salts to react with sulfide (Firer, Friedler, & Lahav, 2008) or by coincubation with ammonium oxidizers that consume nitrite (Peng S. , et al., 2017). Stoichiometric values of iron-containing cultures also suggested a subset of reactions unrelated to Fe^{3+}-reduction, suggesting that the bioavailability of the excess amorphous iron is limited and that concurrent methanogenic reactions may be taking place. Cultivation plans may therefore need to remain cognizant that benzene-oxidizing reactions reliant on Fe^{3+}-reduction may be complicated by incomplete exploitation of ferric iron, even when the required iron oxides are in excess.

In regards to the microbial community of these sediments, the presence of notable primary degrader taxa was established, including *Geobacter* (Fe^{3+}-reducing) and *Peptococcaceae* (NO_3^--reducing), in both clay and sand-based cultures.

These data can ultimately be valuable for helping to define C_6H_6-contaminated environments in Alberta, a province in which such data are highly relevant. Observed lag times and degradation rates serve as convenient guides for laboratory cultivation in regards to forecasting degradation endpoints from *ex situ* sediments, and observed stoichiometries are useful for researchers to confirm energetics and anticipate byproduct generation for new laboratory cultures undergoing establishment. Observed key degrader taxa (*Geobacter* and *Peptococcaceae*) can be further investigated for their candidacy as biomarker populations, the presence and quantity of which can be used to predict contaminant removal rates. Further research may also include work on co-contaminants which inhibit benzene degradation (Edwards, Wilis, Reinhard, & Grbic-Galic, 1992; Cunningham, Rahme, Hopkins, Lebron, & Reinhard, 2001; Da Silva & Alvarez, 2007) such as EtOH, a common additive in gasoline, which can produce a co-solvent effect that enhances benzene solubility in water (Silva, Da Silva, & Alvarez, 2002; Powers, et al., 2001; Ruiz-Aguilar, Fernandez-Sanchez, Kane, Kim, & Alvarez, 2002), resulting in complications in remediation due to the increased expanse of the plume.

These studies were constrained by the logistics of anaerobic culturing which allowed for a limited volume of culture. As such, reproducibility is achieved through repeated removal cycles within each culture as opposed to replication of cultures; well-established cultures require years to decades of cultivation (Taubert, et al., 2012; Luo, Devine, & Edwards, 2016; Luo, et al., 2014), and the acknowledgement of these timelines compelled sharing of these data, such that researchers and industrial partners can appreciate the complications involved. This work is therefore a starting point for the increased surveying of Albertan sediments; such a body of data can move towards the continued development and enrichment of anaerobic benzene cultures, with an aim to ultimately produce cultures for more active implementation through bioaugmentation.

2.6 Acknowledgements

Thanks to NSERC Discovery for financially supporting this research, and to Edwards Lab (University of Toronto) personnel for their assistance in anaerobic microcosm cultivation.

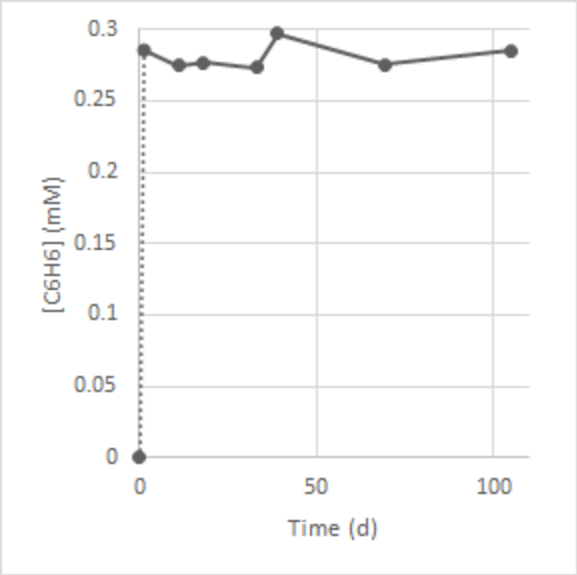

Supplemental 2-1. C6H6 removal in Heat-killed Control (HK)

Samples of culture were heat-sterilized with triple 90 min autoclave cycles, amended with C_6H_6, and maintained in anaerobic conditions over 105 days. C_6H_6 concentrations were monitored by headspace GC analysis. Dotted lines represent C_5H_5 feeding events. Data points represent the average of duplicates.

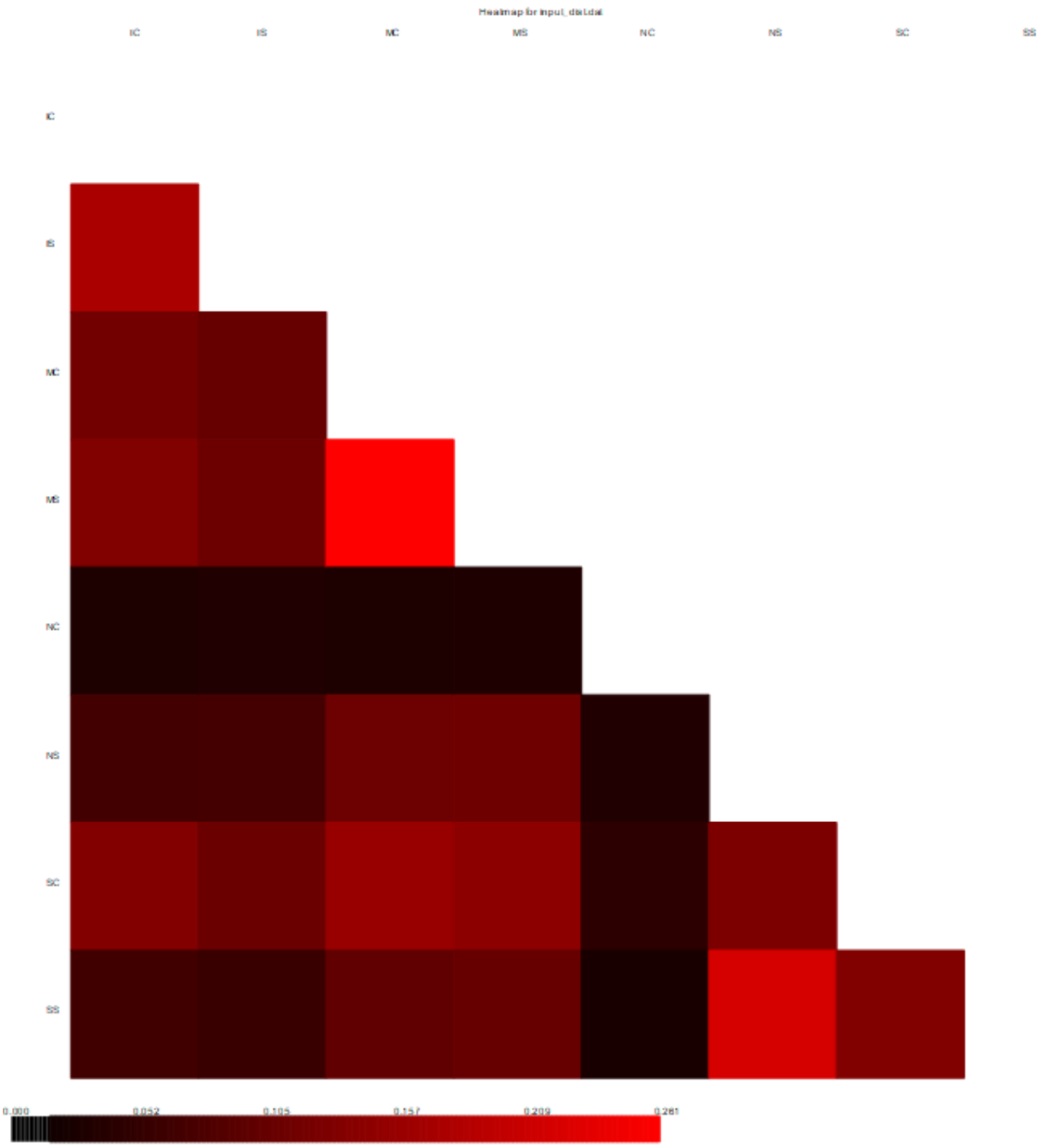

Supplemental 2-2. Similarity Heat Map depicting Beta Diversity between Microcosms

Beta diversity as calculated by the thetaYC method (Yue & Clayton, 2005), the indices of which include both shared and nonshared species populations as derived from 16S rRNA amplicon sequencing. Bi-letter designations are defaulted in alphabetical order. I = iron-reducing, M = methanogenic, N = nitrate-reducing, S = sulfate-reducing; C = clay, S = sand.

3 Iron-reducing Benzene-degrading Cultures Derived from Albertan Sediments: Metagenomics Analysis and Isolation of *Geobacter metallireducens*

3.1 Abstract

Amongst the various redox conditions that have been represented in the anaerobic benzene-degradation literature, it is iron-reduction that has the fewest laboratory advocates. Any groups that establish novel iron-reducing benzene degrading cultures, therefore, have the onus to investigate them thoroughly and compare them to previously reported results, particularly those regarding taxonomic profiles and genetic traits relevant to benzene metabolism. This study interrogated one such culture, derived from Albertan sediments, which had been found to support robust iron-reducing benzene degradation and host substantial populations of an organism with 98% 16S rRNA sequence homology to the reported primary benzene degrader *Geobacter metallireducens*. An attempt to isolate this primary benzene degrader as pure culture was made, and metagenomics sequencing was performed on the mixed culture to verify the *Geobacter* taxon and identify various genes involved in benzene activation. Although the isolation of *Geobacter* was unsuccessful, whole genome sequencing of this culture identified *Geobacter metallireducens* at a species taxonomic level. Neither the putative benzene hydroxylase genes *gmet 0231* and *gmet 0232* were present, nor was the putative benzene carboxylase *AbcDA* or the benzyl-succinate synthase *bssA*, suggesting that benzene enzymatic activities in these cultures were taking place distinct from those reported in the literature.

3.2 Introduction

Bioremediation of benzene contamination is uniquely applicable to the concerns of the oil and gas sector in the province of Alberta, Canada, where the fossil fuel energy industry accounts for a substantial proportion of the provincial economy (Canada Environment & Canada Health and Welfare, 1993; Government of Canada, Environment Canada, & Health Canada, 1993; Government of Alberta, 2019) and places enormous financial liabilities on any cleanup proposals by the affected parties (Dachis, Shaffer, & Thivierge; Singh, 2020). Therefore, bioremediation as a remediation technique is a relatively cost-effective approach that produces minimal environmental disturbance, particularly where indigenous microbes are involved (Azubuike, Chikere, & Okpokwasili, 2016).

The generation of iron-reducing benzene-degrading cultures from Albertan sediments (Lee & Ulrich, 2021), though formative in this regard, had raised further questions as to the specifics of microbial community structures and degradation kinetics. A major challenge for these cultures was to verify the purported mechanisms of iron-reduction, specifically, the activity of *Geobacter metallireducens*, which is the reported primary benzene degrader of iron-reducing cultures (Zhang, Bain, Nevin, Barlett, & Lovley, 2012) that has been isolated in pure culture by the Lovley group alone (Lovley D. R., et al., 1993). The 16S rRNA amplicon sequences of the Alberta cultures demonstrated a 98% homology to that of the Lovley lab (GenBank: JQ799138.1), and the Alberta cultures also hosted auxiliary organisms relevant to anaerobic benzene degradation, namely *Desulfuromonas*, *Methanosarcina*, and *Anaerolineae* (Luo, Devine, & Edwards, 2016; Balch, Fox, Magrum, Woese, & Wolfe, 1979; Keller, Kleinsteuber, & Vogt, 2018). *Geobacter metallireducens*, being the purported primary degrader of iron-reducing

benzene cultures, can be most directly verified via isolation in pure culture as reported previously (Lovley D. R., et al., 1993), following the formulations and protocols established from previous experiments (Lovley & Phillips, 1988; Lovley, Greening, & Ferry, 1984). Although *Geobacter* was observed in Albertan iron-reducing benzene cultures (Lee & Ulrich, 2021), the 16S rRNA amplicon analysis used was limited in its depth of taxonomic identification, and it was imperative to perform whole genome sequencing (WGS) to positively verify organisms to a species level and incorporate putative benzene-degrading gene analysis.

Simplistically, the benzene oxidation pathway in iron-reducing cultures with *Geobacter* is thought to involve the hydroxylation of the highly stable benzene ring to generate a phenol intermediate (Zhang T. , et al., 2013). This phenol, once phosphorylated and carboxylated, is fitted with a Coenzyme A to create the central intermediate of all anaerobic benzene reactions: benzoyl-CoA (Vogt, Kleinsteuber, & Richnow, 2011; Meckenstock & Mouttaki, 2011). This benzoyl-CoA is subsequently metabolized in a manner akin to conventional beta-oxidation (Loffler, et al., 2011; Dong, et al., 2017). The process at play for the first activation of the benzene ring remains unknown, although RNA microarray analysis supports a hydroxylation reaction as the most likely mechanism (Zhang T. , et al., 2013), and implicates the *Geobacter metallireducens* genes *gmet 0231* and *gmet 0232* in particular (Zhang T. , et al., 2013; Zhang T. , et al., 2014). These genes, along with the taxa mentioned previously, were the main points of interest in this study, and were expected to be present in the metagenomes of active iron-reducing benzene-degrading microcosms, alongside populations of *Geobacter metallireducens* that were expected to exist proportionate to culture activity.

3.3 Methods

3.3.1 Cultivation of Iron-reducing Cultures

Iron-reducing cultures derived from Albertan sediments were continuously monitored and maintained as described previously (Lee & Ulrich, 2021), with weekly quantifications of methane and benzene by GC headspace analysis. Three microcosms were analyzed, representing iron-reducing clay (IC), iron-reducing sand (IS), and iron-reducing mixed (IM; a 1:1 combined volume of IC and IS). Soluble iron levels were quantified by ICP-MS (Inductively Coupled Plasma Mass Spectrometry) (iCap Q, ThermoScientific®) with appropriate internal and external standards. Monitoring of iron-reducing cultures continued until a removal rate of 10 µM/d was maintained for three degradation cycles. At that point, 24 mL of culture volume from the most active cultures were taken for DNA extraction and metagenomics analysis.

3.3.2 DNA Extraction of Iron-reducing Cultures

DNA extraction was performed using the FastDNA™ Soil kit and modified according to the manufacturer's instructions to avoid DNA shearing and generate gDNA with average lengths of approximately 15 kb while maximizing lysis (Supplemental 3-1), as maximizing integrity was critical for downstream sequencing quality (Dias, et al., 2014). DNA sequence lengths were quantified with Agilent© ScreenTape and TapeStation Analysis Software 3.1. Such considerations were necessary for maximizing sequencing effectiveness and avoiding biases in favour of particular microbes (Feinstein, Sul, & Blackwood, 2009; Guo & Zhang, 2013; Vishnivetskaya, et al., 2014; Corcoll, et al., 2017). Two extraction kits were tested,

Dynabeads™ (Invitrogen®) and FastDNA™ for Soil (MolecularBio®), and modified to optimize extraction.

3.3.3 Genetic Analysis of Iron-reducing Cultures

Whole Genome Sequencing (WGS) was performed by University of Alberta MBSU facilities using the NextSeq Mid-Output 300 Cycle chip for an output data yield of approximately 30 GB. Library preparation was performed using the Illumina DNA Prep kit (Cat# 20018704), and quality-checked using an HS-DNA chip bioanalyzer. Analysis of WGS data was performed using the pipelines and tools developed at the Human Microbiome Project at EMBL (Bork & Zeller, 2021), including the NGLess toolkit (Coelho, et al., 2019) for genome assembly, proGenomes toolkit (Mende, et al., 2017) and eggNOG (Huerta-Cepas, et al., 2019) for annotation. mOTUs2 tools and the mOTUs database was used (Milanese, et al., 2019) for clustering and referencing, and iPath (Darzi, Letunic, Bork, & Yamada, 2018), iTOL (Letunic & Bork, 2019), Enterotyping (Costea, et al., 2018), and SIAMCAT (Wirbel, et al., 2020) tools were used for visualization. All metagenomics analyses were performed by Dr. Nabeel Mian in the Ulrich Lab of the University of Alberta. Data are publicly available on GenBank, Accession #PRJNA821538

qPCR primers targeting *Geobacter metallireducens, Methanosarcina, Anaerolineae, Desulfuromonas,* and *Hydrogenophilaceae,* as well as the genes *gmet 0231, gmet 0232,* and *ppsA* were designed using Primer Express™ software, using MGB minor groove and Taqman™ discrimination predictions at a minimum-maximum temperature of 58-60ºC (Table 3-1). Triplicate qPCR reactions were prepared from extracted DNA using the ThermoFisher™ DyNAmo Flash SYBR Green qPCR Kit as directed by the manufacturer. These reactions were amplified and analyzed by the BioRad™ CFX96 Real-Time Detection system under the

following conditions: initial denaturation at 95℃ for 7 min, followed by 40 cycles of denaturation at 95℃ for 10 sec and annealing/extension at 59℃ for 30 sec with data acquisition, and final melting curve processing from 65-95℃ at 0.5℃ increments with a 10 sec plate reading. Cq (Cycle Quantification) values were averaged between triplicates and converted to copy number by semi-log standard curves. Standards were established with 4 serial 10-fold dilutions of 16S rRNA sequences cloned into ThermoFisher™ TOPO4 plasmids. *Bac* (Bacteria), *Peptococcaceae, Deltaproteobacterium* ORM2*,* and *abcA* gene primers were provided by Edwards Lab at the University of Toronto.

3.3.4 Isolation of *Geobacter metallireducens*

The dominating presence of a *Geobacter* taxon in the Alberta iron-reducing cultures, with 98% 16S rRNA sequence homology to the primary benzene degraders described in the literature (Abu Laban, Selesi, Jobelius, & Meckenstock, 2009; Zhang T. , et al., 2013), offered an opportunity to attempt an isolation of *Geobacter* for the generation of a pure benzene-degrading culture. These protocols were adapted from previous isolations (Lovley, Greening, & Ferry, 1984; Lovley & Phillips, 1988), characterized by the use of slant tubes in anaerobic conditions, with phosphate buffer containing nitrate (as sodium nitrate) and then ferric iron (iron (III) citrate) as terminal electron acceptors and acetate as a carbon source. These experiments yielded pink colonies that were subsequently grown in liquid media as pure cultures. The formulations used were unchanged from these previous protocols, which reported the isolation of *Geobacter metallireducens* as pink colonies on agar that could also be expanded in liquid media. Later iterations of isolations in this study incorporated alterations such as the use of benzene over

acetate as a carbon source at a liquid concentration of 0.28 μM, the use of agarose rather than agar as a growth medium, and the use of Petri plates in place of Hungate tubes.

Table 3-1. qPCR Oligonucleotides for Anaerobic Benzene-degrading Iron-reducing Cultures.

Source Sequence	GenBank Accession Number	qPCR Oligonucleotide Sequence (5'-3')	
		Forward	**Reverse**
Bac 1055..1392	n/a	ATGGCTGTCGTCAGCT	ACGGGCGGTGTGTAC
Geobacter metallireducens	JQ799138.1	AGCAGCCGCGGTAATACG	GATTTATTGGGCGTAAAGCGC
gmet 0231 263106..264068	GSE33794	CCGCCATGGGAAAGGAA	CTCTACAACGCCAGCGACAA
gmet 0232 264085..264930	GSE33794	TCCCGGTACTGCTCGATGAG	ACATCTTCCCGCAGCAGC
ppsA 475..613	GSE33794	AGCGTGGTCACTGAAGGAAT	AAAAGACGTAGGCGGCATAG
Methanosarcina	KT216122.1	GGGCACGAACCGGATTAGAT	CGTAAACGATGCTCGCTAGGT
Desulfuromonas	KY891252.1	CCGCCGCGGTAATACG	GGAATTATTGGGCGTAAAGCG
Anaerolineae ornatilinea	MF661877.1	GGCCTGCGTCCCATCA	TACCAAGGCGATGACGGG
Hydrogenophilaceae thiobacillus	MN880335.1	ACCTGGGAATGGCATTTTGA	TCAGAGGGGGGTGGAATTC
Peptococcaceae 634..743	KJ522755.1	GRATYTCTTGAGGGTATGAG	CAGTTGTATGCCAGAAAGCC
abcA 254..373	KJ522755.1	GGCGCGAAATCCAGGATACA	GGTCGAACAGGTTGACGTCT
Deltaproteobacteria ORM2 168..422	KT025834.1	GAGGGAATAGCCAAAGGTGA	GAGCTTTACGACCCGAAGAC

Bespoke qPCR-ready oligos were synthesized to interrogate iron-reducing cultures. The Bac primer pair targeted general bacterial sequences, based on conserved 16S rRNA regions. Peptococcaceae, Deltaproteobacteria ORM2, Geobacter, Methanosarcina, Desulfuromonas, Anaerolineae, and Hydrogenophilaceae taxa were also targeted via their 16S rRNA sequences.

When culture plates or tubes yielded growth, six colonies were picked for 16S rRNA sequencing identification. Colony polymerase chain reactions (PCR) targeting the 16S rRNA V3-4 regions (IL-F: TCG TCG GCA GCG TCA GAT GTG TAT AAG AGA CAG CCT ACG GGN GGC WGC AG; IL-R: GTC TCG TGG GCT CGG AGA TGT GTA TAA GAG ACA GGA CTA CHV GGG TAT CTA ATC C) was performed to generate sequences for analysis and identification, using Thermo Scientific© Phusion High-Fidelity DNA Polymerase (cat# F-530S) according to manufacturer's instruction. The conditions for the reaction were as follows: initial denaturation at 95ºC for 30", then denaturation at 95ºC for 10", annealing at 56ºC for 30", extension at 72ºC for 15", cycling 25 times, with a final extension at 72ºC for 5'. Amplicons were separated by gel electrophoresis and extracted by gel extraction using Invitrogen© QIAEX II (cat# 20021) kits according to the instructions of the manufacturer. Sanger sequencing was performed by the MBSU DNA Core at the University of Alberta.

3.4 Results and Discussion

3.4.1 Whole Genome Sequencing of Iron-reducing Cultures

The techniques involved in DNA extraction from active iron-reducing mixed cultures required extensive modification and optimization to attain an optimal input of unsheared DNA (Supplemental 3-2) for WGS inputs, minimizing the fragmentary effect of the lysis method while maximizing yield and quality of DNA. The unaltered mechanochemical lysis protocols generated DNA lengths of 5 kb unsuitable for downstream analysis, while magnetic methods failed to extract detectable quantities of DNA entirely, and lysis conditions had to be iterated

continuously to finally yield proper 15 kb DNA strands in suitable quantities for sequencing (Supplemental 3-2). Specifically, magnetic Dynabeads failed to extract DNA (Supplemental 3-2), while FastDNA in its unaltered protocol yielded sheared DNA to lengths of approximately 3-5 kb, and multiple optimizations of the FastDNA protocol were executed in several configurations to maximize final DNA length, including: decreasing the speed of the BeadBeater step, decreasing the time of the BeadBeater step, using the vortex rather than the BeadBeater, and decreasing the time of the vortex step (Supplemental 3-2). Ultimately, using vortex extraction at maximum speed for 5-10 minutes yielded optimal DNA lengths for metagenomic analysis.

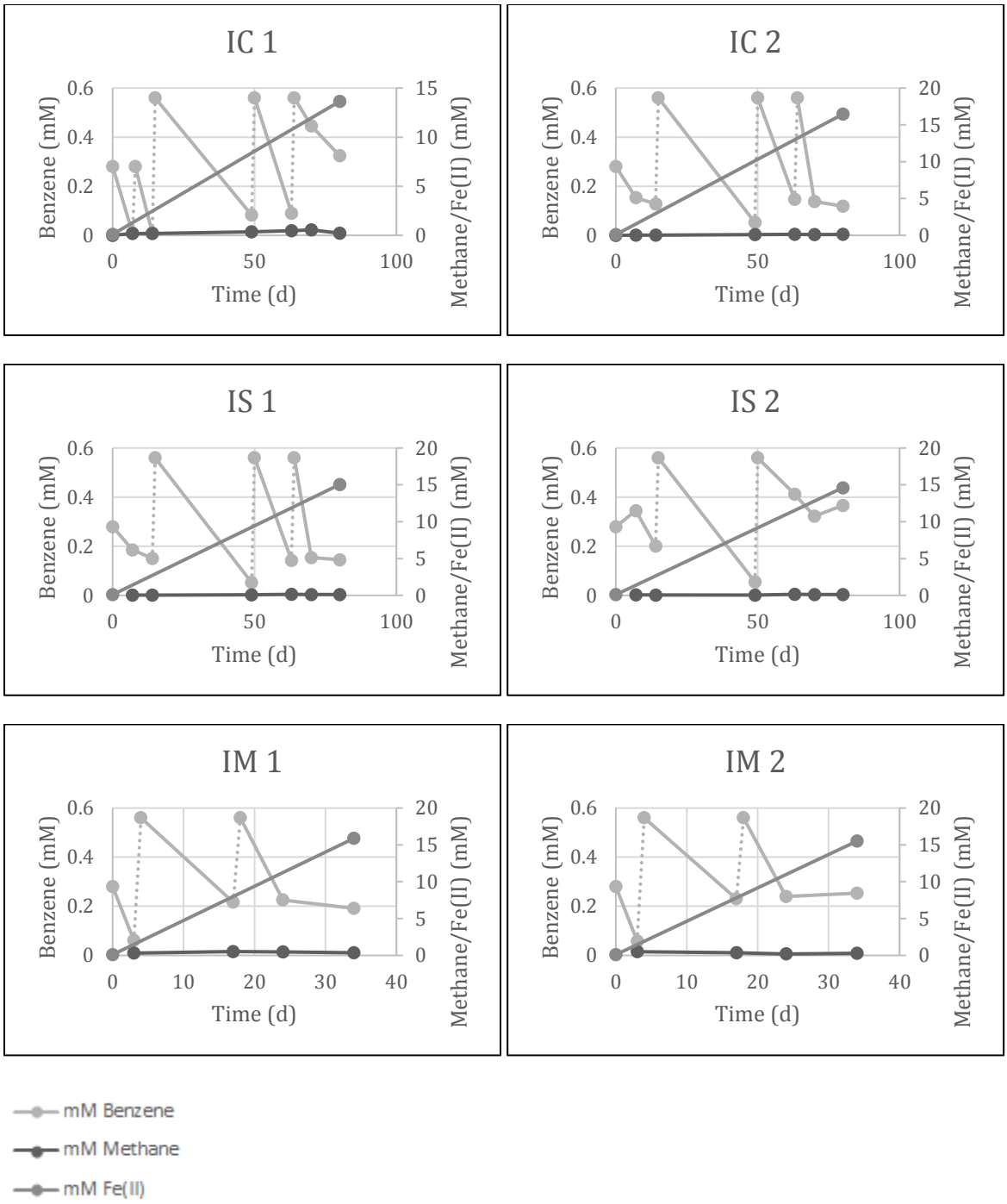

Figure 3-1. Degradation curves for Iron-reducing Cultures.

Degradation profiles of Iron-reducing cultures derived from Albertan sediments (Lee and Ulrich 2021) 80 days prior to metagenomics harvesting. Bi-letter designations represent redox condition and sediment type. IC = Iron-reducing Clay; IS = Iron-reducing Sand; IM = Iron-

reducing Mixed (cultures generated from a 1:1 volume mixture of IC and IS cultures). Each sediment was represented by two microcosm bottles.

Culture		Degradation Rate (μM/d)	Stoichiometric Ratio (mol Fe : mol C6H6)	Culture Volume (L)
IC	1	22.89	8.51	0.18
	2	21.36	11.00	0.18
IS	1	20.85	9.02	0.18
	2	11.73	17.80	0.18
IM	1	37.37	17.71	0.20
	2	36.35	17.78	0.20

Table 3-2. Degradation Metrics of Iron-reducing Cultures.

Degradation rates and stoichiometries of iron-reducing cultures, calculated from the final 80 days of cultivation prior to metagenomics harvesting. Bi-letter designations represent redox condition and sediment type. IC = Iron-reducing Clay; IS = Iron-reducing Sand; IM = Iron-reducing Mixed (cultures generated from a 1:1 volume mixture of IC and IS cultures). Each sediment was represented by two microcosm bottles.

	Clay	Sand	Mixed
bp Count	3,060,137,044	3,192,970,698	3,200,874,321
Sequence Count	17,851,868	18,367,102	18,564,253
Mean Seq Length	171 ± 41	174 ± 42	172 ± 41
Mean GC %	60 ± 10	58 ± 9	58 ± 10
Duplicate Reads	6,108,337	8,607,253	5,971,425
Quality Controlled bp Count	2,067,215,436	1,764,760,916	2,226,838,675
Quality Controlled Sequence Count	11,675,497	9,705,382	12,537,437
Quality Controlled Mean Seq Length	177 ± 46	182 ± 49	178 ± 46
Quality Controlled Mean GC %	59 ± 10	59 ± 10	58 ± 11
Protein Predictions	6,134,255	4,183,596	6,827,771
rRNA Predictions	57,396	45,096	52,878
Aligned Proteins	2,654,632	1,819,795	3,034,735
Aligned rRNAs	7,173	5,661	3,710
# Species	398	228	426

Table 3-3. Sequencing Metrics of Iron-reducing Cultures

Sequencing produced approximately 18 million reads from each sample (Table 3-3), of 171-174 bp in length and 58-60% GC content. Quality control protocols removed approximately 6-9 million reads, and alignments yielded 228-426 species and 1-3 million aligned protein features (Table 3-3). Rarefaction curves (Supplemental 3-3) demonstrated that the sequencing process sampled all microcosms extensively in terms of their intrasample alpha diversity, and beta diversity heatmaps and Newick trees indicated a greater similarity between Clay (IC) and Mixed (IM) samples with a divergence in the Sand (IS) microcosms, which may account for observed differences in culture activity.

WGS analysis of the IC, IS, and IM microcosms indicated a preponderance of bacterial *Geobacter metallireducens* GS-15 populations at 10.95, 23.27, and 11.73% respectively (Figure

3-2). Additional *Geobacter* species were also prominent in all samples, including *Geobacter sulfurreducens*, *Geobacter uraniireducens*, *Geobacter* sp. FRC-32, *Geobacter bemidjiensis*, and *Geobacter* sp. M18. Said species were not known to be primary degraders of benzene, but the high representation of *Geobacter* was reflected in the abundance of chemotaxis genes, of which *Geobacter* is particularly noted for among anaerobic organisms (Aklujkar, et al., 2009) (Supplemental 3-5). *G. metallireducens* GS-15 organisms have previously been reported to metabolize monoaromatics (Aklujkar, et al., 2009), but the putative benzene hydroxylases *gmet 0231* and *gmet 0232* were not found in the genetic milieu of either IC, IS, or IM cultures (Supplemental 3-5), distinguishing these *Geobacter* from those described in the literature as primary benzene degraders (Lovley D. R., et al., 1993), suggesting that these genes may not be necessary nor sufficient for anaerobic benzene degradation in iron-reducing cultures, and further implicating these genes as more likely to be regulators rather than hydroxylases (Zhang T. , et al., 2014) that are related to but not essential for benzene metabolism. Other genes associated with benzene degradation downstream of methylation such as *bss* (Heider, 2007; Leutwein & Heider, 2002; Leutwein & Heider, 2001; Leuthner & Heider, 2000) were absent in IC/IS/IM microcosms, as were the speculated benzene carboxylase genes described in nitrate-reducing cultures, *abcA* and *abcD* (Abu Laban, Selesi, Rattei, Tischler, & Meckenstock, 2010) (Supplemental 3-5).

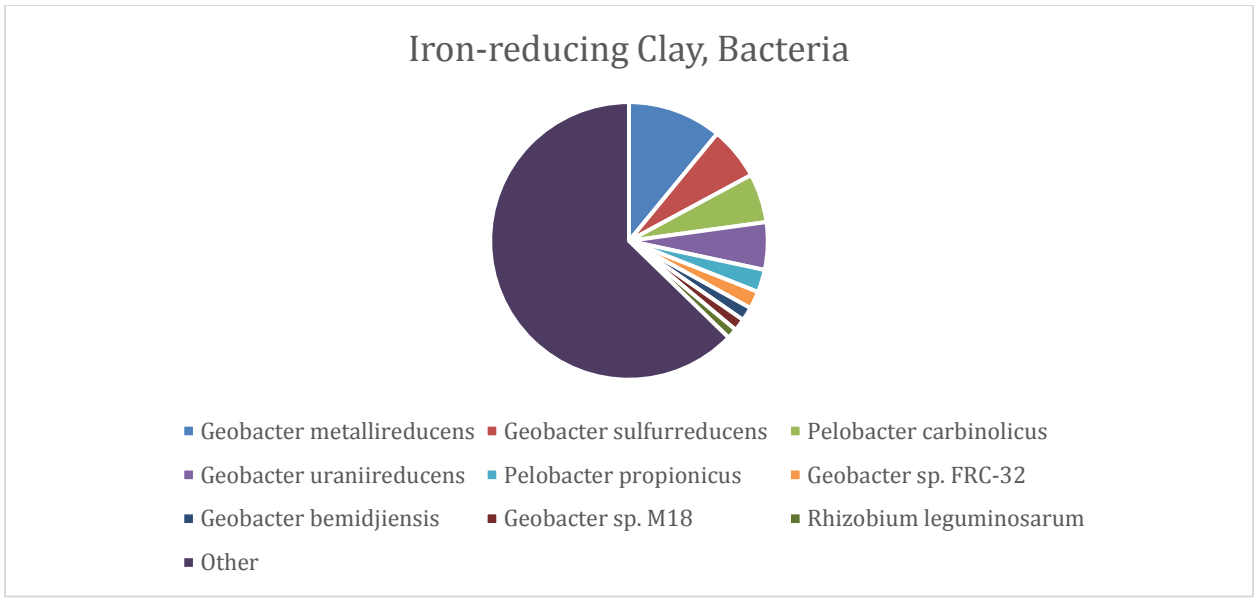
Iron-reducing Clay, Bacteria
Geobacter metallireducens
Geobacter sulfurreducens
Pelobacter carbinolicus
Geobacter uraniireducens
Pelobacter propionicus
Geobacter sp. FRC-32
Geobacter bemidjiensis
Geobacter sp. M18
Rhizobium leguminosarum
Other

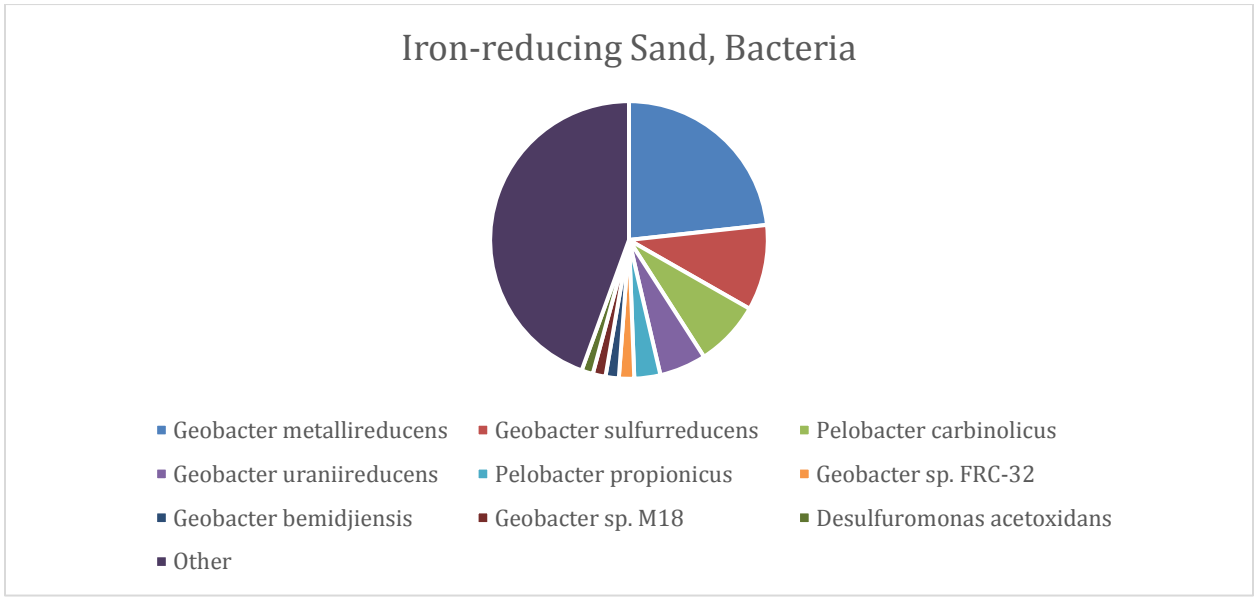
Iron-reducing Sand, Bacteria
Geobacter metallireducens
Geobacter sulfurreducens
Pelobacter carbinolicus
Geobacter uraniireducens
Pelobacter propionicus
Geobacter sp. FRC-32
Geobacter bemidjiensis
Geobacter sp. M18
Desulfuromonas acetoxidans
Other

Iron-reducing Mixed, Bacteria

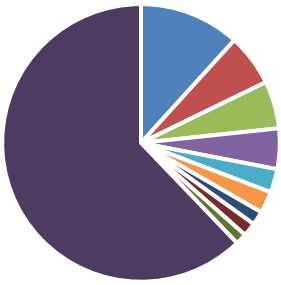

- Geobacter metallireducens
- Geobacter sulfurreducens
- Pelobacter carbinolicus
- Geobacter uraniireducens
- Pseudomonas stutzeri
- Pelobacter propionicus
- Bradyrhizobium japonicum
- Geobacter sp. FRC-32
- Geobacter bemidjiensis
- Other

Iron-reducing Clay, Archaea

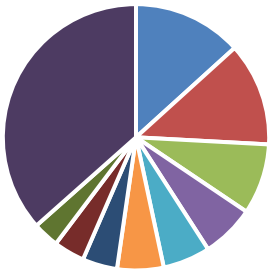

- Methanothermobacter thermautotrophicus
- Methanosarcina mazei
- Methanothermus fervidus
- Methanobrevibacter smithii
- Methanosarcina acetivorans
- Methanosarcina barkeri
- Methanobrevibacter ruminantium
- Methanococcoides burtonii
- Methanosaeta thermophila
- Other

Figure 3-2. Microbial Community Profiles of Iron-reducing Benzene-degrading Cultures.

Auxiliary taxa such as *Desulfuromonas* were also prominent in the cultures (Figure 3-2), and likely play a peripheral role (Luo, Devine, & Edwards, 2016). *Pelobacter* such as *Pelobacter propionicus* and *Pelobacter carbinolicus* were also present (Figure 3-2), and distinct from the specific acetogenic *Pelobacter acetylenicus* described in fermentative hydrocarbon-degrading cultures (Rabus, et al., 2016), but *Pelobacter*-related organisms have been well-documented in BTEX-degrading cultures as auxiliaries to primary degraders (Aburto-Medina & Ball, 2015; Vogt,

Kleinsteuber, & Richnow, 2011). Other documented degradation-associated taxa were present in high proportions as well, including *Methanosarcina* (Balch, Fox, Magrum, Woese, & Wolfe, 1979) and *Methanosaeta* (Cruz Viggi, et al., 2014). These two taxa dominated the archaeal reads (Figure 4-2), comprising 56.63-65.18% of archaeal populations, and have previously been observed in benzene-degrading cultures (Lee & Ulrich, 2021) so their presence was expected. Functionally, they may serve as Direct Interspecies Electron Transfer (DIET) partners for *Geobacter* species (Lu, Luo, Shao, & He, 2016; Wang, Li, Gao, & Wang, 2018), but more comprehensive analysis needs to be done to assert the existence of DIET phenomena in the iron-reducing cultures.

Because the analysis of the metagenomics data of these cultures was limited in scope, the functional primary activation gene for benzene degradation in these iron-reducing cultures remains unknown. Future efforts should be directed towards the creation of standardized genomic libraries for the cross-referencing of new data with previously-acquired metagenomic information for comparative analysis (Dias, et al., 2014; Ngara & Zhang, 2018), and should expand the scope of metagenomics analysis to generate associative biplots and metabolic pathway statistics that could illuminate the functional qualities of the iron-reducing cultures, which would provide further insight about these mixed cultures.

Ultimately, the isolation of *Geobacter metallireducens* from Albertan iron-reducing cultures was unsuccessful, and the identification of benzene activation genes in the metagenomes of active cultures was inconclusive. Nevertheless, *Geobacter metallireducens* remained the most prominent bacterial population in active iron-reducing benzene degrading cultures, and warrants further investigation into its potential role as the primary mediator of benzene oxidation in these consortia.

3.4.2 qPCR Analysis of Iron-reducing Cultures

The oligos designed to target *Geobacter*, *Methanosarcineae, Anaerolineae, Desulfuromonas,* and *Hydrogenophilaceae*, historically the 5 most abundant and literature-relevant OTUs in the Albertan iron-reducing cultures (Lee & Ulrich, 2021) were unable to achieve any observable amplification in qPCR analysis (data not shown). Oligos targeting putative benzene-related genes *gmet 0231, gmet 0232,* and *ppsA* in *Geobacter* (Zhang T. , et al., 2014) also failed to amplify, even when melting temperatures were adjusted for annealing optimization (data not shown). Due to time constraints, further attempts to troubleshoot these primers could not be made. These oligos were intended to serve as tools to correlate culture activity with copy numbers of benzene degraders or benzene degrading enzymes, and currently none of the synthesized primers have any demonstrated ability to estimate culture activity as bioindicator genes in the iron-reducing cultures tested.

3.4.3 *Geobacter* Isolation

The isolation of *Geobacter* proceeded according to the protocols described previously by the Lovley group (Lovley & Phillips, 1986; Lovley, et al., 1989), but failed to isolate *Geobacter*. These series of experiments utilized a two-step process of isolation, beginning with nitrate-reducing conditions with acetate as a carbon source. Nitrate-reducing slant tubes (agar medium, acetate carbon source) yielded growth after 14 days of incubation at 30ºC (Supplemental 3-1), as did nitrate-reducing slant tubes using benzene as a carbon source. Iron-reducing slant tubes and Petri dishes failed to yield growth, whether using agar or agarose as growth medium substrata. Six colonies resulting from nitrate-reducing slant tubes were subjected to Colony PCR. All colonies shared similar morphologies and 16S rRNA sequences. These sequences did

not align to any known taxa at species-level, and only shared 96% homology to bacteria found in miscellaneous environmental samples with little overt functional relation. These include an uncultured bacterium LMP12_16S_OTU_0019 from an Illinois wetland (KY802203.1), a calcium-precipitating *Terrabacter terrigena* from a karst cave in Hungary (MT415115.1), and a Nigerian *Janibacter indicus* related to kerosene biodegradation (MN515054.1). Homology to *Geobacter metallireducens* 16S rRNA genes (JQ799138.1) only reached 86% similarity, far beneath species-level identification prerequisites. After these series of isolations, time and equipment constraints necessitated a cessation of experimental attempts, although future research may implement Petri dishes sealed within a specialized anaerobic jar apparatus and saturated with atmospheric benzene vapour to provide a more ideal growing condition for *Geobacter* (Suri, Gassara, Stanislav, & Voordouw, 2019).

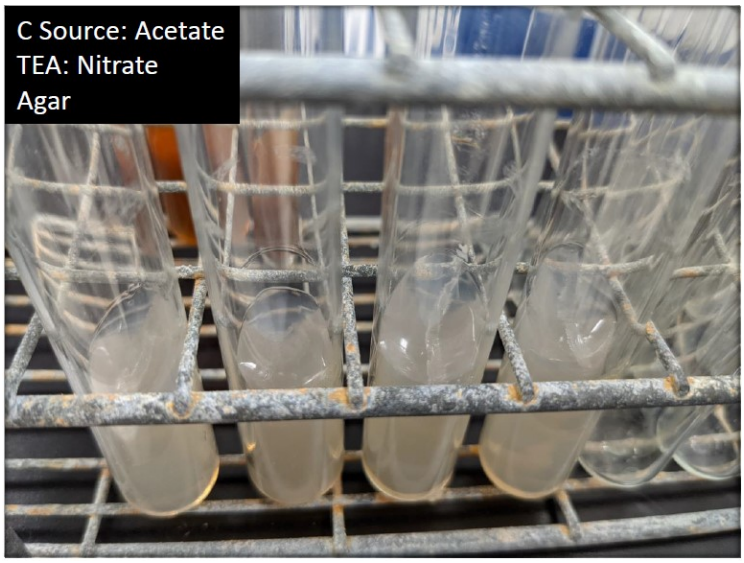

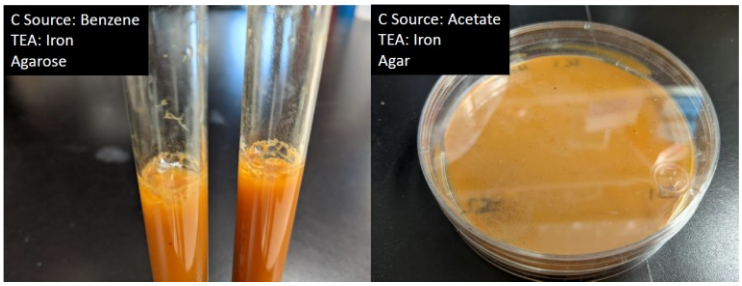

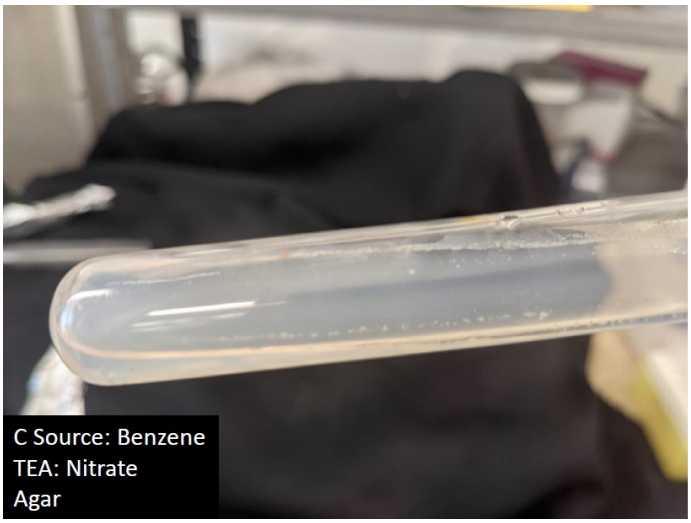

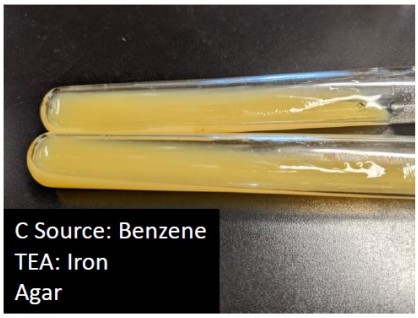

Supplemental 3-1. Isolation attempts for Geobacter metallireducens.

Isolations were attempted using various configurations of carbon sources, TEAs, medium substrata, and glassware/plasticware. Carbon sources included acetate or benzene, TEAs

included nitrate or iron, media included agar or agarose, and glassware/plasticware included Hungate tubes or Petri dishes.

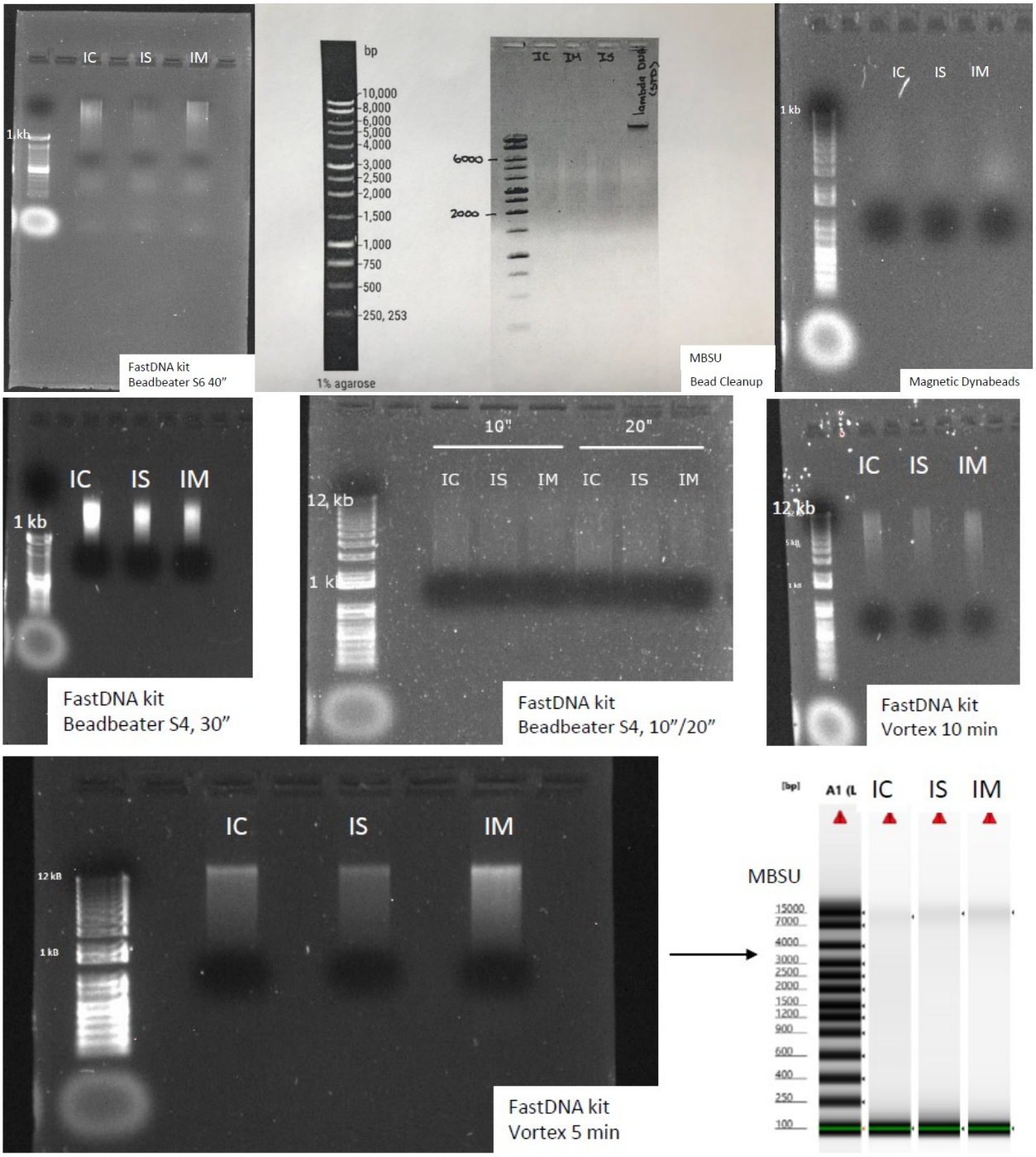

Supplemental 3-2. DNA Extraction Optimization of Iron-reducing Benzene-degrading Cultures.

Multiple extraction techniques were tested with the aim of attaining non-sheared DNA. Two kits were used: FastDNA for Soil (MolecularBio) and Dynabeads (Invitrogen). FastDNA extraction protocols utilize the BeadBeater device, set at speeds of 4-6 m/s, or the vortex at max speed. IC = iron clay; IS = iron sand; IM = iron mixed. Final image (bottom-right) represents the final sequenced samples as visualized by the Tapestation apparatus.

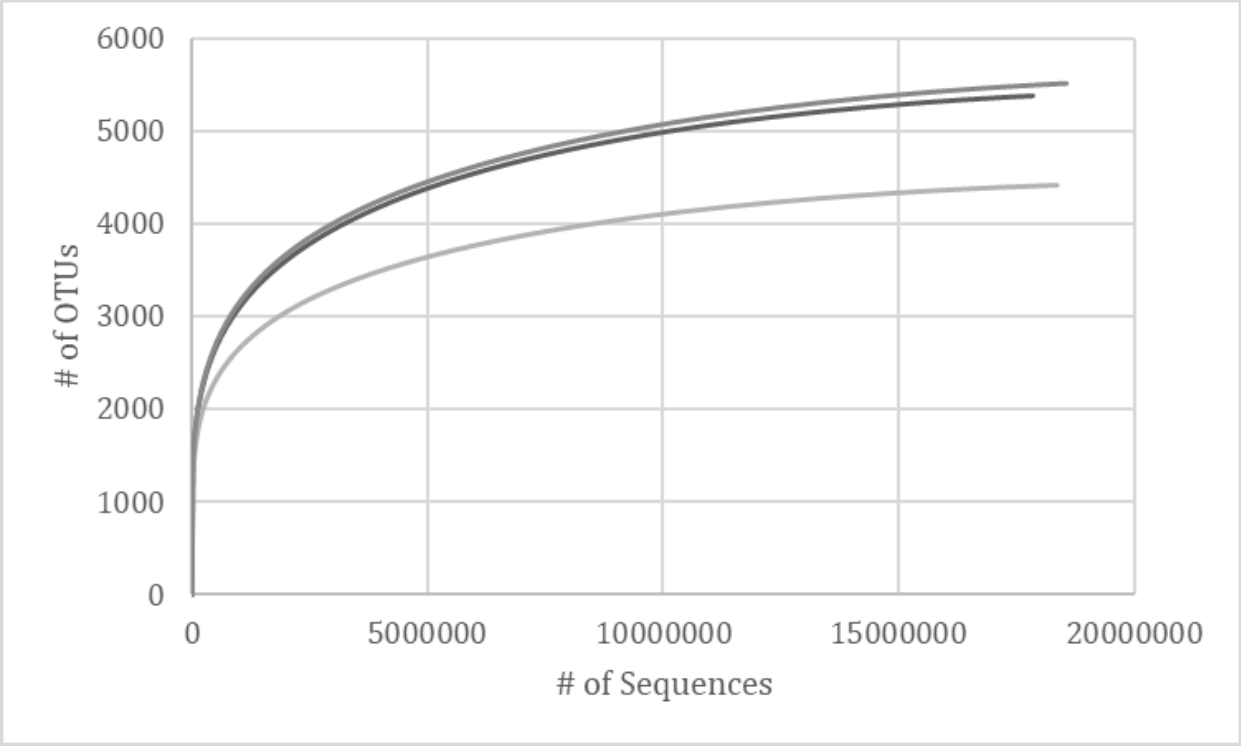

Supplemental 3-3. Rarefaction Curves for Iron-reducing Cultures.

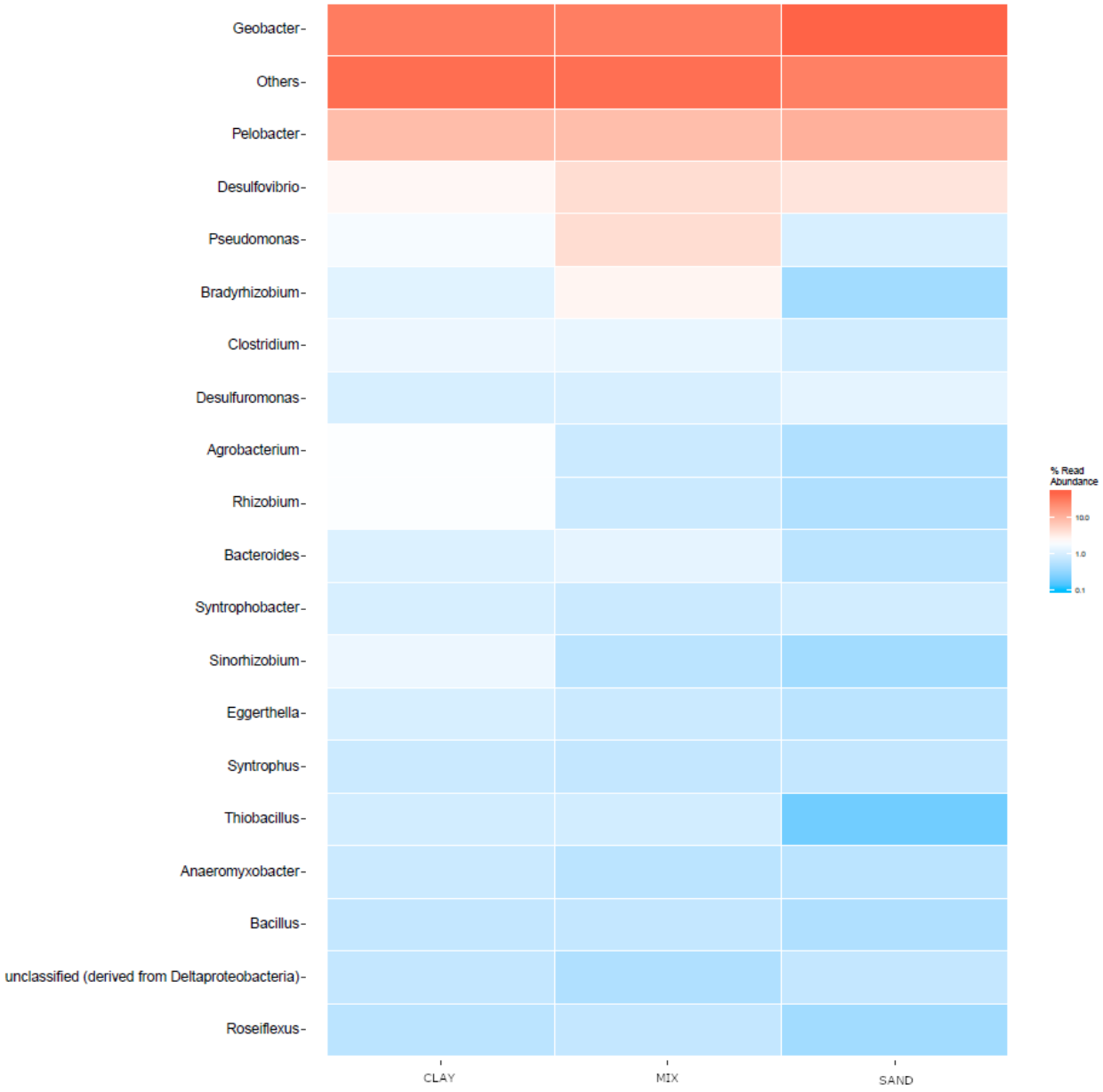

Supplemental 3-4. Heatmap Visualization of Iron-reducing Cultures.

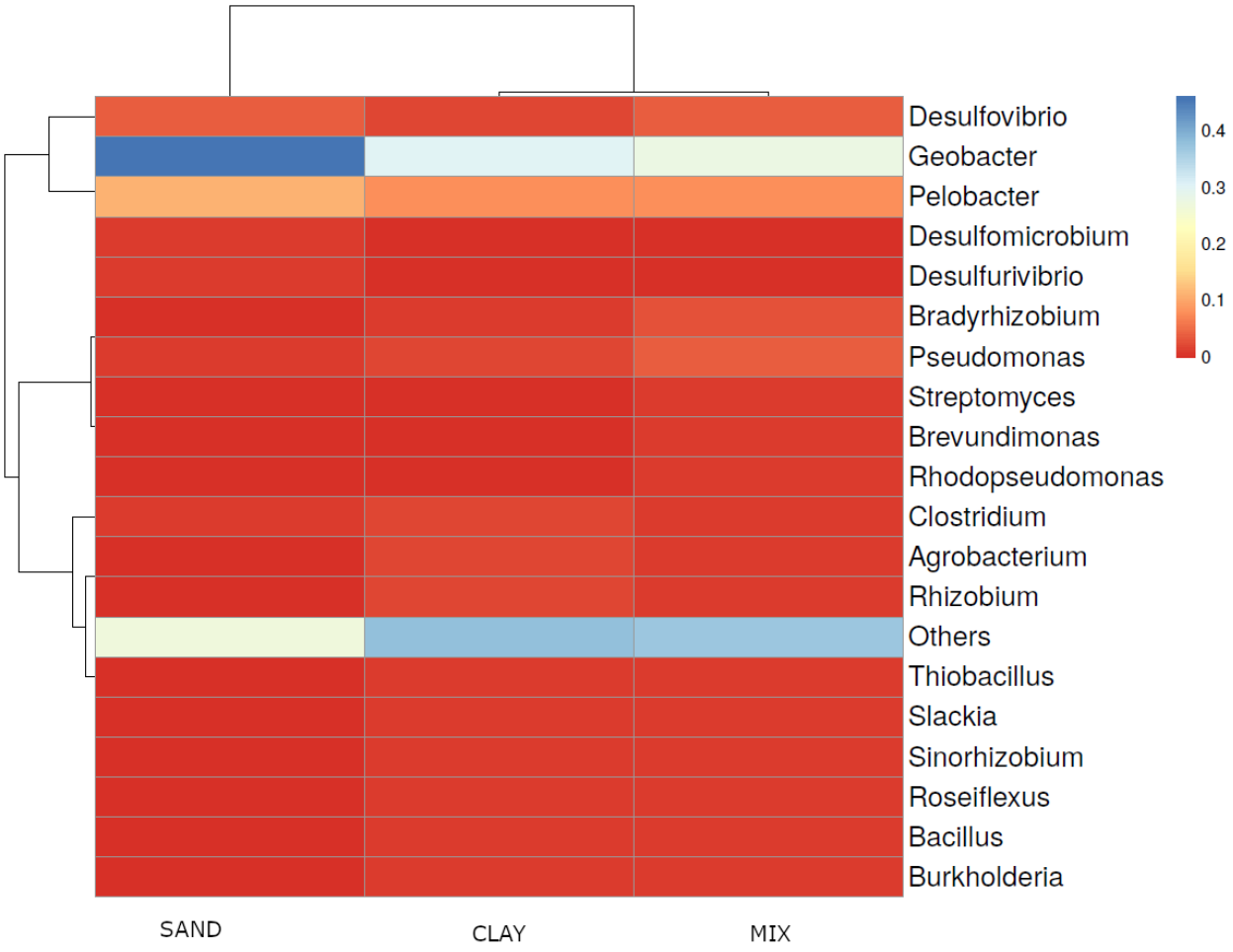

Supplemental 3-5. Genetic Analysis of IC, IS, and IM Microcosms.

Metagenomic analysis available in Metagenomics.xlsx.

4 Enhancing Iron Dissolution in Iron-reducing Benzene Cultures with External Chelators

4.1 Abstract

Previously, iron-reducing benzene degrading microcosms established from Albertan sediments, although capable of robust and repeated benzene removal, exhibited iron stoichiometries incongruous with theoretical values. Because the terminal electron acceptor used in these cultures was an insoluble ferric oxide known as ferrihydrite, it was reasoned that bioavailability was the limiting factor for iron-reduction in the microcosms, and that amendments that could mediate the dissolution of iron oxides could promote iron-reduction processes thereby. This study evaluated the efficacy of chelators such as oxalic acid, a low molecular weight organic acid (LMWOA) and its potential synergy with a siderophore analogue, acetohydroxamic acid (aHA), in comparison with a chelator with known capability for promoting benzene oxidation in iron-reducing cultures, nitrilotriacetic acid (NTA). Oxalic acid and aHA was found to effectively enhance the performance of iron-reducing benzene cultures, to a degree comparable to NTA, and both chelators were associated with the expansion of the reported primary benzene degrader *Geobacter metallireducens*. Because of the potential carcinogenicity of NTA (Canada, Nitrilotriacetic Acid, 1990), the efficacy of LMWOA and siderophore-promoted iron dissolution could be more amenable to remediation strategies, and inform biostimulation efforts in the *ex situ* culturing of iron-reducing microcosms.

4.2 Introduction

Benzene is a priority contaminant known for its recalcitrance, solubility in water, and carcinogenicity (Canada Environment & Canada Health and Welfare, 1993), and the difficulty of its bioremediation is exacerbated by the tendency for contaminated sites to become exhaust oxygen and become anaerobic (Weelink, van Eekert, & Stams, 2010), which may include the use of nitrate, sulfate, or carbon dioxide as an electron acceptor. This study focusses on ferric iron processes; besides being a terminal electron acceptor, iron is essential for the activity of cytochromes, ferredoxins, and iron-sulfur metalloproteins, and is crucial for the activity of iron-reducing organisms (Bertrand, et al., 2015). Iron typically forms oxyhydroxide compounds and is typically associated with mineral structures: in poorly-drained soils, ferric iron usually exists as lepidocrocite, maghemite, magnetite, ferrihydrite, and ferroxite (Cornell & Schwerfmann, 2003), while in well-drained soils, ferric iron typically exists as crystalline goethite and hematite (Cornell & Schwerfmann, 2003). However, these iron oxides have very low solubility at neutral pH (Schwertmann & Cornell, 2008) and are therefore very limited in bioavailability for dependent microorganisms (Lindsay, 1988).

Iron-reducing benzene degradation has a very heavy stoichiometric dependence on ferric iron ions (Vogt, Kleinsteuber, & Richnow, 2011), so the low bioavailability of ferric iron is a major hindrance to this respiratory group, even though ferric iron is a potent terminal electron acceptor that has a relatively high redox potential (ΔE^0 = +36 V) (Silva, Ruiz-Aguilar, & Alvarez, 2005; Lueders, 2017). The high concentrations of iron in the natural environment, the relatively low toxicity of iron-reduction byproducts, and the high potential energy yield makes iron-reduction an ideal respiratory strategy for anaerobic benzene degradation. It is therefore imperative to

investigate novel means to induce the dissolution of ferric iron from iron oxides and maintain a robust pool of iron for respiration during the oxidation of benzene in a laboratory setting.

Previous experiments have demonstrated the efficacy of organic acid chelators such as humic acids, EDTA (Ethylenediaminetetraacetic acid), and NTA (nitrilotriacetic acid) for enhancing metabolic activity (Lovley, Woodward, & Chapelle, 1994; Lovley, Woodward, & Chapelle, 1996; Lovley D. R., Coates, Woodward, & Phillips, 1995; Lovley D. R., Coates, Blunt-Harris, Phillips, & Woodward, 1996) in those iron-reducing cultures. Furthermore, previous abiotic experiments have also demonstrated the ability of siderophores, small secreted biological chelators (Kraemer, 2004) that can exhibit plurispecific activity (D'Onofrio, et al., 2010; Guan, Kanoh, & Kamino, 2001), to solubilize iron minerals (Dhungana, Anthony, & Hersman, 2007) and synergistically augment the iron dissolution capabilities of organic acids (Loring, Simanova, & Persson, 2008; Wang, Schenkeveld, Kraemer, & Giammar, 2015; Reichard, Kretzschmar, & Kraemar, 2007). Siderophore concentrations in sediments can range from approximately 8-1800 μM (Hersman, Lloyd, & Sposito, 1995), but alone, they are less efficacious at iron dissolution, most likely due to steric hindrance (Reichard, Kretzschmar, & Kraemar, 2007), while low molecular weight organic acids (LWMOAs) alone demonstrate high turnover (Xu & Gao, 2008) and relatively lower complex formation rate constants. However, a synergy exists between LWMOAs and siderophores, as they can functionally complement each other (Lin, et al., 2018) to enhance iron dissolution; this effect has been seen with siderophores in combination with complex organic matter as well (Mikutta & Kretzschmar, 2008), and iron that is bound by heterogenous high molecular weight organic acids have been observed to be bioavailable for siderophore capture (Kuhn, Maurice, Neubauer, Hofmann, & von der Kammer, 2014). However, no study has yet attempted to use siderophores and organic acids in combination to enhance contaminant degradation in an iron-reducing context with living microbial cultures.

All ferric iron oxides have Euclidean octahedral geometries (Cornell & Schwerfmann, 2003) with six oxygen or hydroxide ions. This structure is not unique to iron, and can be formed with multiple ions; furthermore, non-iron metallic cations can be incorporated into the ferric oxide structure. It is the arrangement of the octahedra that determines the classification of these ferric oxides. Ferrihydrite, for example, is very poorly crystalline - it resembles hematite, and is characterized by a set of octahedra with radial symmetry along the c plane, but with substitutions of oxygen with water and hydroxide, or by the absence of some oxygen components entirely. Ferrihydrite is therefore ideal for iron-reduction culturing because its lack of crystallization prevents formation of large matrices and maximization of surface area (200 m^2 g^{-1}) (Cornell & Schwerfmann, 2003), a property which promotes biological activity. Neither is ferrihydrite a synthetic artifact; it is a common naturally-occurring mineral in drainage systems, water body sediments, and hydromorphic soils (Cornell & Schwerfmann, 2003)

The goal of this study is to evaluate the combined effect of iron-chelating ligands and organic acids on the dissolution of ferrihydrite and the performance of iron-reducing, benzene-degrading cultures. Iron-reducing cultures established in previous scholarship have identified *Geobacter metallireducens* (Zhang, Bain, Nevin, Barlett, & Lovley, 2012; Abu Laban, Selesi, Rattei, Tischler, & Meckenstock, 2010) as a primary benzene degrader, and have quantified degradation rates of approximately 0.006 mM d^{-1} (Kunapuli, Lueders, & Meckenstock, 2007). The cultures used in this study, inoculated by sediments from a mine-lease site in Northern Alberta as described previously (Holden, Donahue, & Ulrich, 2011), were known to contain these community members as well. Based on previous studies (Holmen, Sison, Nelson, & Casey, 1999), the organic iron complexes may also affect secondary members of the microbial profile in conjunction with the primary degrader *Geobacter metallireducens*, which utilizes ferric iron through direct contact (Childers, Ciugo, & Lovley, 2002; Reguera, et al., 2005). Chelators, whether they be bona fide siderophores or organic acids, would be expected to generate a

soluble pool of iron from iron oxide, as ferric iron bound to organic matter is readily accessed by siderophores due to their high binding constants (Kuhn, Maurice, Neubauer, Hofmann, & von der Kammer, 2014; Schwabe, Anke, Szymanska, Wiche, & Tischler, 2018). The combination of siderophore chelators and LMWOAs with regards to iron dissolution introduces a number of interacting chemical mechanisms, including complexation of iron ions, coprecipitation of insoluble forms, and adsorption of organic acids onto iron aggregates (Kleber, et al., 2015; Akafia, Harrington, Bargar, & Duckworth, 2014; Kang, et al., 2019), but nevertheless, the chelators would be expected to synergistically enhance iron mineral weathering (Cheah, Kraemer, Cervini-Silva, & Sposito, 2003; Saad, et al., 2017; Cervini-Silva & Sposito, 2002), which is a principal mediating factor in promoting benzene degradation in iron-reducing cultures (Lovley & Woodward, 1996), although as noted, complex organic matter in the mixed culture may protect against siderophore-based iron-oxide dissolution (Poggenburg, Mikutta, Liebmann, Koch, & Guggenberger, 2018).

4.3 Methods

4.3.1 Culturing of Iron-reducing Benzene Degraders

Iron-reducing cultures were enriched from clay and sand sediments from the Athabasca region of Alberta as described previously (Holden, Donahue, & Ulrich, 2011). Cultures were infused with 40 mL of mineral media (Edwards & Grbic-Galic, 1994), and amended with 2% v/v insoluble Fh ($(Fe^{3+})_2O_3 \bullet 0.5H_2O$, ferrihydrite) and 0.28 µM liquid concentration of benzene. Methanogenic cultures did not receive Fh. Maintenance cultures were contained within sterile 250 mL bottles and sealed with Mininert™ caps, and all manipulations were performed within an

anaerobic chamber (Coy Laboratory Products, Madison, WI) (atmosphere 5/5/90% v/v/v $H_2/CO_2/N_2$). Microcosms were stored in anaerobic conditions at 25℃ in the absence of light. Actively degrading iron-reducing cultures were used for this study, with degradation rates of 1.27E-02 mM d^{-1}. Methanogenic cultures demonstrated active degradation rates of 5.08E-03 mM d^{-1}. These cultures were diluted 1:10 v/v with anaerobic mineral media and monitored within a single degradation cycle over a 112-day period. Heat sterilization was performed via three 90 min autoclave cycles.

Twenty-four microcosms were established, each with 40 mL of culture sealed within serum bottles with butyl stoppers and amended with neat benzene to an initial liquid concentration of 0.28 mM. Acetohydroxamic acid (aHA) (Costa, et al., 2020) was used as an analogue for hydroxamates like desferrioxamine B (DFO) (Holmen, Sison, Nelson, & Casey, 1999), a commercially available and extensively studied trihydroxamate siderophore (Crumbliss and Harrington 2009). Experimental chelator concentrations of 2 mM were identical to the concentrations of nitrilotriacetic acid (NTA) used in previous experiments with benzene-degrading iron-reducing cultures (Lovley, Woodward, & Chapelle, 1996).

Table 4-1. Methanogenic and Iron-reducing Sample Treatment Matrix.

	Benzene		Killed Control		No-benzene Control	
Untreated	M H2O B	I H2O B	M H2O K	I H2O K	M H2O B-	I H2O B-
Nitrilotriacetic Acid	M NTA B	I NTA B	M NTA K	I NTA K	M SYN B-	I NTA B-
aHA + Oxalic Acid	M SYN B	I SYN B	M SYN K	I SYN K	M SYN B-	I SYN B-

Microcosms were established in triplicates: M = methanogenic; I = iron-reducing. Benzene was amended to a liquid concentration of 0.28 mM: B = benzene; K = killed control; B- = benzene-free control. Chelators were amended to a final concentration of 2 mM in equal volumes: H2O = untreated; NTA = nitrilotriacetic acid; SYN = synergy of acetohydroxamic acid and oxalic acid, 1 mM each.

4.3.2 C_6H_6 and CH_4 Analysis

Benzene and methane quantification were performed via headspace analysis with an Agilent™ 7890A FID (flame ionization detector) and an HP-1 methylsiloxane (30 m x 320 µm x 0.25 µm) column. The method was as follows: the injector was set to 17.735 psi with septum purge flow 3 mL/min, the column was set to 350℃ 4.5 mL/min, the oven was set to 50℃ 4.5 min, and the detector was set to 250℃ and 45 mL/min hydrogen, 450 mL/min air, 25 mL/min helium. Injections used 100 µL manual headspace volumes extracted with gas-locking syringes (Sigma-Aldritch™ VICI Series A-2) under anaerobic conditions. The error for C_6H_6 concentration measurements was ±6.24%. Calibration was performed with external standards and the detection limit was 0.01 mM benzene and 0.03 mM methane. Daily rates were determined by calculation of total removal over the total number of days of culturing. Stoichiometric values were determined by calculating the molar ratios of Fe(II) or methane to the quantity of benzene

degraded, or by calculating the molar ratios of the chelators to the quantity of benzene degraded.

Equation 4-1. Chemical Redox Equations for Benzene, NTA, aHA, and Oxalic Acid.

Methanogenic Half-reaction

$$CO_2 + 6H^+ + 8e^- \leftrightarrow CH_4 + 2H_2O$$

Iron-reducing Half-reaction

$$Fe^{3+} + e^- \leftrightarrow Fe^{2+}$$

Benzene:

Half-reaction

$$C_6H_6 + 18H_2O \leftrightarrow 6HCO_3 + 36H^+ + 30e^-$$

Methanogenesis

$$C_6H_6 + 3.75CO_2 + 10.5H_2O \rightarrow 6HCO_3 + 13.5H^+ + 3.75CH_4$$

Iron-reducing

$$C_6H_6 + 30Fe^+ + 18H_2O \rightarrow 6HCO_3^- + 36\,H^+ + 30Fe^{2+}$$

Nitrilotriacetic Acid (NTA):

Half-reaction

$$C_6H_9O_6N + 13H_2O \leftrightarrow 6HCO_3^- + HNO + 28H^+ + 18e^-$$

Methanogenesis

$$C_6H_9O_6N + 8.5H_2O + 2.25CO_2 \rightarrow 6HCO_3^- + HNO + 2.25CH_4 + 14.5H^+$$

Iron-reducing

$$C_6H_9O_6N + 13H_2O + 18Fe^{3+} \rightarrow 6HCO_3^- + HNO + 28H^+ + 18Fe^{2+}$$

Acetohydroxamic Acid (aHA):

Half-reaction

$$C_2H_5O_2N + 5H_2O \leftrightarrow 2HCO_3^- + HNO + 12H^+ + 16e^-$$

Methanogenesis

$$C_2H_5O_2N + H_2O + 2CO_2 \rightarrow 2HCO_3^- + 2CH_4 + HNO + 2CH_4$$

Iron-reducing

$$C_2H_5O_2N + 5H_2O + 16Fe^{3+} \rightarrow 2HCO_3^- + HNO + 12H^+ + 16Fe^{2+}$$

Oxalic Acid:(OXA):

Half-reaction

$$C_2H_2O_4 + 2H_2O \leftrightarrow 2HCO_3^- + 2H^+ + 4e^-$$

Methanogenesis

$$C_2H_2O_4 + H^+ + 0.5CO_2 + H_2O \rightarrow 0.5CH_4 + 2HCO_3^-$$

Iron-reducing

$$C_2H_2O_4 + 2H_2O + 4Fe^{3+} \rightarrow 4Fe^{2+} + 2HCO_3^- + 2H^+$$

Saprophytic:

Half-reaction

$$C_5H_7O_2N + 14H_2O \leftrightarrow 5HCO_3^- + HNO + 29H^+ + 24e^-$$

Methanogenesis

$$C_5H_7O_2N + 3CO_2 + 8H_2O \rightarrow 5HCO_3^- + HNO + 11H^+ + 3CH_4$$

Iron-reducing

$$C_5H_7O_2N + 14H_2O + 24Fe^{3+} \rightarrow 5HCO_3^- + HNO + 29H^+ + 24Fe^{2+}$$

4.3.3 Fe(II) Quantification

At 112 days of monitoring, when benzene levels reached 10% of initial concentrations, samples were taken to quantify the generation of ferrous iron and relate these quantities to benzene removal metrics for stoichiometric analysis. 1 mL of culture volume was extracted anaerobically and filtered through a 0.2 μm syringe filter, and the filtrate was diluted 5000x with 1% nitric acid. Soluble iron was analyzed using ICP-MS (Inductively Coupled Plasma Mass Spectrometry) (iCap Q, ThermoScientific®) with appropriate internal and external standards.

4.3.4 16S rRNA Community Analysis and Population Quantification

At day 112 of culturing, when benzene levels reached 10% of initial concentrations, 1 mL of the culture volume for the highest-performing cultures was centrifuged at 8000 xg for 3 min, and

DNA extraction on collected biomass was performed with FastDNA™ kits as per manufacturer instructions. Primary PCR of the V3-V4 region of the 16S rRNA gene was performed by Phusion™ polymerases using the following oligonucleotides, specific for *Archaea* and *Bacteria*: 16S rRNA V3-4 IL-F (TCG TCG GCA GCG TCA GAT GTG TAT AAG AGA CAG CCT ACG GGN GGC WGC AG) and 16S rRNA V3-4 IL-R (GTC TCG TGG GCT CGG AGA TGT GTA TAA GAG ACA GGA CTA CHV GGG TAT CTA ATC C). PCR cleanup was performed by QIAEX™ kits (Qiagen™), and prepared samples were delivered to TGAC DNA core at the University of Alberta for Illumina-MiSeq™ analysis. All kit-based techniques were performed as directed by the manufacturer. Raw fastq file reads were processed by the Mothur process for 16S rRNA community analysis, with DNA library preparation and analytic workflows adapted from previously-developed pipelines (Schloss, et al., 2009). Visualizations were performed by Krona (Ondov, Bergman, & Phillippy, 2013), Phinch (Bik and Pitch Interactive, n.d.), and MEGA7 (Kumar, Stecher, & Tamura, 2016). Data are available on GenBank, Accession #PRJNA821360.

4.4 Results and Discussion

4.4.1 Benzene Removal Rate and Iron/Methane Stoichiometry

Although previously investigated by researchers, the iron dissolution effects of the chelators in this system were verified abiotically prior to culture experiments (Supplemental 4-3) using phosphate-buffered media and 10% v/v ferrihydrite to replicate experimental conditions. Chelators behaved as expected, with NTA causing the greatest dissolution of ferric iron, while methanol controls had little influence on soluble iron concentrations. The reported synergistic effect between aHA and OXA was also observed, and the amendments tested did not cause

any alteration in pH at experimental concentrations of 2 mM. Heat-killed controls also showed negligible benzene loss over the experimental period, while benzene-free controls showed methane production disproportionate to stoichiometric values as expected from amendment consumption alone, suggesting a substantial saprophytic presence in the consortia that may be due to decay, which expands as the rate of substrate consumption declines (Rittmann & McCarty, 2001) (Supplemental 4-1, Supplemental 4-2). This speculation was supported by the stoichiometric ratios of methane in the live experimental cultures (Table 4-2), which were higher than theoretical values where only the methane contributions of the tested amendments were accounted for (Equation 4-1). Iron-reducing cultures, as expected, exhibited less stoichiometric methane generation than methanogenic cultures, and relatively low iron stoichiometries when compared to historical values (Table 4-2) (Lee & Ulrich, 2021). Although iron stoichiometric ratios aligned well with theoretical values in iron-reducing cultures treated with NTA (Table 4-2), there was minimal soluble iron detected in both the aHA and oxalic acid-treated cultures as well as the untreated cultures. Though treated samples exhibited higher iron stoichiometric ratios than untreated samples as predicted, these results suggest an greater basal prominence of methanogenesis in the chelator-treated cultures than was expected.

Table 4-2. Stoichiometric Ratios in Methanogenic and Iron-reducing Cultures.

Culture	Chelator	Stoichiometry (x mol : mol C6H6)	
		Methane	Ferrous Iron
Methanogenic	H2O	7.95	n/a
	NTA	3.95	n/a
	SYN	7.71	n/a
Iron-reducing	H2O	3.15	2.69
	NTA	0.08	29.72
	SYN	3.49	3.61

Chelator conditions are represented by tri-letter designations. H2O = water, untreated; NTA = nitrilotriacetic acid, positive control; SYN = synergy of aHA (acetohydroxamic acid) siderophore analogue and OXA (oxalic acid) low molecular weight organic acid. Cultures were amended with equal volumes of chelator in water and maintained anaerobically.

Nevertheless, both the positive control NTA and the experimental synergistic treatment SYN (aHA + OXA) amendments had a statistically significant ($P < 0.05$) positive effect on benzene removal in iron-reducing cultures (Figure 4-5, 3-6). NTA (nitrilotriacetic acid) had the most marked effect on iron-reducers as expected (Lovley, Woodward, & Chapelle, 1994), and its potency as demonstrated in abiotic conditions was borne out biotically, with NTA treatments having the greatest effect on benzene-degrading activity (Figure 4-6, Supplemental 4-3). The synergy of aHA and oxalic acid was also effective at promoting benzene removal, although not to the extent of NTA (Figure 4-6). Conversely, neither of the chelator treatments had any statistically significant effect on methanogenic cultures, and benzene degrading activity was not altered regardless of the presence of NTA or aHA and oxalic acid (Figure 4-4, 3-6). Future studies may elect to interrogate higher concentrations of chelators and establish a concentration-dependent effect, although iron dissolution would be expected to show

diminishing returns upon increases in chelator concentrations, most likely due to depletion of surface complexation opportunities (Liermann, Kalinowski, Brantley, & Ferry, 2000). Other studies may also investigate the connection of chelators with direct interspecies electron transfer (DIET), which is known to be mediated through contact between *Geobacter* and its microbial partners via organic acids (Lovley D. R., 2017).

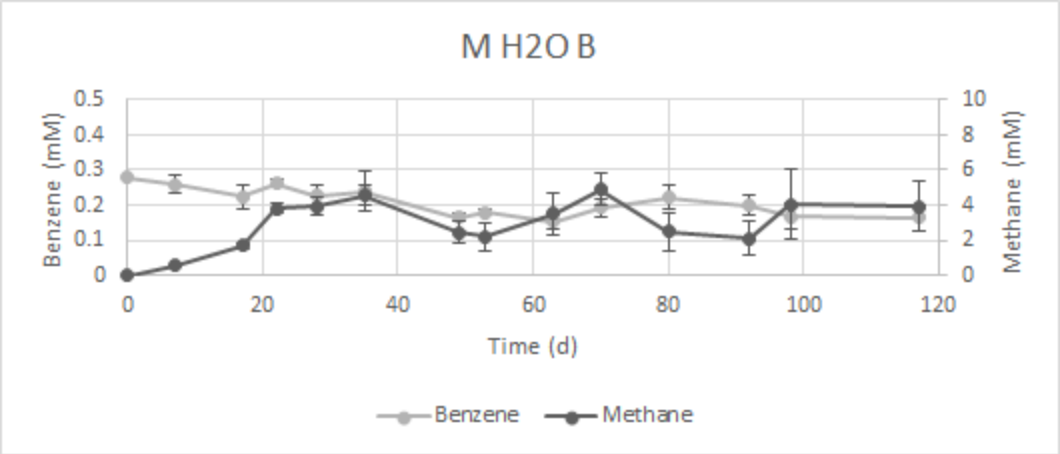

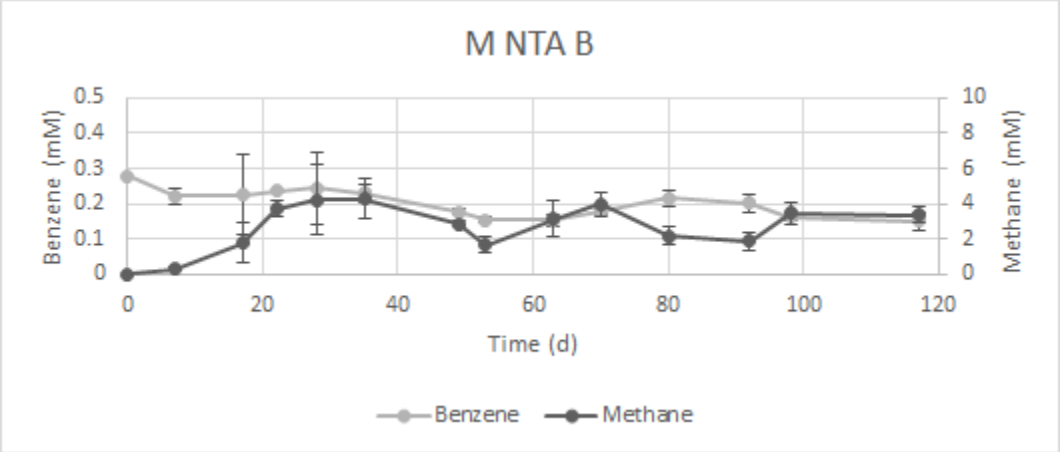

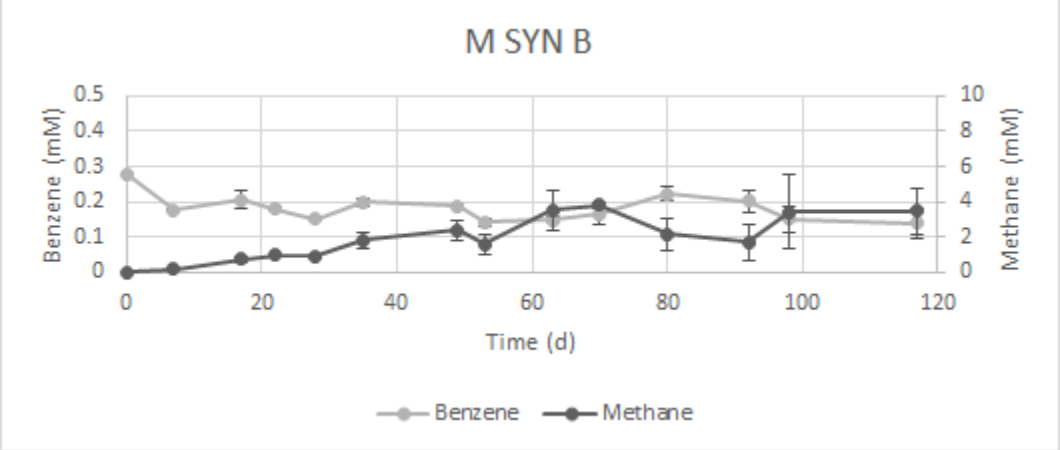

Figure 4-1. Degradation Curves for Methanogenic Culture Conditions.

Benzene and methane concentrations were determined by headspace GC. Datapoints were averaged between triplicates. M = methanogenic; H2O = water/untreated; NTA = nitrilotriacetic

acid; SYN = synergy, aHA + oxalic acid; B = benzene. Error bars represent one standard deviation.

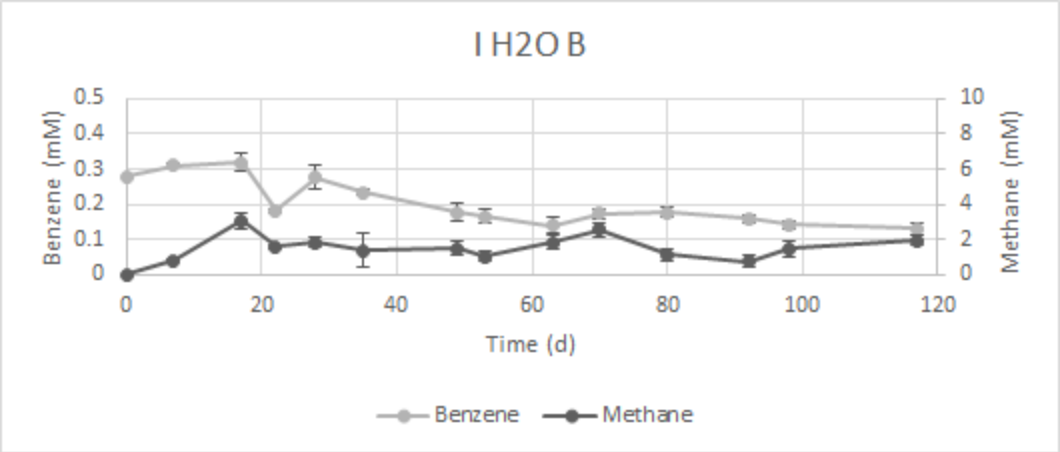

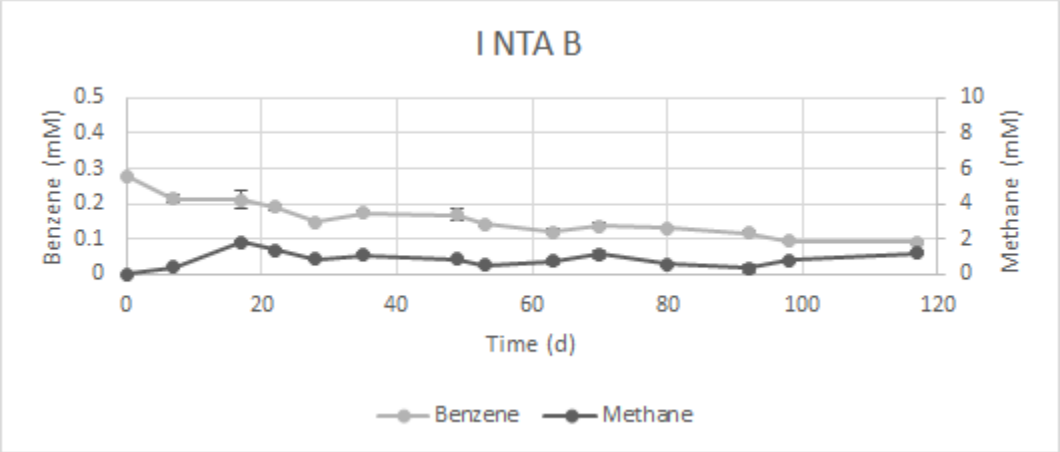

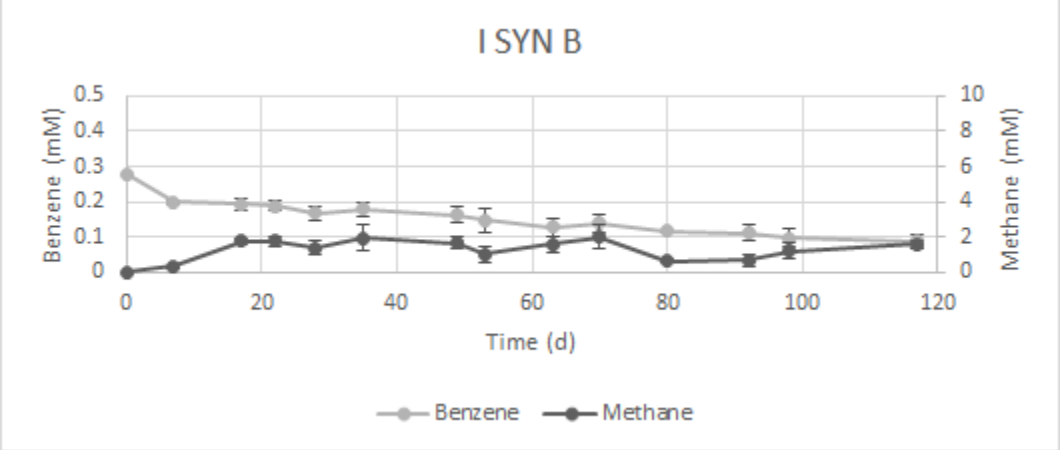

Figure 4-2. Degradation Curves for Iron-reducing Culture Conditions.

Benzene and methane concentrations were determined by headspace GC. Datapoints were averaged between triplicates. I = iron-reducing; H2O = water/untreated; NTA = nitrilotriacetic

acid; SYN = synergy, aHA + oxalic acid; B = benzene. Error bars represent one standard deviation.

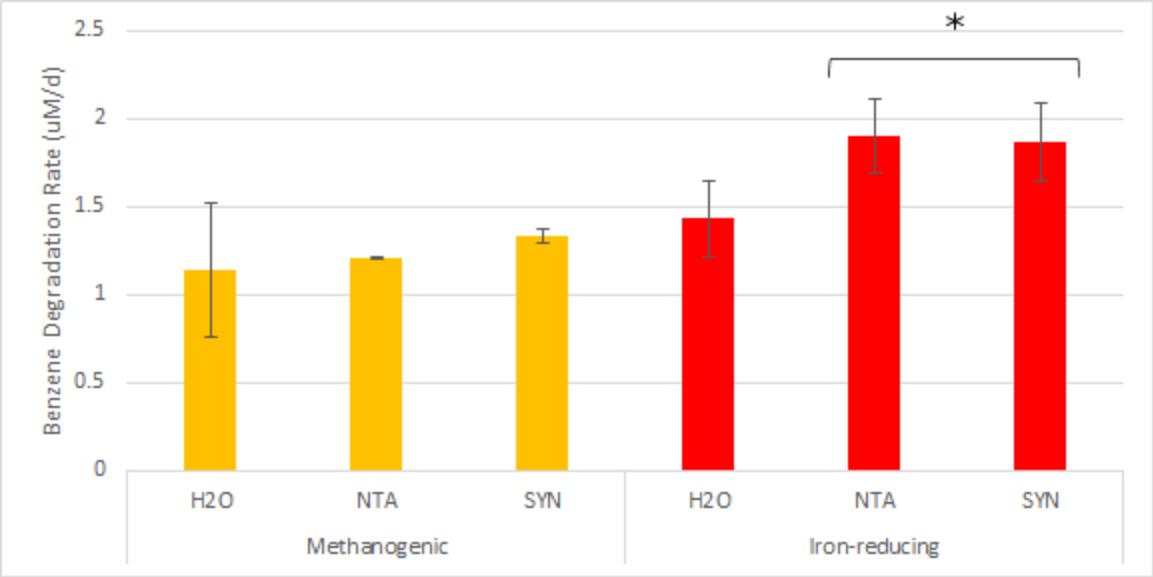

Figure 4-3. Degradation Rates of Methanogenic and Iron-reducing Microcosms.

Total benzene removal amounts were divided by total time of cultivation. Asterisks represent statistical significance as pertaining to the appropriate untreated control (p-value < 0.05). H2O = water/untreated; NTA = nitrilotriacetic acid; SYN = synergy, aHA + oxalic acid. Error bars represent one standard deviation.

4.4.2 Microbial Community Analysis and Quantification

All microcosms tested demonstrated high alpha diversity via Shannon Indices (Figure 4-7, 3-8), and rarefaction curves indicated that the implemented sequencing did not exhaustively sample the microcosms to saturation (Supplemental 4-4). All samples had >97% sequencing coverage, although iron-reducing samples had greater observed OTU richness than methanogenic samples. Newick trees and beta diversity heatmaps (using Jaccard Indices and Yue and Clayton Theta Similarity Coefficient protocols respectively) demonstrated microbial community divergence between untreated and chelator-treated iron-reducing microcosms, particularly NTA treatments, with relatively minor divergence between methanogenic microcosms (Supplemental 4-5), further suggesting a biostimulatory effect from chelator amendments in iron-reducing

cultures specifically.

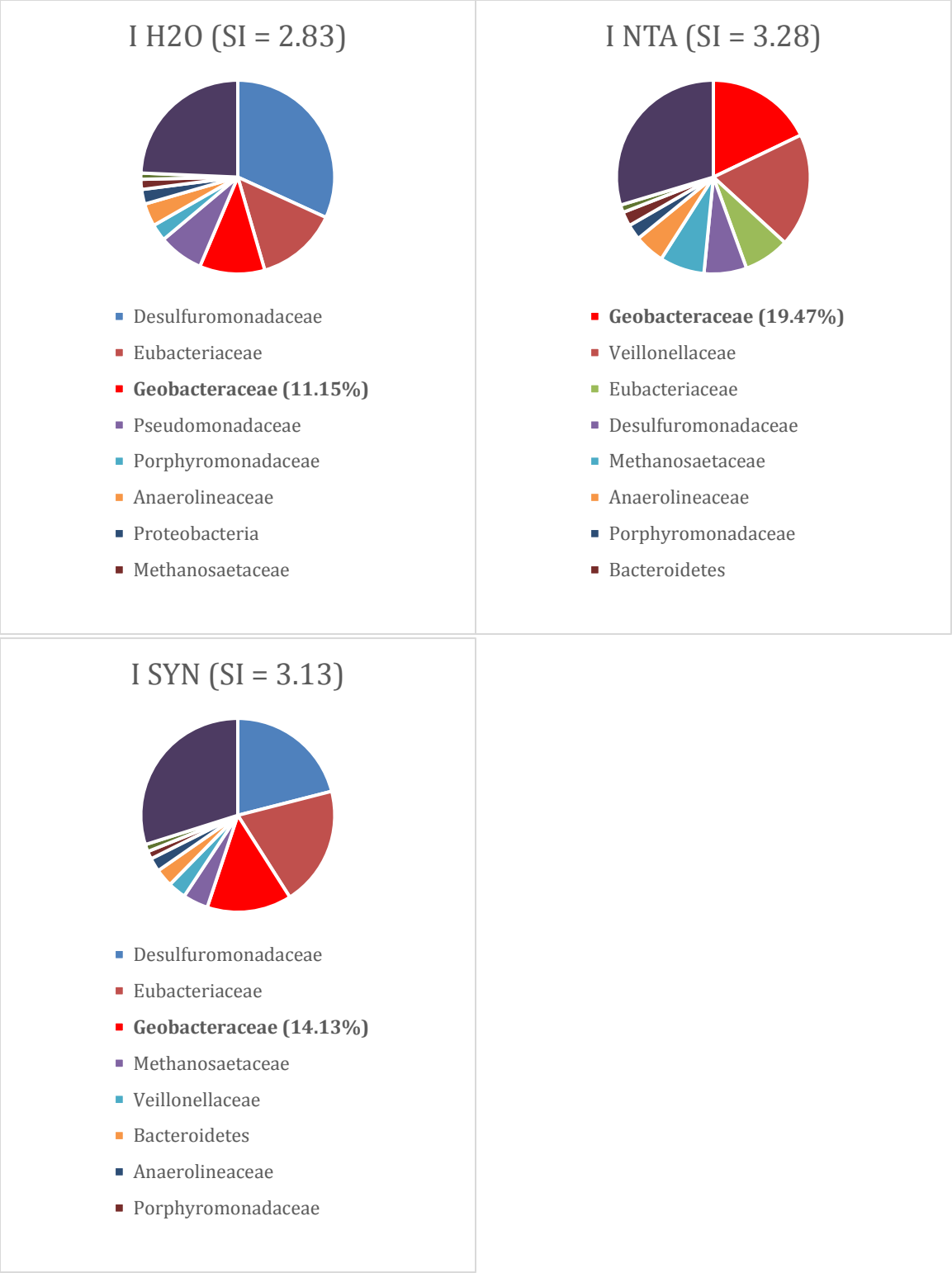

Figure 4-4. Microbial Profiles of Iron-reducing Benzene-degrading Microcosms.

16S rRNA amplicon sequencing analysis of iron-reducing cultures. I = iron-reducing; H2O = water, untreated; NTA = nitrilotriacetic acid; SYN = synergy of oxalic acid and acetohydroxamic acid; SI = Shannon Index. Red designates Geobacteraceae organisms in all cultures.

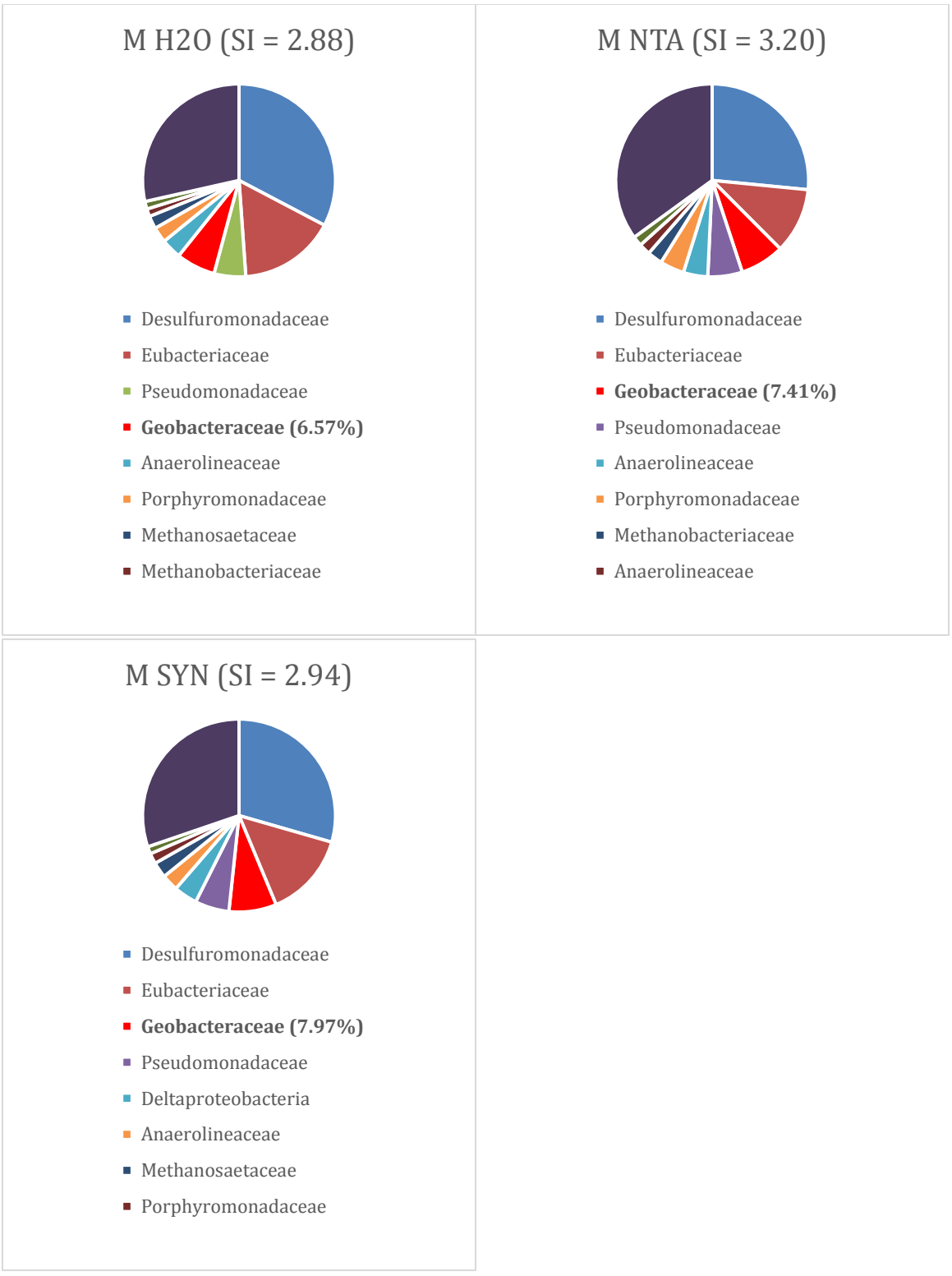

Figure 4-5. Microbial Profiles of Methanogenic Benzene-degrading Microcosms.

16S rRNA amplicon sequencing analysis of methanogenic cultures. M = Methanogenic; H2O = water, untreated; NTA = nitrilotriacetic acid; SYN = synergy of oxalic acid and acetohydroxamic acid; SI = Shannon Index. Red designates Geobacteraceae organisms in all cultures.

Degradation was enhanced in iron-reducing cultures treated with chelators (Figure 4-6), and these metrics were reflected in the commensurate expansion of the *Geobacter* population, with 98.87% 16S rRNA homology to reported primary degraders (GenBank Accession# JQ799138.1), in the chelator-treated iron-reducing cultures but not the methanogenic samples (Figure 4-7, 3-8). The prominence of *Geobacter* in methanogenic samples was unexpected, as previous maintenance cultures did not exhibit notable populations of these organisms (Lee & Ulrich, 2021); cross-contamination from iron-reducing cultures was unlikely, due to inter-sample heat sterilization of needles, and separate syringes being used exclusively within triplicates during the headspace monitoring phase. Furthermore, although *Geobacter* has been observed to reduce other metals such as manganese (Levar, Hoffman, Dunshee, & Toner, 2017), these ions were never present within the culture medium used in this study. Nevertheless, the final populations of *Geobacter* taxa manifested according to expectations in the iron-reducing cultures, with the siderophore and LMWOA treatments demonstrating an expansion of *Geobacter* interposed between that of the untreated and the NTA positive control samples (Figure 4-7). The structure of aHA is a linearized form of the desferrioxamine B molecule, so although *Geobacter* is not known to exhibit siderophore receptors, the uptake of aHA complexes may be less specific. *Geobacter metallireducens* may also be acquiring iron from oxalic acid complexes. Future experiments may elect to investigate the properties of these chelators further and elucidate the detailed mechanisms in which they promote benzene metabolisms. Previously documented benzene-degradation auxiliary taxa such as *Desulfuromonadaceae* (Luo, Devine, & Edwards, 2016)., *Methanosaeta* (Cruz Viggi, et al., 2014)*, Anaerolineae* (Keller, Kleinsteuber, & Vogt, 2018)*,* and *Methanosarcineae* (Balch, Fox, Magrum, Woese, & Wolfe, 1979) were also present in both methanogenic and iron-reducing microcosms, reflecting the prominence of methanogenesis in both cultures. However, known primary degraders in methanogenic cultures such as *Deltaproteobacterium* ORM2a (Luo, Devine, & Edwards, 2016) were not represented in these cultures, nor were other primary degraders from sulfur or nitrate-reducing microcosms

such as *Clostridiaceae* JN18 or *Peptococcaceae*, respectively (Noguchi, Kurisu, Kasuga, & Furumai, 2014; Alfreider & Vogt, 2007; Sakai, Kurisu, Yagi, Nakajima, & Yamamoto, 2009; Luo, et al., 2014; Luo, Devine, & Edwards, 2016; Musat, Wilkes, Behrends, Woebken, & Widdel, 2010; Oka, et al., 2008; Bedard, Ritalahti, & Loffler, 2007; Zaan, et al., 2012).

Previous experiments had demonstrated the ability of NTA to enhance benzene degradation in iron-reducing cultures, and this study in turn demonstrated that the effects of siderophores and low molecular weight organic acids may have similar biostimulatory potential while lacking the carcinogenicity of NTA, making them more potentially amenable to remediation strategies. aHA had been chosen as a relatively plurispecific siderophore analogue, as it was a foundational chemical component of desferrioxamine B, already characterized in the literature as being used by a wide variety of microorganisms including *Streptomyces coelicolor* (Barona-Gómez et al. 2006; Ronan et al. 2018), *Streptomyces pilosus* (Codd, Richardson-Sanchez, Teffer, & Gotsbacher, 2018), *Staphylococcus aureus* (Endicott, Lee, & Wencewicz, 2017), and *Anthrobacter simplex* (Winkelmann, 1991), among others (Hider & Kong, 2010). Still, as a member of the hydroxamate class of siderophores, desferrioxamine B bears the specificities inherent therein, precluding its use by those bacteria that do not bear the proper receptors and limiting its potential biostimulatory application. In addition, linearization of the desferrioxamine B siderophore is inversely correlated with iron affinity (Codd, Richardson-Sanchez, Teffer, & Gotsbacher, 2018), and further interrogations may elect to introduce a more comprehensive panel of hydroxamates for testing. The known synergy of aHA (acetohydroxamic acid) and oxalic acid in dissolving ferric iron observed in abiotic conditions (Supplemental 4-2) correlated with its effect on living cultures, and the relationship between these two entities may be worthy topics for follow-up experiments, which should incorporate an assay for quantifying the turnover of external chelators (Schwabe, Anke, Szymanska, Wiche, & Tischler, 2018) and therefore their

contribution as carbon sources for the consortium. This may yield further insight as to their metabolic fate, though multiple iterations of the derivatization protocols may be necessary to optimize the procedure for mixed cultures with complex chemistries.

Other factors may persist in biotic treatments: biological chelators are not limited to binding ferric iron, and organic matter that can be produced by microorganisms is known to contain substantial amounts of other metals such as aluminum, zinc, and copper - however, the transfer of non-iron metals to siderophores from organic matter is generally limited (Kuhn, Maurice, Neubauer, Hofmann, & von der Kammer, 2014), so it is unlikely that the transfer of these metals can account for differences in metabolic activity which may result from the use of alternative terminal electron acceptors. However, the extraction of iron from organic matter by biological chelators has also been seen to affect the size distribution of the organic material (Kuhn, Maurice, Neubauer, Hofmann, & von der Kammer, 2014), an effect that can potentially cascade into changing availabilities of these metals. Furthermore, the mechanisms that mediate the transfer of iron from organic matter to chelators have been previously examined (Kuhn, Maurice, Neubauer, Hofmann, & von der Kammer, 2014), and are thought to involve cation exchange, and iron can also be transferred between chelators upon changing pH levels (Crumbliss & Harrington, 2009), so sequestration is not necessarily permanent. These phenomena, among others, may partially account for the complications evident when transposing abiotic dissolution data to biotic samples, and should be investigated in more detail for future studies.

Furthermore, the potential utility of siderophores may not be limited to iron dissolution. Another property of hydroxamic acids is their ability to oxidize ferrous iron into the ferric form (Farkas, Enyedy, Zekany, & Deak, 2001), which may regenerate Fe^{3+} from Fe^{2+} and maintain iron-reduction reaction processes thereby. This process reduces one of the hydroxamate groups into an amide, generating desferrioxamine B-monoamide, and interestingly, DFO-monoamide-Fe^{3+}

complexes have been seen to be highly reactive molecules that can remediate other contaminants such as nitroaromatics (Kim, Duckworth, & Strathmann, 2009). The ability of siderophores to act as protectants against oxidative stress may be important in cultivating anaerobic cultures, and it is known that *G. metallireducens* can express oxidative stress defense enzymes in the presence of aromatic compounds (Heintz, et al., 2009). Siderophore amendments may thus alleviate the metabolic burden of generating such enzymes. Additionally, desferrioxamine B utilization is relatively plurispecific, and a representative operon from *Streptomyces coelicolor* contains 6 DFO-associated genes, where *desA-D* are biosynthetic, *desE* encodes a receptor, and *desF* encodes a reductase (Ronan, et al., 2018). Another relatively plurispecific siderophore is enterobactin, of the catechol family (Peralta, et al., 2016; Hider & Kong, 2010), which is evidenced by *tonB* receptor genes in multiple G- bacteria. Detailed metagenomic surveys of iron reducers for such genes may therefore illuminate candidate taxa that may benefit from chelator amendment.

Lastly, aHA and oxalic acid may potentially be able to improve the performance of other cultures derived from sediments distinct to those used in this study. For example, the colloidal fraction of the Horse River, a tributary of the Athabasca which flows through the natural bitumen beds in Northern Alberta, is enriched in iron minerals (Gibson, et al., 2012), and this colloidal fraction dictates the bioavailability of elements like iron, where trace element forms are categorized as truly dissolved (1-450 nm; >1 kDa), colloidal (1-1000 nm), and particulate (>450 nm) (Wilkinson & Lead, 2007; Cuss, et al., 2018). The combination of fossil fuel materials with iron materials may result in the propagation of iron-reducing benzene-degrading microorganisms, and if sediment material from this region is ever cultivated anaerobically to survey for such bacteria, the identity of such organisms can provide unique insights into the mechanisms they use to mobilize iron and make them bioavailable. These data can direct new studies into iron dissolution strategies that can aid in the cultivation of iron-reducers for benzene degradation.

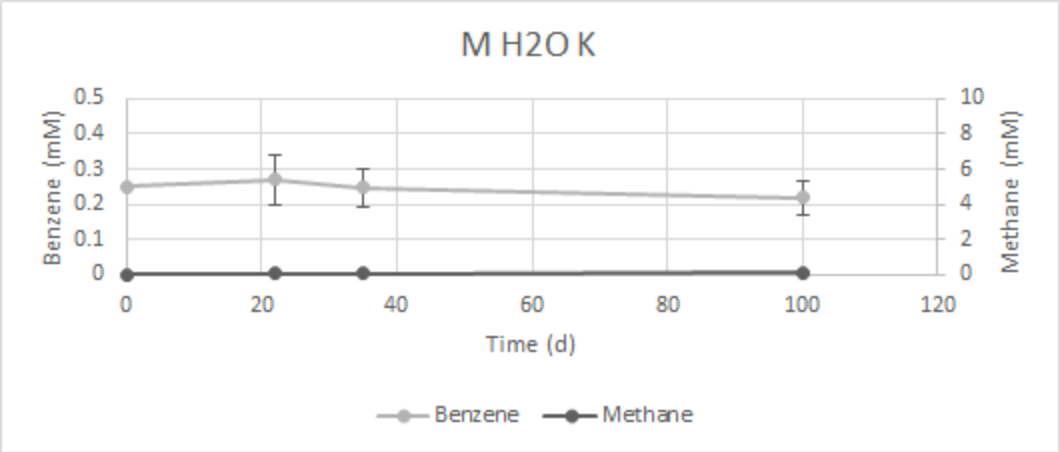
M H2O K
Benzene (mM)
Methane (mM)
Time (d)
Benzene
Methane

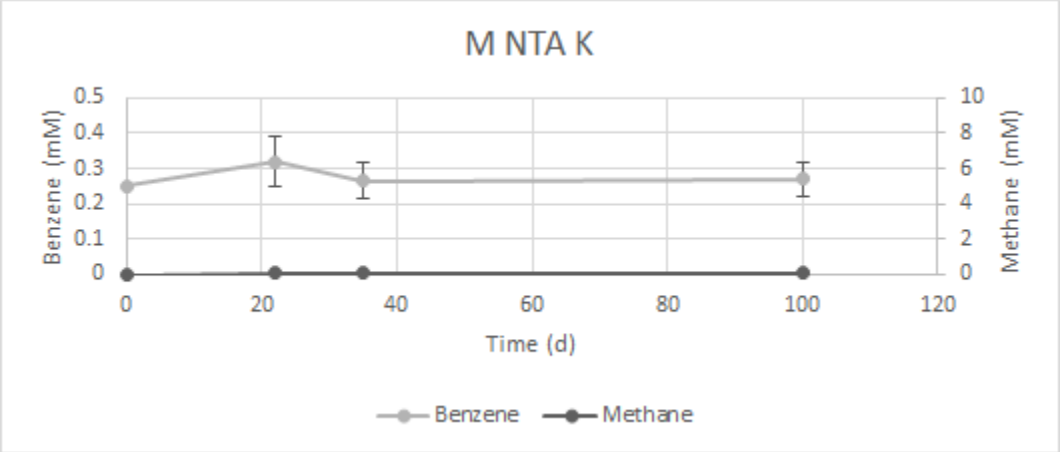
M NTA K
Benzene (mM)
Methane (mM)
Time (d)
Benzene
Methane

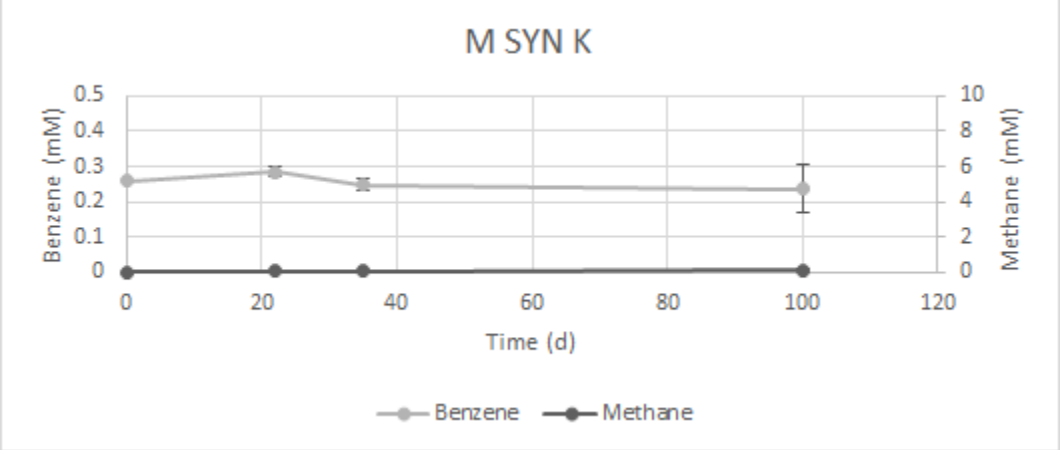
M SYN K
Benzene (mM)
Methane (mM)
Time (d)
Benzene
Methane

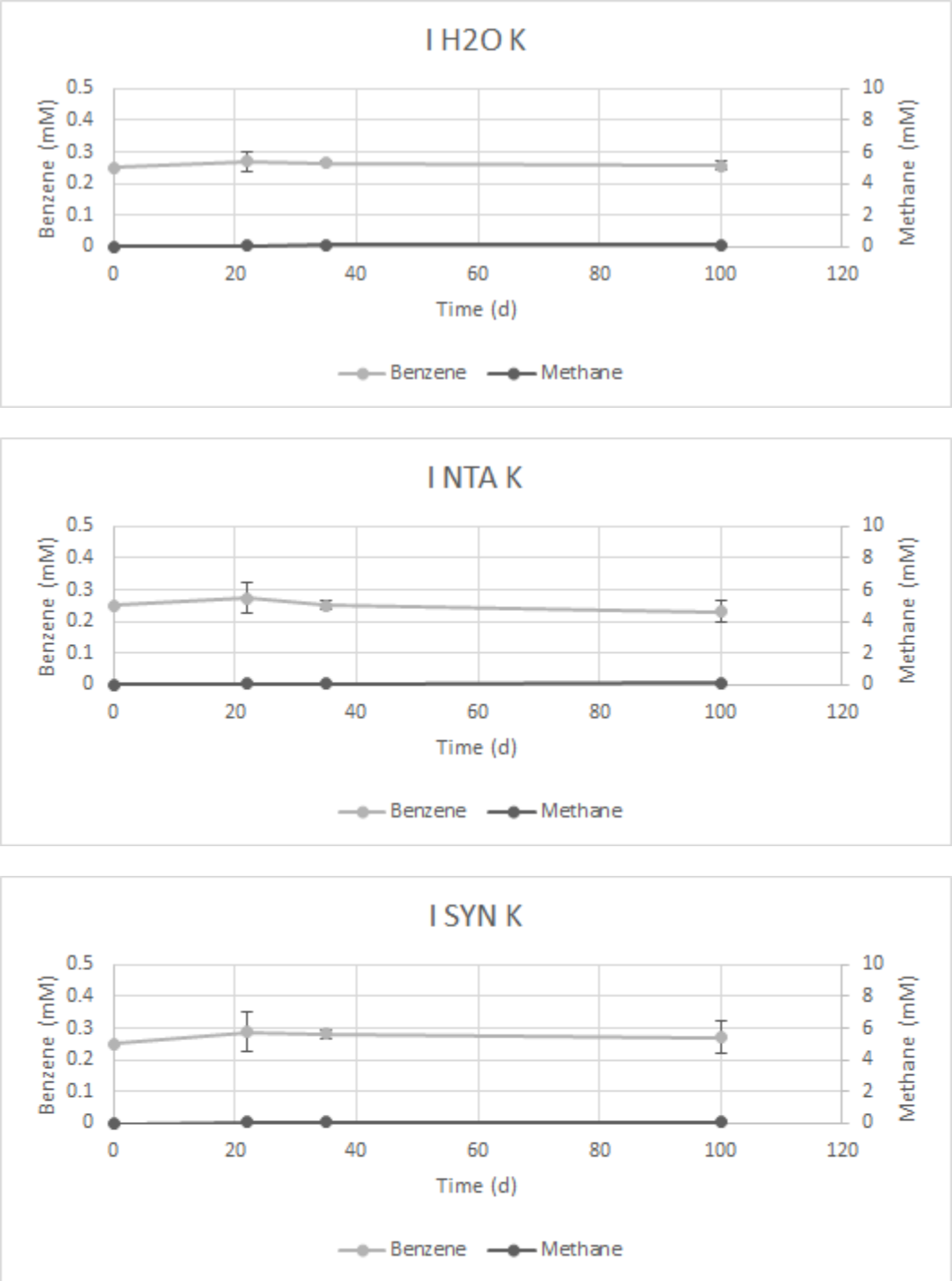

Supplemental 4-1. Benzene Removal in Heat-killed Controls.

Cultures were sterilized by three separate 90 min autoclave cycles over 72 hours and benzene levels were monitored by headspace GC. M = methanogenic; I = iron-reducing; H2O =

water/untreated; NTA = nitrilotriacetic acid; SYN = synergy, aHA + oxalic acid; K = killed controls. Error bars represent one standard deviation.

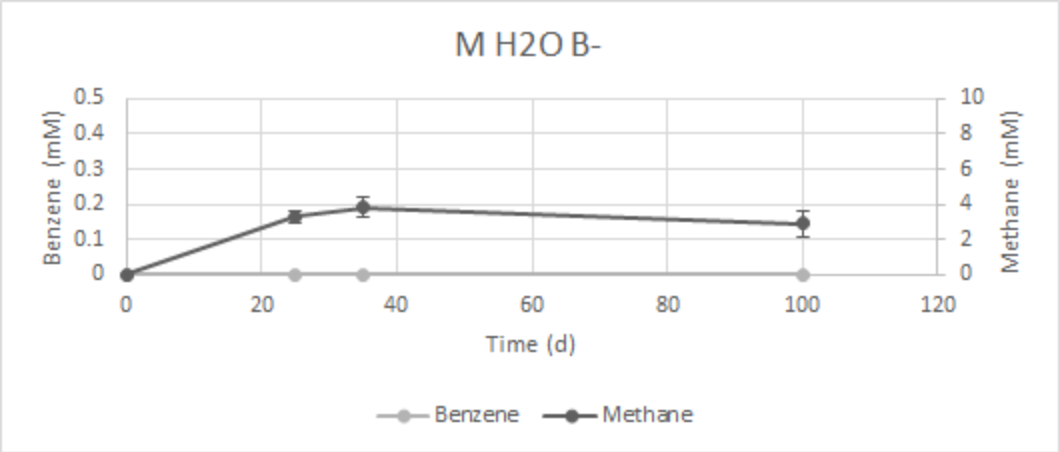
M H2O B-
Benzene (mM)
Methane (mM)
Time (d)
Benzene
Methane

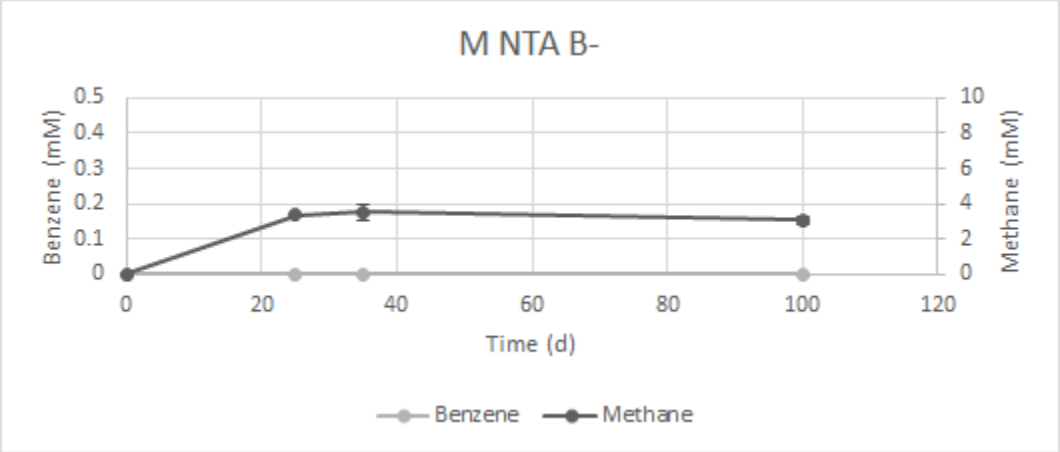
M NTA B-
Benzene (mM)
Methane (mM)
Time (d)
Benzene
Methane

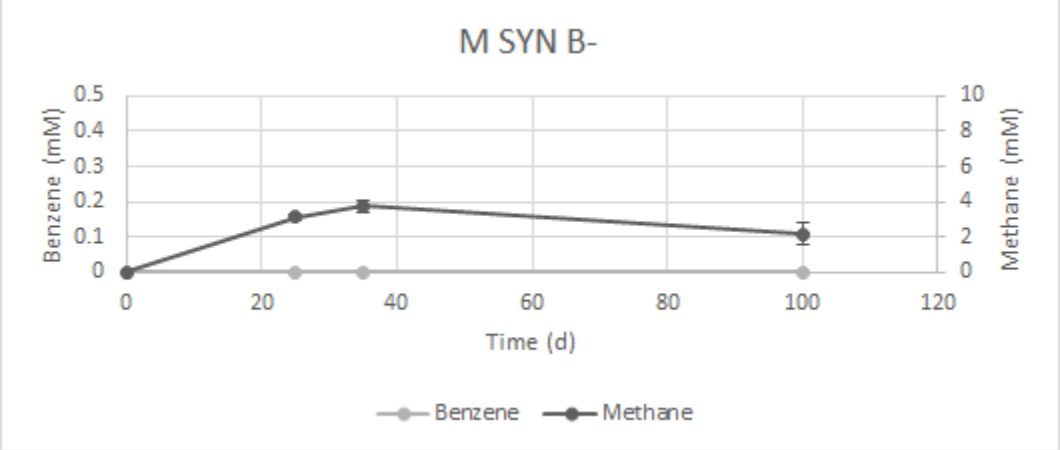
M SYN B-
Benzene (mM)
Methane (mM)
Time (d)
Benzene
Methane

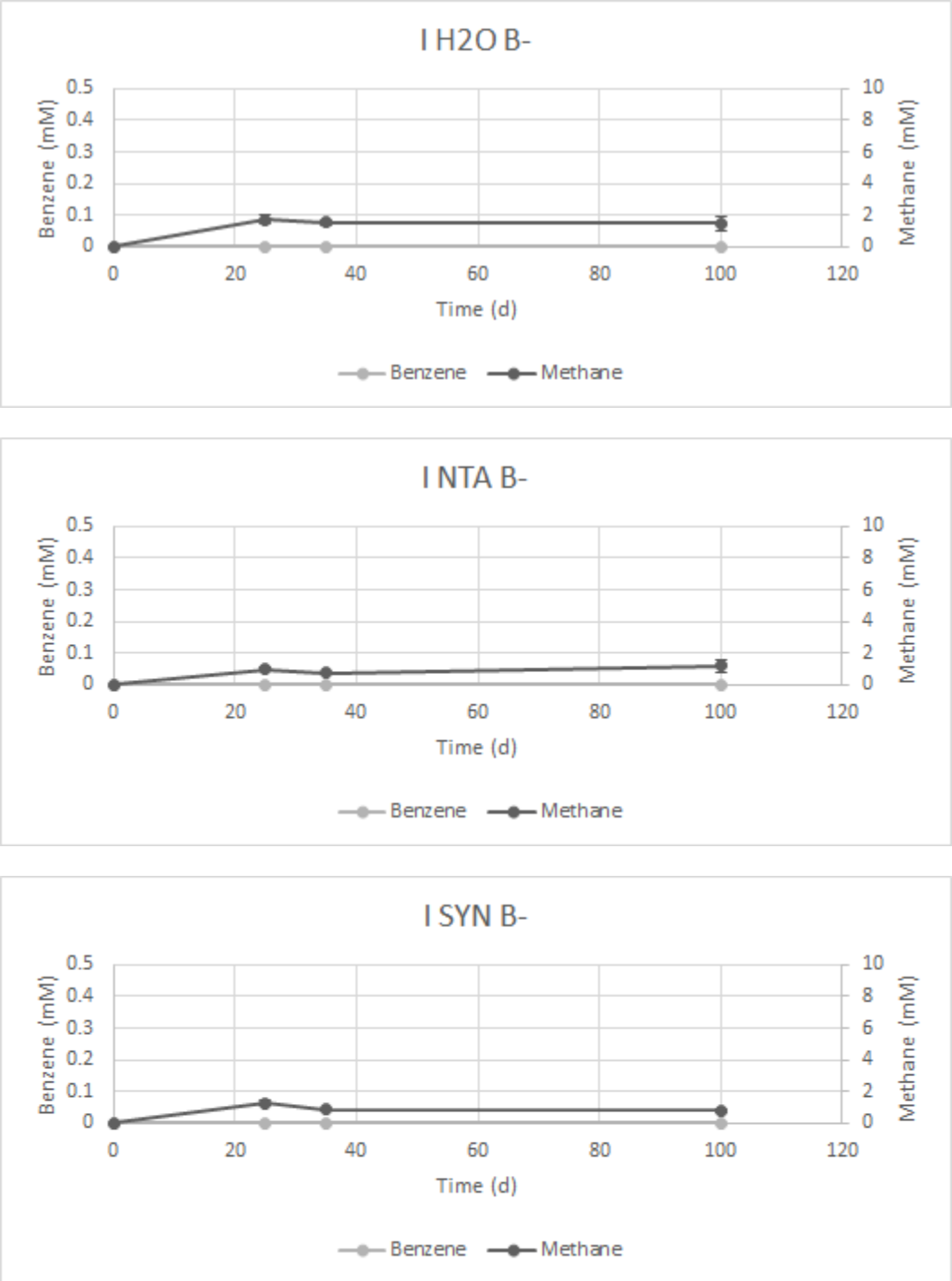

Supplemental 4-2. Methane Production in Benzene-free Controls.

Benzene and methane concentrations were determined by headspace GC. Datapoints were averaged between triplicates. M = methanogenic; I = iron-reducing; H2O = water/untreated;

NTA = nitrilotriacetic acid; SYN = synergy, aHA + oxalic acid; B- = no-benzene controls. Error bars represent one standard deviation.

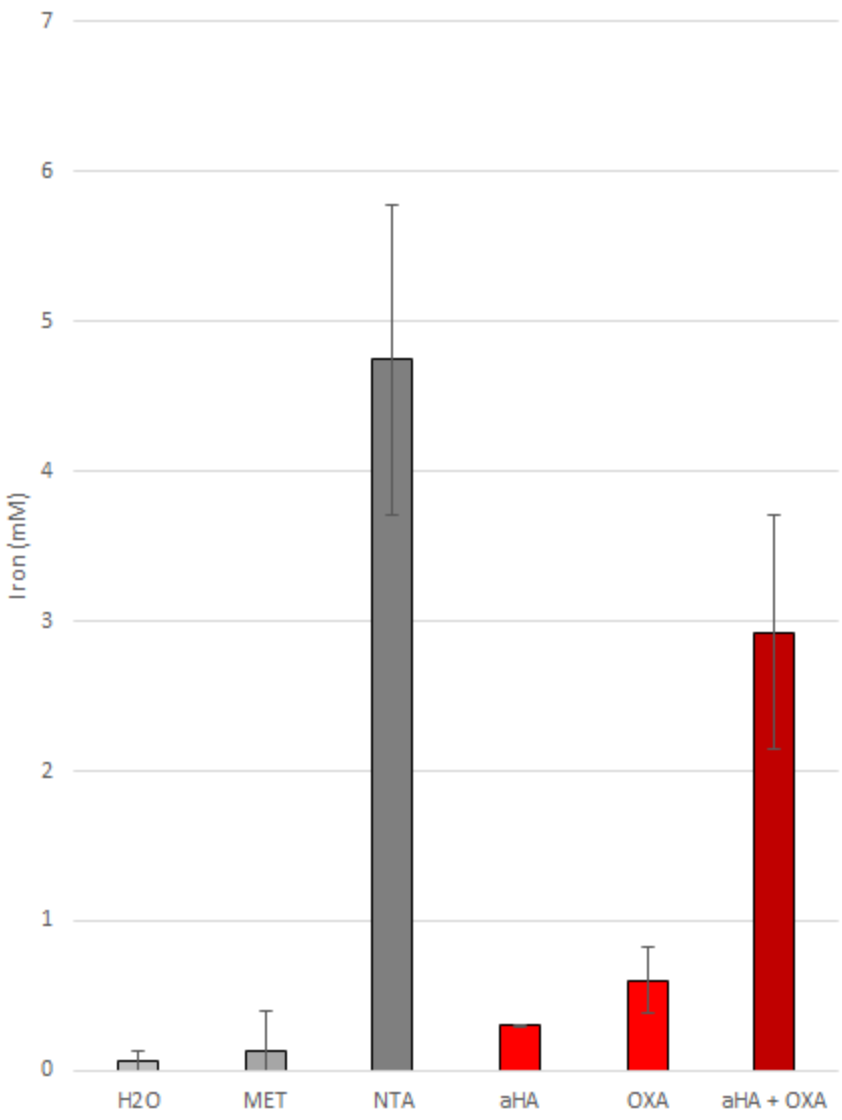

Supplemental 4-3. Abiotic Dissolution of Ferrihydrite.

Media-only controls were established with 10% v/v ferrihydrite and incubated with light exclusion for 48 h before total soluble iron quantification using ICP-MS. pH levels did not change upon addition of chelator amendments. H2O = untreated/water; MET = methanol, representing a non-chelating carbon source; NTA = nitrilotriacetic acid, representing a positive control; aHA = acetohydroxamic acid alone, representing hydroxamate siderophore; OXA = oxalic acid alone, representing low molecular weight organic acid; aHA + OXA = acetohydroxamic acid and oxalic acid, representing the synergy of the two. Error bars represent one standard deviation.

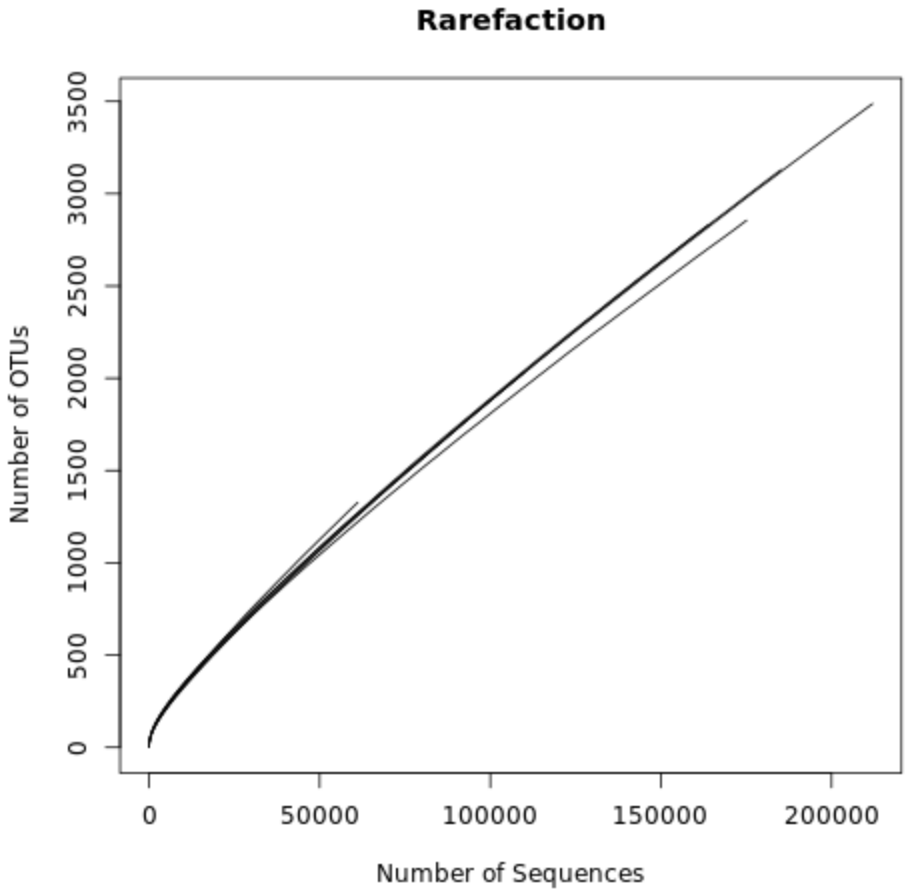

Supplemental 4-4. Rarefaction Curves for Benzene-degrading Microcosms.

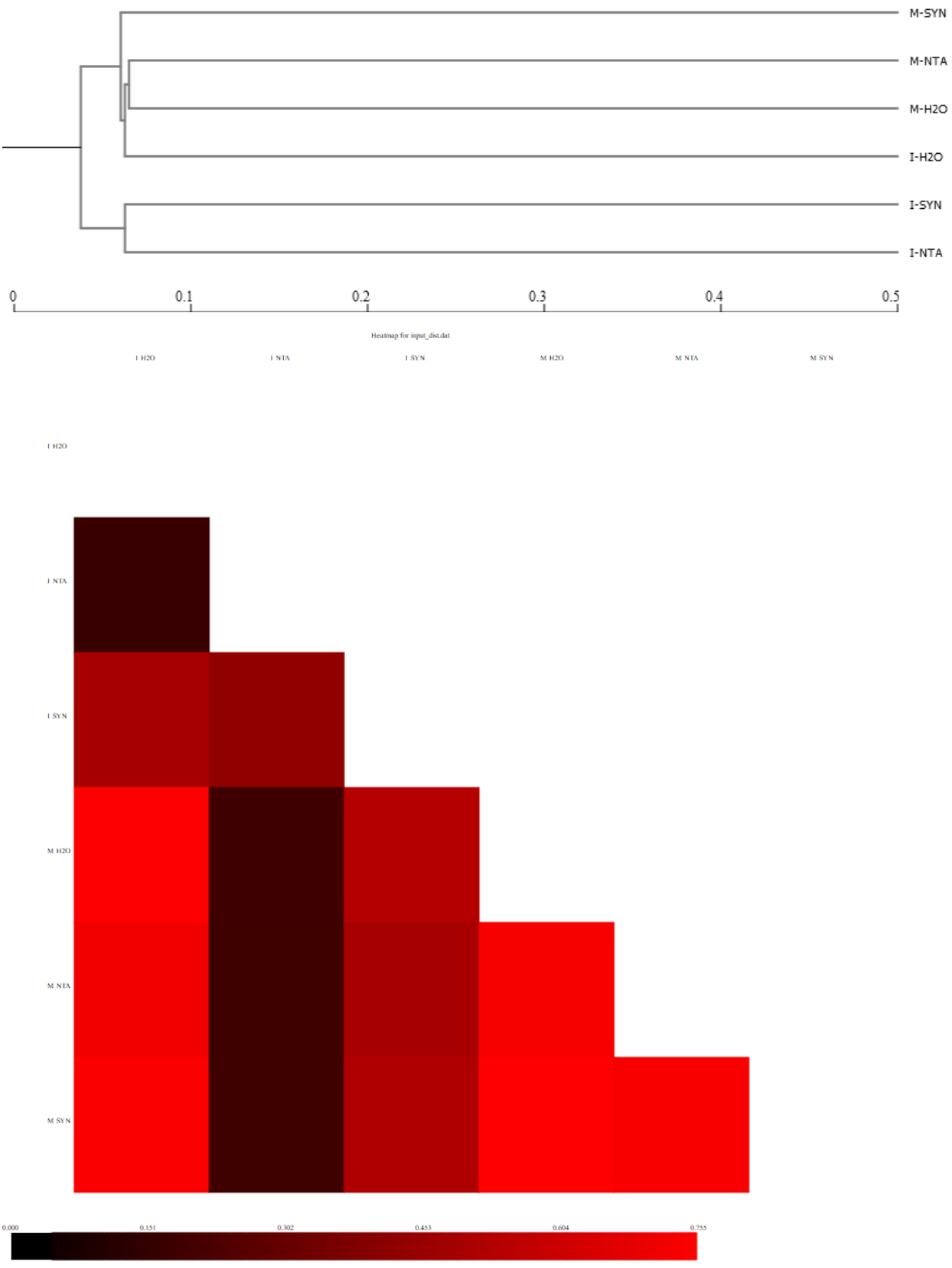

Supplemental 4-5. Beta Diversity Analysis of Benzene-degrading Microcosms.

Beta diversity between samples was visualized using Newick trees and heatmaps using jclass and thetayc protocols respectively, with distances estimated by Phylip matrices. I = iron-reducing; M = methanogenic; H2O = untreated, water; NTA = nitrilotriacetic acid; SYN = synergy of acetohydroxamic acid and oxalic acid.

5 The Contribution of Magnetite to Benzene Degradation in Iron-reducing Cultures

5.1 Abstract

Iron-reducing cultures are the least represented respiratory group within the anaerobic benzene degrading scholarship, and novel iron-reducing benzene degrading cultures warrant extensive comparative investigations to establish reproducibility of results. Robust benzene degradation has been observed in iron-reducing cultures derived from Albertan sediments, and various studies regarding the genetic traits of the culture and the iron utilization of its microbial constituents have been implemented. This study is a continuation of previous biostimulation efforts in the Alberta iron-reducing benzene degrading cultures, and evaluates the potential for magnetite minerals to promote their metabolic activity, with the intent to either provide growth surfaces or to enhance electroconductivity for *Geobacter* nanowires thought to be resident in the culture. Unfortunately, the cultures that were prepared for the experiment lost all benzene-degrading activity upon establishment, representing a substantial and irreparable loss of culture volume, and the investigation could not continue. Future attempts should implement various hydrogen-excluding controls to minimize the possibility of similar culture-arresting events.

5.2 Introduction

Benzene is a priority contaminant common to industrial fossil fuel processes (Canada Environment & Canada Health and Welfare, 1993), and its bioremediation is typified by

anaerobic conditions (Weelink, van Eekert, & Stams, 2010) and lethargic removal rates (Vogt, Kleinsteuber, & Richnow, 2011), resulting from its high chemical stability. Consequently, the establishment of cultures that can degrade benzene has been difficult, but the scholarship has identified certain taxa that are capable of accomplishing the critical first activation of the benzene ring that initiates the process (Noguchi, Kurisu, Kasuga, & Furumai, 2014; Alfreider & Vogt, 2007; Sakai, Kurisu, Yagi, Nakajima, & Yamamoto, 2009; Luo, et al., 2014; Luo, Devine, & Edwards, 2016; Musat, Wilkes, Behrends, Woebken, & Widdel, 2010; Oka, et al., 2008; Zhang, Bain, Nevin, Barlett, & Lovley, 2012; Bedard, Ritalahti, & Loffler, 2007; Zaan, et al., 2012). This activation of benzene is thought to involve either carboxylation into benzoate, methylation into toluene, or hydroxylation into phenol (Vogt, Kleinsteuber, & Richnow, 2011; Meckenstock & Mouttaki, Anaerobic Degradation of Non-Substituted Aromatic Hydrocarbons, 2011), all of which divert to a central metabolite, benzoyl-CoA (Vogt, Kleinsteuber, & Richnow, 2011; Meckenstock & Mouttaki, Anaerobic Degradation of Non-Substituted Aromatic Hydrocarbons, 2011), which is subsequently metabolized as acetyl-CoA (Dong, et al., 2017).

The latter process is suggested by differential expression experiments to be the purview of *Geobacter metallireducens* (Zhang T. , et al., 2013; Zhang T. , et al., 2014), previously demonstrated to degrade benzene in an iron reducing context (Zhang, Bain, Nevin, Barlett, & Lovley, 2012; Abu Laban, Selesi, Rattei, Tischler, & Meckenstock, 2010). Iron-reducing anaerobic degradation of benzene is characterized by multiple metabolic advantages, including the high redox potential of ferric iron and the low relatively toxicity of ferrous iron (Silva, Ruiz-Aguilar, & Alvarez, 2005; Lueders, 2017; Abbasian, Lockington, Mallavarapu, & Naidu, 2015). Notably, *Geobacter* does not utilize extracellular electron shuttling to reduce ferric iron (Nevin & Lovley, 2000); instead, it mediates iron reduction through direct physical contact with quinol and porin-cytochrome-based electron relays that transfer electrons to the outer membrane (Levar, Chan, Mehta-Kolte, & Bond, 2014; Zacharoff, Chan, & Bond, 2016; Lloyd, et al., 2003; Rotaru

A.-E. , et al., 2014; Liu Y. , et al., 2014; Shi, et al., 2016). These relays can take the form of membrane-bound nanowires (Reguera, et al., 2005), whose precise composition is contentious within the scholarship, and is thought to comprise either stacked hemes of OmcS (outer membrane cytochrome S) polymers (Wang, et al., 2019) or Type IV PilA (pilin A) subunits (Liu X. , et al., 2019). These constituents are thought to be the main contributors to the electrotransfer activity of the nanowire, and are therefore logical targets for external experimental enhancement.

A potential amendment worth consideration is magnetite ($Fe(II)Fe(III)_2O_4$), a ferrimagnetic, highly-conductive iron oxide consisting of both ferric and ferrous iron in an ordered crystalline structure that coordinates its cubic vertices with oxygen (Cornell & Schwerfmann, 2003). This mineral is widely implicated in redox interactions within bioremediation contexts (Zhou, Xu, Yang, & Zhuang, 2014; Zhuang, Tang, Wang, Hu, & Zhou, 2015; Li, et al., 2015; Zhang & Lu, 2016; Cruz Viggi, et al., 2014; Baek, Jung, Kim, & Lee, 2017; Yamada, Kato, Ueno, Ishii, & Igarashi, 2015), and electron transfer processes in *Methanosarcina* (Kato, Hashimoto, & Watanabe, 2012), *Methanosaeta* (Cruz Viggi, et al., 2014), and especially *Geobacter* (Kato, Hashimoto, & Watanabe, 2012), in which it is thought to externally reconstitute the properties of OmcS in the nanowire (Liu F. , et al., 2015). That is, nanoscale magnetite is capable of restoring the electron transfer of nanowires normally provided by OmcS, thus absolving the need for *Geobacter* to shoulder the metabolic burden of synthesizing cytochromes *de novo*. The introduction of magnetite can therefore potentially alleviate energy costs and improve the metabolic ability of *Geobacter* to traffic electrons to ferric iron. Furthermore, the taxa (*Geobacter, Methanosaeta*) that have previously been demonstrated to be positively affected by magnetite additions are notable due to their abundance and co-occurrence in anaerobic iron-reducing benzene-degrading cultures (Lee & Ulrich, 2021). However, no study to date has

evaluated the utility of magnetite for enhancing the degradation of a notoriously stable contaminant such as benzene in an iron-reducing context.

In this research, the effect of magnetite on anaerobic benzene degradation capability in cultures based on sediments from the province of Alberta (Lee & Ulrich, 2021), where benzene contamination risks are commensurate with the ubiquity of the oil and gas industry (Economic Dashboard - Oil Production, 2019), associated underground storage units (Government of Canada, Environment Canada, & Health Canada, Benzene. Priority Substances List Assessment Report, 1993; Government of Canada P. S., 2019), and orphan wells (Dachis, Shaffer, & Thivierge; Natural Resources Canada, 2020) are addressed. Benzene removal, methane production, and the expansion of known primary degrader taxa such as *Geobacter* will be used as metrics for culture performance. It is expected that the introduction of magnetite will positively affect the kinetics of benzene removal, while the influence of silica controls is expected to be minimized to a sorption effect. Neither magnetite nor silica amendments, existing on the nanometer scale, are expected to play any role as a growth substratum, so it is hypothesized that only nanomagnetite would cause the expansion of *Geobacter* primary degrader taxa.

5.3 Methods

5.3.1 Culture Source

Iron-reducing cultures were cultivated and maintained as previously described (Lee & Ulrich, 2021). All manipulations were performed in an anaerobic chamber with an atmosphere of 5/5/80 % hydrogen/carbon dioxide/nitrogen, while culture bottles were maintained with a headspace of 10% carbon dioxide mix balanced with nitrogen. Cultures in sterile serum bottles were diluted 50% v/v with previously-defined anaerobic mineral media (Edwards & Grbic-Galic, 1994) and amended with 10% v/v ferrihydrite ($Fe_5HO_8 \cdot 4H_2O$) as a terminal electron acceptor source.

Anaerobic-conditioned benzene was amended with a glass syringe to a liquid concentration of 0.28 mM, and experimental concentrations (5 g/L) of 50% magnetite slurry were provisioned with sterile syringes. Media-only formulations were prepared to gauge the sorption effect of each experimental treatment condition in isolation.

Microscale magnetite was synthesized as previously described (Schwertmann & Cornell, 2008), as was nanoscale magnetite (Y. S. Kang et al. 1998). Nanoscale (10 nm) silica spheres were provided by Sigma Aldritch (637238-50G), and microscale (10 μm) silica spheres were provided by Materium© (MAT540). Nanoscale magnetite was intended to determine the effect of supplanting nanowire conductivity, while microscale magnetite was intended to determine the effect of providing growth surfaces for degrader populations. Micro and nanoscale silica beads were intended to isolate and control for the conductive and growth-surface properties of magnetite.

Table 5-1. Treatment Conditions for Iron-reducing Cultures.

Treatments (10 mM)	Treatment Role
Killed Control	Killed Control
H2O	Untreated Control
Microsilica	Control, nonconductive
Nanosilica	Control, nonconductive
Micromagnetite	Control without nanowire conductivity
Nanomagnetite	Experimental, nanowire conductivity

5.3.2 Benzene and Methane Quantification

Benzene and methane were quantified with headspace Gas Chromatography (GC) as previously described (Lee & Ulrich, 2021). The method was as follows: the injector was set to a pressure of 17.735 psi with septum purge flow of 3 mL/min, the column was set to 350℃ at 4.5 mL/min, the oven was set to a temperature of 50℃ for 4.5 min, and the detector was set to 250℃ with a flow of 45 mL/min hydrogen, 450 mL/min air, and 25 mL/min helium. Injections used 100 µL of headspace volumes extracted via gas-locked syringes (Sigma-Aldritch™ VICI Series A-2) under anaerobic conditions. C_6H_6 concentration measurements had an error of ±6.24%. Calibration was performed with external standards, with a detection limit of 0.01 mM benzene and 0.03 mM methane.

5.3.3 Iron Quantification

Although iron quantification was not performed due to the circumstances of the experiment, 1 mL of the sample volume was to be harvested and filtered through a 0.2 μm syringe filter, and the filtrate diluted 5000x in 1% nitric acid. Total soluble iron was to be analyzed using ICP-MS (Inductively Coupled Plasma Mass Spectrometry) (iCap Q, ThermoScientific®) in conjunction with internal and external standards.

5.4 Results and Discussion

Although the synthesis of magnetite and cultivation of iron-reducing inocula was successful (characterized by degradation rates of 12 μM/d and stoichiometries of 18.1 mol Fe(II): 1 mol C_6H_6), and the materials used exhibited some sorption capacity (Figure 5-1) (Table 5-1), the culture, once introduced into experimental bottles, failed to retain its original activity, even in untreated controls, and exhibited no detectable benzene degradation. This loss of activity was unprecedented in this research group, and may have been caused by a shift in microbial community that polarized towards hydrogenotrophic methanogens, already extant in various benzene-degrading consortia (Sakai, Kurisu, Yagi, Nakajima, & Yamamoto, 2009; Lee & Ulrich, 2021; Luo, Devine, & Edwards, 2016; Noguchi, Kurisu, Kasuga, & Furumai, 2014), as hinted by the accumulation of methane in experimental microcosms. This shift may have been due to the acclimatization process for glassware, which necessitated the placement of experimental material into the anaerobic chamber for at least 24 hours for the sake of extracting residual oxygen. The atmosphere in the chamber contained 5% hydrogen, which may have been used by taxa such as *Hydrogenophilaceae* to dominate the consortium and competitively exclude primary benzene-degraders. However, this phenomenon did not seem to occur in previous

experiments that involved anaerobic cultures (Lee & Ulrich, 2021), so questions remain that require comprehensive empirical analysis to elucidate. This experiment, as it was, represented a major expenditure of maintenance culture volume that required a substantial amount of time to attain and a large amount of effort to replace for other experiments. Considering the investment of effort in growing this culture volume, a repetition of the experiment was therefore not possible within the allotted timeframe, but the failure of the cultures to initiate was still noted here as a cautionary event for later studies. Future experimental attempts may elect to sparge all experimental bottles after the introduction of culture, and replace the microcosm headspace with a formulation of gas that includes nitrogen and carbon dioxide without hydrogen. However, expanding existing maintenance culture volumes (such that compromised experimental cultures would merely be temporary setbacks rather than terminating factors) remains the surest defense against such difficulties, and should be the priority for researchers intending to perform anaerobic benzene culturing experiments.

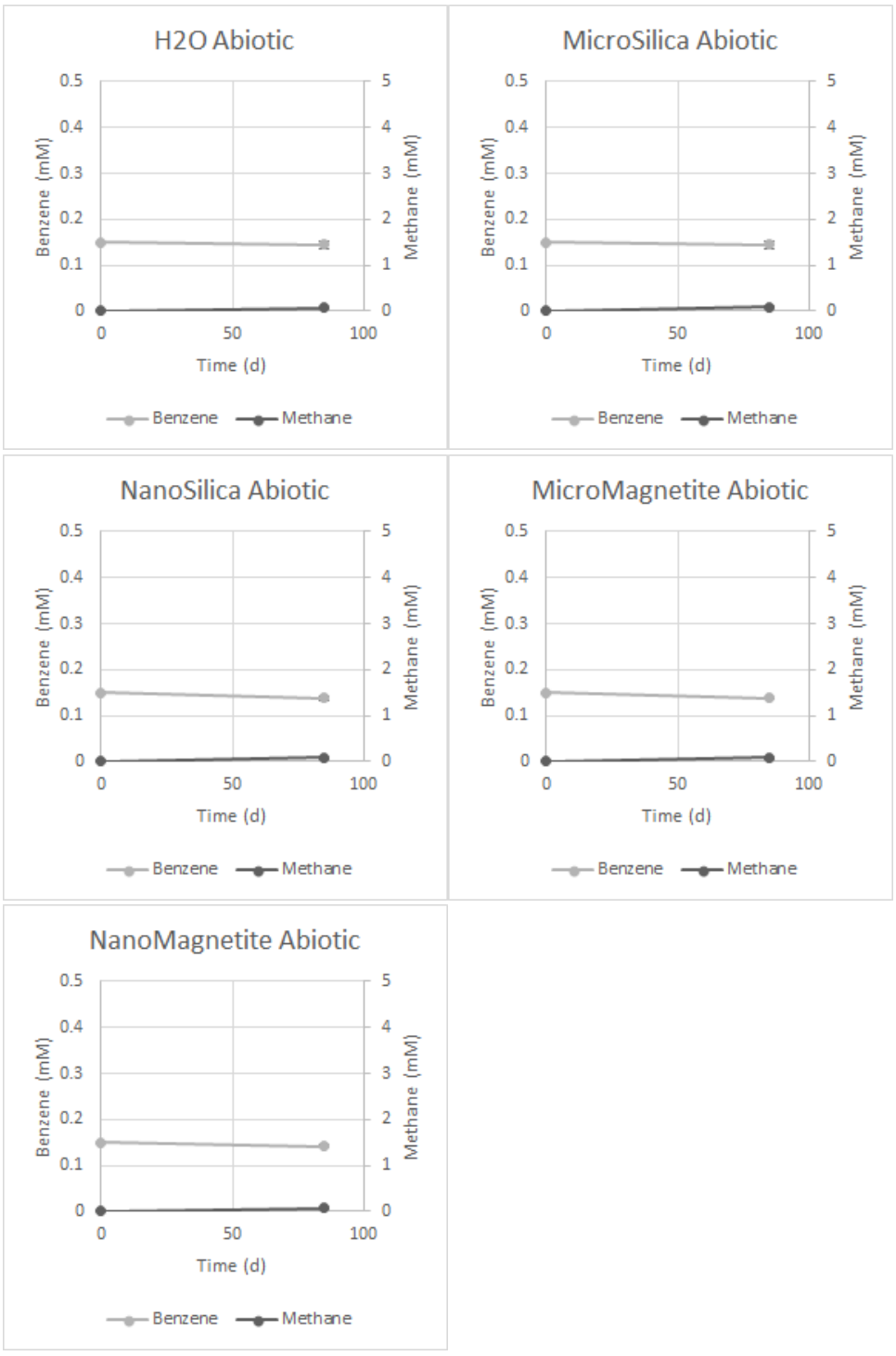

Figure 5-1. Abiotic Benzene Sorption and Heat-killed Controls.

Triplicate control specimens devoid of live cultures were monitored by headspace GC. H2O Abiotic represents untreated samples. MicroSilica Abiotic represents samples containing microscale silica. NanoSilica Abiotic represents samples containing nanoscale silica.

MicroMagnetite Abiotic represents samples containing microscale magnetite. NanoMagnetite Abiotic represents samples containing nanoscale magnetite.

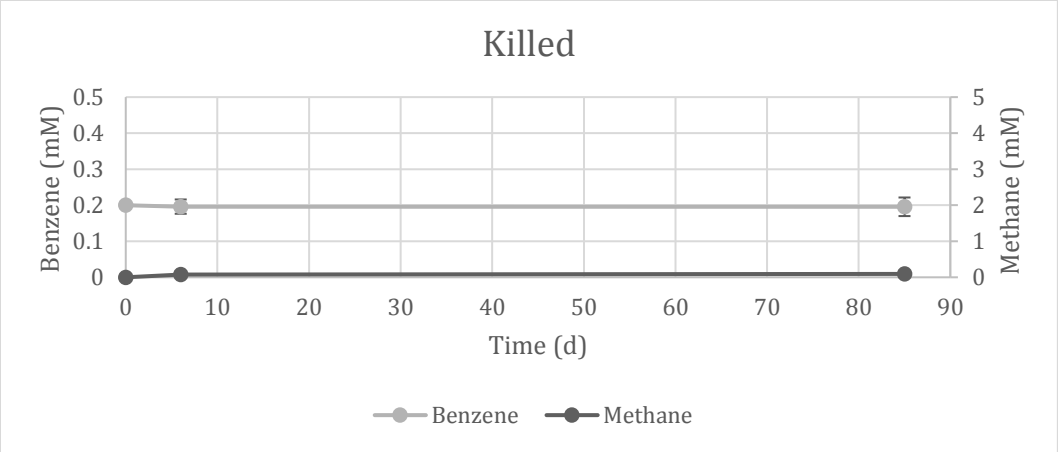
Killed
Benzene (mM)
Methane (mM)
Time (d)
Benzene
Methane

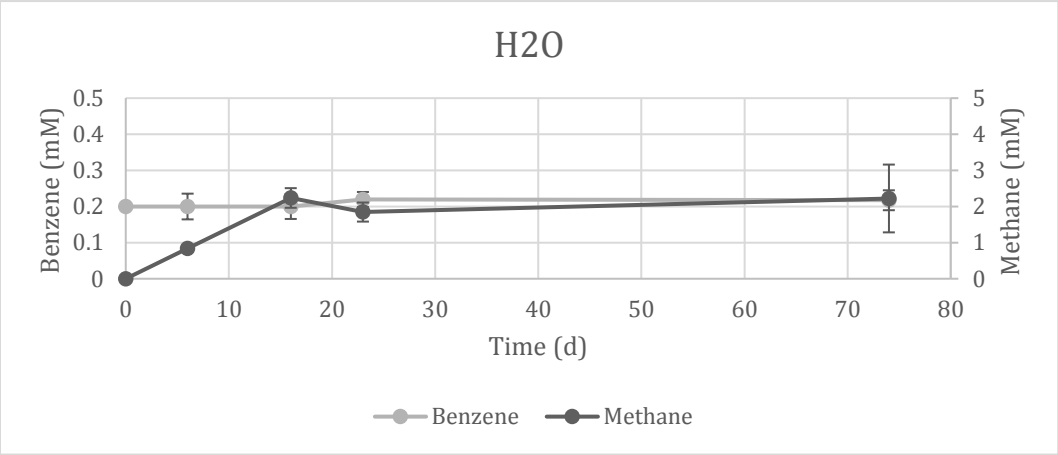
H2O
Benzene (mM)
Methane (mM)
Time (d)
Benzene
Methane

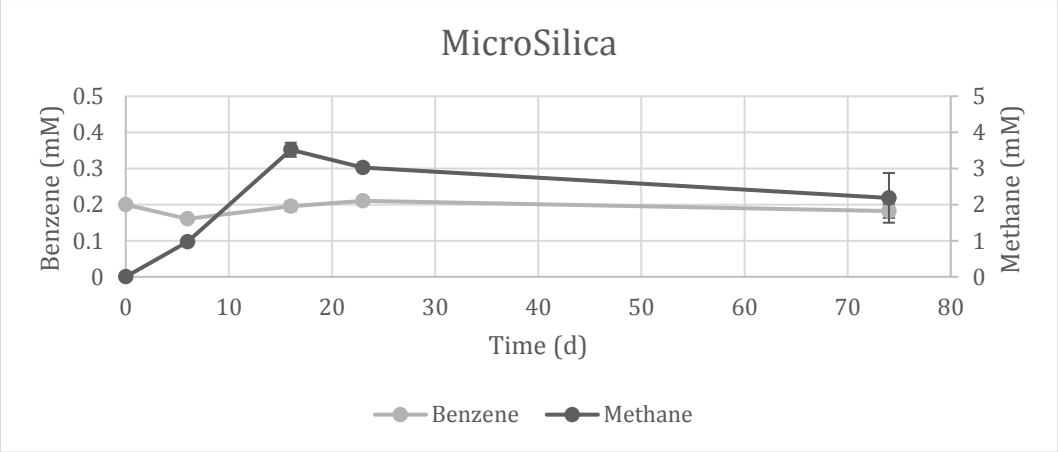
MicroSilica
Benzene (mM)
Methane (mM)
Time (d)
Benzene
Methane

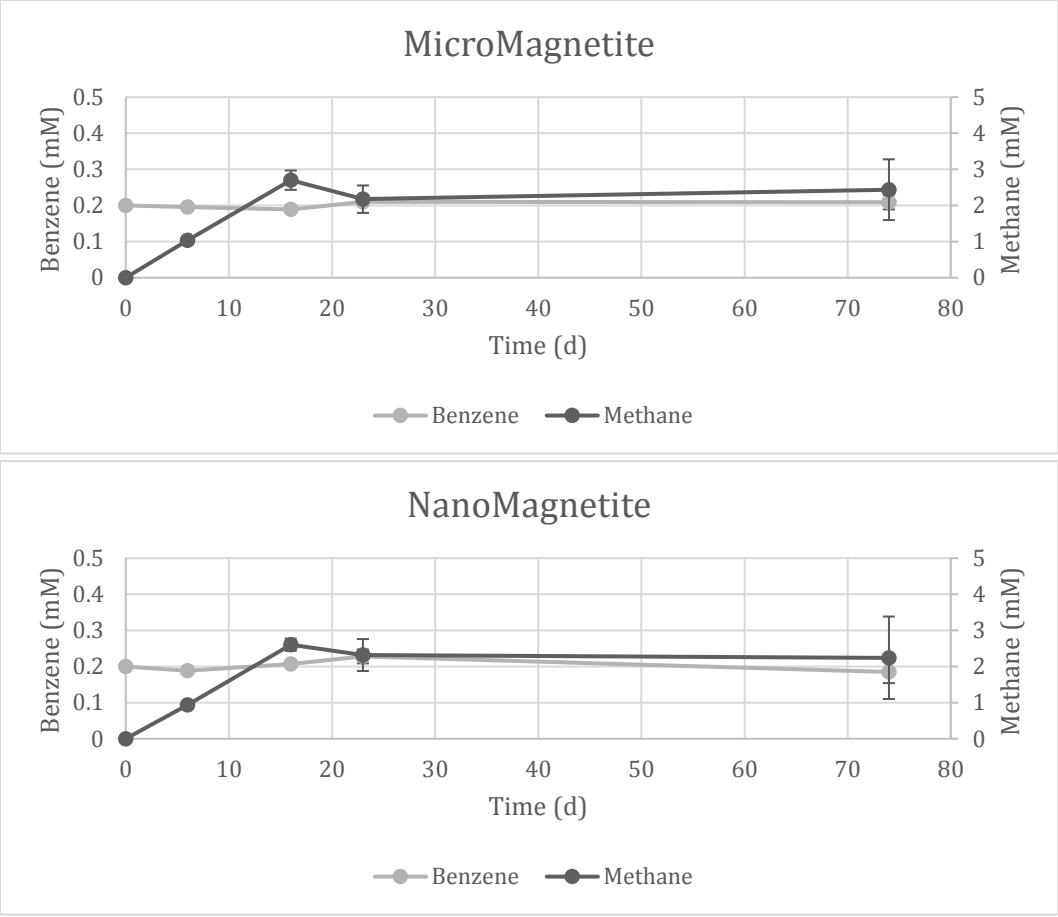

Figure 5-2. Degradation Curves of Live Iron-reducing Cultures

Triplicate live cultures treated with either silica or magnetite at micro and nano scales were monitored by headspace GC. Both methane and benzene levels were quantified over a period of 75 days. H2O represents untreated samples. MicroSilica represents samples containing microscale silica. NanoSilica represents samples containing nanoscale silica. MicroMagnetite represents samples containing microscale magnetite. NanoMagnetite represents samples containing nanoscale magnetite.

Table 5-2. Abiotic Benzene Sorption onto Amendment Materials.

No-culture Controls (10 mM)	Benzene Sorption (µM/d)
H2O	0.07
Microsilica	0.24
Nanosilica	0.21
Micromagnetite	0.13
Nanomagnetite	0.20

Abiotic controls were monitored by headspace GC, and sorption rates were calculated in order to attribute removal rates in live cultures to the microbes alone.

Table 5-3. Benzene Removal Metrics in Amended Cultures.

Treatments (10 mM)	Benzene Removal (μM/d)	Methane Production (μM/d)
Killed Control	0.05	1.05
H2O	0.23	29.60
Microsilica	0.24	29.07
Nanosilica	0.21	28.00
Micromagnetite	0.13	32.53
Nanomagnetite	0.20	29.87

Live cultures amended with micro or nano scale silica or magnetite were monitored by headspace GC over a period of 75 days, and removal rates were calculated as described previously (Lee & Ulrich, 2021).

Further considerations can be made in future experiments in terms of genetic and signaling analysis of biofilm formations. In terms of attached growth, single planktonic microbes that adopt a sessile lifestyle gain a multitude of fascinating emergent traits that can be relevant in a bioremediation context, and amendments such as magnetite that can potentiate these properties can be worthy avenues of study. Although not an anaerobic example, the *lux* genes of *Vibrio cholerae* can be quite illuminating in demonstrating how this growth shift occurs. For *V. cholerae*, quorum sensing is the key: the LuxS enzyme in this species synthesizes autoinducer molecules (Schauder, Shokat, Surette, & Bassler, 2001), which, upon reaching threshold concentrations, transduces a signal to activate a repressor of a repressor, allowing the transcription of virulence genes, including those responsible for biofilm formation (Hurley &

Bassler, 2017). Quorum signaling via the Agr system is critical for biofilm formation in *Staphylococcus* as well (Novick & Geisinger, 2008); this system regulates the production of phenol-soluble modulins that themselves regulate biofilm maturation (Le, et al., 2019), and quorum sensing also determines lectin and fimbriae expression in *Burkholderia cenocepacia* H111 (Inhulsen, et al., 2012). Environmental cues can also initiate biofilm formation. In *Pseudomonas*, the Wsp protein (O'Connor, Kuwada, Huangyutitham, Wiggins, & Harwood, 2012) receives signals indicative of surface contact, and transduces these signals to accumulate intracellular pools of secondary messenger cyclic diguanylate (Hengge, 2009) and activate the secretion of the adhesin LapA (Monds, Newell, Gross, & O'Toole, 2007). Signal transduction also regulates the production of the exopolysaccharide Psl in *P. aeruginosa* (Irie et al. 2010), and the secretion of pyoverdine, a siderophore, is determinative for its microcolony morphology (Yang, Nilsson, Gjermansen, Givskov, & Tolker-Nielsen, 2009), indicating the importance of nutritional factors, particularly ferric iron, in attachment and sessile growth (Harmsen, Yang, Pamp, & Tolker-Nielsen, 2010). The chemical signals and genetic mechanisms that underpin biofilm formation in benzene-degrading consortia would be worthy avenues for future study.

Future research may also investigate the microbial community in biofilm formation for benzene degraders, specifically the spatial distribution of primary degraders and their microbial partners. Upon colonization of a growth surface, bacteria in biofilms typically develop a species-dependent architecture, and the individual species of a consortium can change dramatically according to both environmental signals (Klausen, et al., 2003) and the integration of other community members (Nielsen, Tolker-Nielsen, Barken, & Molin, 2000; Wolfaardt, Lawrence, Robarts, Caldwell, & Caldwell, 1994). This conditional morphology will necessarily influence the metabolism of the consortium whole, and colocalization of different species on a surface can allow anaerobic respiration of said material (eg. ferric iron), as well as intercellular interactions

such as DIET (direct interspecies electron transfer); this may be achieved through adjacent cytochrome-to-cytochrome interactions (McGlynn, Chadwick, Kempes, & Orphan, 2015), long-range cable filaments (Vasquez-Cardenas, et al., 2015), nanowires (Liu X. , et al., 2019), and by the abiotic conductive subsurface itself (Chen, et al., 2014; Chen, et al., 2014; Kato, Hashimoto, & Watanabe, 2012).

However, biofilms are not merely beneficial for addressing the immediate nutritional and metabolic requirements of the member cells; they can be protective as well, expanding the tolerance or resistance of microbes against environmental factors. Although well-documented in pathogens, studies on genetic changes that characterize biofilm-based organisms in an anaerobic bioremediation context are still in their infancy. In a disease context, these can include antibiotics or immune defenses in the host organism (Vestby, Gronseth, Simm, & Nesse, 2020; Costerton, et al., 1987), but in an environmental context, these factors most likely manifest as mechanical stressors or toxic compounds. In either case, the mechanisms for doing so share commonalities, including the desensitizing behavior of extracellular materials (Flemming & Wingender, 2010), and inducible genetic changes in member organisms that result in a resistant phenotype (Park, et al., 2014). The foundation of the biofilm is the extracellular matrix (ECM) composed of extracellular polymeric substances (EPS) (Flemming & Wingender, 2010), which itself includes polysaccharides, proteins (both structural and enzymatically active), lipids, nucleic acids, and biopolymers (Wingender, Neu, & Flemming, 1999). This matrix immobilizes and stratifies constituent cells in a specific architecture, and can affect oxygen tolerance in strict anaerobes, as the EPS limits aerobic diffusion in the surface-adjacent layers (Beer, Stoodley, Roe, & Lewandowski, 1994) and establishes a respiratory gradient that culminates in microbial and metabolic heterogeneity within the biofilm architecture. Lipids for example appear to have a role in adhesion for *Acidithiobacillus ferrooxidans* and *Leptospirillum ferrooxidans*, both of which can attach to iron-containing minerals and facilitate bioleaching and

biocorrosion (Sand & Gehrke, 2006). The EPS itself can act as a nutrient bank and recycling depot, and be degraded enzymatically as seen in stromatolite-based cyanobacteria (Decho, Visscher, & Reid, 2005), although this degradation can also mediate detachment and subsequent colonization of new surfaces (Ma, et al., 2009; Petrova & Sauer, 2016). EPS structural proteins like fimbriae and polysaccharides like cellulose in *Escherichia coli* and *Salmonella typhimurium* can cross-link and stabilize biofilm (Zogai, Nimtz, Rohde, Bokranz, & Romling, 2001), bracing it against mechanical stress, to which most biofilms behave in a viscoelastic manner (Stoodley, Cargo, Rupp, Wilson, & Klapper, 2002). Furthermore, extracellular DNA can be the medium of horizontal gene transfer in biofilms, enhanced by proximity and sessility, as seen in the acquisition of antibiotic resistance genes in immobilized *Staphylococcus aureus* (Savage, Chopra, & O'Neill, 2013) and the increased copy number of resistance plasmids in biofilm-bound *Enterococcus faecalis* (Savage, Chopra, & O'Neill, 2013; Cook & Dunny, 2013). Biofilm bacteria also appear to be especially mutable and capable of rapid evolution, generating resistance strains at higher frequency than in their planktonic counterparts (Bae & Jeon, 2013; Yonezawa, et al., 2013). Therefore, future researchers could also investigate the resilience of anaerobic benzene-degrading biofilms to environmental stressors such as oxygen, or toxic byproducts of nitrate and sulfate-reduction such as nitrite and sulfide.

Other growth substrata may also be interrogated for effectiveness in promoting biofilm formation in benzene-degrading cultures. In a wastewater treatment context, the initial adhesion of anaerobic microbes to solid media appeared to be most effective when the surface support was both hydrophilic and positively charged (Siddique, Suraksa, Horprathum, Oaew, & Cheunkar, 2019). This preference for hydrophilic over hydrophobic surfaces was demonstrated in an array of anaerobic dechlorinating bacteria as well (Schie & Fletcher, 1999). In contrast, the membrane hydrophilicity of a myriad of *Clostridium difficile* strains did not appear to correlate with their

abilities to initiate biofilm formation on abiotic surfaces (Pantaleon, et al., 2018). *Shewanella putrefaciens* demonstrated differential growth patterns when adhered to smooth glass slides, glass wool, or graphite paper (Melzer, et al., 2015), with monolayer and eventual multilayer stacks on the former and single cell attachments observed on the latter two materials, albeit with increased cell density on graphite paper. Sulfate-reducing benzene-degrading microcosms have been observed to require a solid subsurface amendment such as sand, lava granules, or amberlite for stable, sustained benzene removal (Herrmann, Kleinsteuber, Neu, Richnow, & Vogt, 2008), and microscopic evaluations demonstrated substantial cell colonization in lava granules, possibly on account of its relatively high surface area (Herrmann, Kleinsteuber, Neu, Richnow, & Vogt, 2008), whereas amberlite did not host biomass, although this was thought to be an artifact of microscopy preparation. In a comparison of dehalogenating bacteria *Desulfomonile tiedjei*, *Syntrophomonas wolfei*, *Syntrophobacter wolinii*, and *Desulfovibrio* sp. strain G11, all of which have negatively charged membranes, it was found that a starvation nutritional state could significantly polarize *S. wolfei* and *Desulfovibrio* sp. strain G11 towards a sessile phenotype (Schie & Fletcher, 1999). Intriguingly, *S. wolfei* and *D tiedjei* adherence to the glass substratum also benefited with the addition of a coating of positively charged ferric iron (Schie & Fletcher, 1999), which allowed them to form monolayers over the surface. Metal-organic coatings comprising a zirconium nanometer-thick monolayer encompassing anaerobic *Morella thermoacetica* have also been demonstrated to improve survivability in oxic environments (Ji, Zhang, Liu, Yaghi, & Yang, 2018). Furthermore, solid amendments are not limited to being merely inert attachment points for sessile growth, but may also serve as active components of microbial metabolism. Zero-valent iron can support microbial growth for anaerobes such as *Geobacter sulfurreducens* ACL_{HF}, most likely using direct metal-to-microbe electron transfer based on outer membrane cytochromes OmcS and OmcZ (Tang, Holmes, Ueki, Palacios, & Lovley, 2019). Zero-valent iron on a micrometer scale,

in conjunction with fibrous activated carbon amendments, also supported anaerobic dechlorination processes, mediated mostly by quinones, chromene, and pyrone that allowed electron transfer (Vogel, Kopinke, & Mackenzie, 2019); the rate of this process was comparable to nanoscale zero-valent iron-amended cultures.

Other materials that could be applicable to benzene-degrading cultures have also been previously interrogated for their efficacy in promoting contaminant degradation. Carbonaceous amendments appear to bolster anaerobic metabolisms through biomass retention (Zhao, Zhang, Woodard, Nevin, & Lovley, 2015) and, if conductive, through mediation of DIET processes (Zhang, et al., 2018). Biochar for example can promote the growth of methanogens such as *Methanosaeta* and *Methanosarcina*, and reduces ammonium and acid load (Lu, Luo, Shao, & He, 2016; Wang, Li, Gao, & Wang, 2018), ultimately improving methane and hydrogen production (Sunyoto, Zhu, Zhang, & Zhang, 2016). These effects, as well as a more rapid recovery from souring, were also observed with carbon cloth (Dang, et al., 2016); the co-promotion of *Methanosarcina* and *Sporanaerobacter/Enterococcus* in this system suggests an important role of DIET in these processes. DIET also appears to play a part with granulated activated carbon amendments, which are more effective at improving anaerobic digestion performance when they are made more conductive with magnetite (Peng H. , et al., 2018). This is further illustrated with graphene, which is more conductive and more effective per-mass equivalent than activated carbon in augmenting methane production in anaerobic digesters (Lin, et al., 2017). Conductive carbon-based surfaces therefore appear to be a foundation for promoting syntrophy (Liu F. , et al., 2012), and are especially effective at increasing methanogen populations (Yang, et al., 2017) through the provision of a conductive link to DIET partners (Yan, et al., 2017; Wang, Li, Gao, & Wang, 2018). Carbon materials can also retain hydrogen partial pressure and mitigate acid shock (Zhao, Li, Quan, & Zhang, 2017), providing a suitable microenvironment for methanogenesis and DIET respectively to take place.

Table 5-4. Substrata candidates for further study in anaerobic degradation of priority contaminants.

Substratum Material	**Mechanism**	**Reference**
Lava granules	Increased surface area	(Herrmann, Kleinsteuber, Neu, Richnow, & Vogt, 2008)
Fe(III) coating on glass	Electropositivity	(Schie & Fletcher, 1999)
Zirconium nanosphere coat	Oxygen exclusivity	(Ji, Zhang, Liu, Yaghi, & Yang, 2018)
Zero-valent iron	Metal-microbe e^- transfer	(Tang, Holmes, Ueki, Palacios, & Lovley, 2019)
Magnetite	DIET	(Peng H. , et al., 2018)
Carbonaceous amendments	Biomass retention Acid shock resistance Methanogen growth DIET	(Zhao, Zhang, Woodard, Nevin, & Lovley, 2015) (Zhao, Li, Quan, & Zhang, 2017) (Lu, Luo, Shao, & He, 2016) (Peng, et al., 2018)

These amendments would therefore be appropriate candidates for further study, as materials that could potentially enhance the performance of benzene degrading cultures by providing growth surfaces and/or enhancing electroconductivity for iron-reducing metabolisms.

6 The Functional Characterization of Putative Benzene Carboxylase AbcA

6.1 Abstract

The cultivation of anaerobic benzene degrading cultures is a time-intensive process, due to the low redox potentials of the culturing conditions combined with the chemical stability of benzene itself. The *in vitro* synthesis of benzene-degrading enzymes as recombinant proteins, however, would remove the strenuous culturing requirements of these microcosms, and facilitate benzene removal capabilities in well-characterized model microorganisms such as *Escherichia coli*. This study investigates the possibility of synthesizing a fusion construct, containing a double tag with hexahistidine and biotin, with the putative benzene carboxylase gene from *Peptococcaceae* known as AbcDA. It was expected that soluble recombinant AbcDA protein, isolated and immobilized on resin, would be capable of degrading benzene in a cell-free environment. Although the AbcD subunit fusion construct was successfully cloned and expressed, the AbcA construct failed to materialize as soluble protein in spite of multiple expression attempts, and subsequent experiments could not take place. Future investigators may elect to use alternative expression systems more phylogenetically proximal to *Peptococcaceae* in order to maximize the possibility of generating soluble protein, or redesigning the fusion constructs with alternative amino acid tags that can further promote hydrophilicity and solubility.

6.2 Introduction

Isolation of primary degraders of benzene in mixed anaerobic cultures is affected by the intricate syntrophic relationships that allow such metabolisms (Hermann, et al., 2010; Morris, Henneberger, Huber, & Moissl-Eichinger, 2013; Gieg, Fowler, & Berdugo-Clavijo, 2014) and this fastidiousness complicates the generation of pure cultures, which is a critical prerequisite for the execution of classical microbiological manipulations. These difficulties are exacerbated by redox conditions that yield lower metabolic rates relative to oxygen (Vogt, Kleinsteuber, & Richnow, 2011; Abbasian, Lockington, Mallavarapu, & Naidu, 2015; Philipp & Schink, 2012), which increases the time burden required for cultivation - the doubling times of which can range from days to months (Meckenstock & Mouttaki, Anaerobic Degradation of Non-Substituted Aromatic Hydrocarbons, 2011). However, molecular and bioinformatics methods can bypass the necessity of traditional microbiological culturing techniques, and facilitate the identification of organisms and genes of interest. These methodologies have illuminated previously-inaccessible information about metabolic pathways and associated bacterial taxa in anaerobic benzene-degrading mixed cultures. The genes and the enzymatic pathways that facilitate the degradation of benzene are of great interest to remediators, and can be used as biomarkers for monitoring and prognosis or as active benzene-degrading entities *eo ipso*.

Benzene, a fully conjugated six-carbon annulene, is chemically and energetically stable due to the delocalization of pi electrons along the planar ring. Therefore, an activation step that disrupts this delocalization is critical for downstream oxidation. All benzene mineralization pathways proposed to date begin with the addition of a hydroxyl, methyl, or carboxyl group to one of the ring carbons in order to generate phenol, toluene, and benzoate, respectively (Vogt, Kleinsteuber, & Richnow, 2011). This tripartite divergence is the first step and most critical for the subsequent mineralization of benzene.

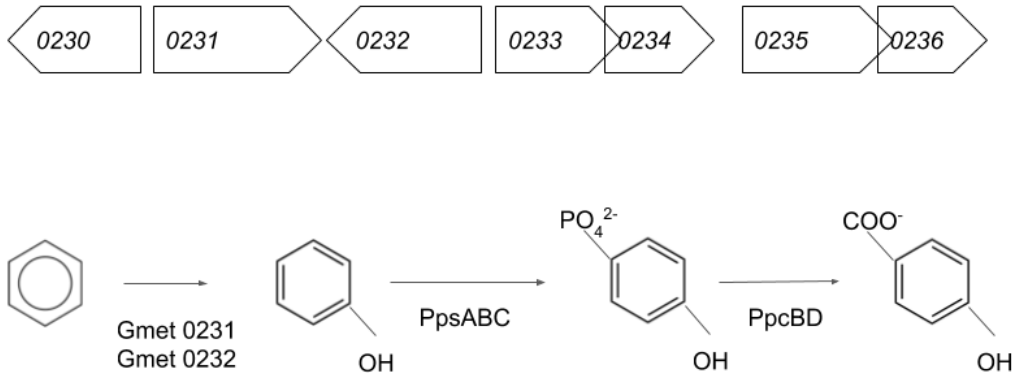

Figure 6-1. gmet Operon (Geobacter metallireducens) and Proposed Pathway for Hydroxylation-activated Benzene Degradation.

Gmet = Geobacter metallireducens; Pps = phenylphosphate synthase; Ppc = phenylphosphate carboxylase (T. Zhang et al. 2014, 2013).

The first purported method of benzene activation is hydroxylation, which produces phenol - evidence of hydroxylation has been observed in *Geobacter metallireducens* by SIP (stable isotope probing) (Zhang T. , et al., 2013), and putative hydroxylation-related genes have been identified by microarray analysis and mutagenesis (Zhang T. , et al., 2014). These genes, specified as *gmet 0231* and *gmet 0232*, are colocalized on one operon but have no homology to previously known hydroxylases. They may instead act as regulators for constitutively-expressed hydroxylases that may be activated post-transcription, or conversely, they may represent a yet uncharacterized enzymatic structure with benzene hydroxylase activity. Currently, there are no biochemical data available on gene products Gmet 0231 and Gmet 0232 that confirm hydroxylation activity. Reactions subsequent to hydroxylation include phosphorylation and

carboxylation, as well as a final addition of a coenzyme A to form benzoyl CoA (Zhang T. , et al., 2013).

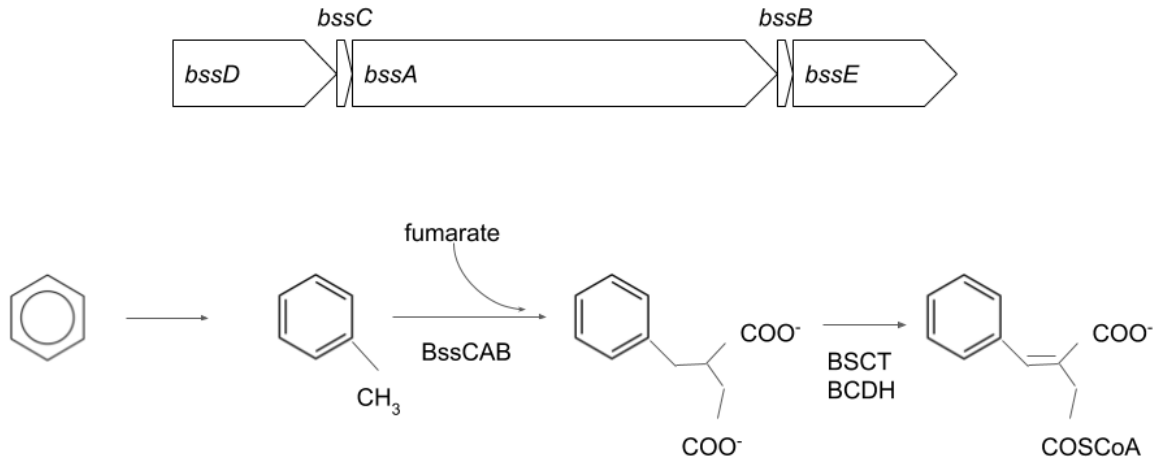

Figure 6-2. bss Operon (Thauera aromatica) and Proposed Pathway for Methylation-activated Benzene Degradation.

Bss = benzylsuccinate synthase; BSCT = benzylsuccinate-CoA transferase; BCDH = benzylsuccinate-CoA dehydrogenase (Heider, 2007; Leutwein & Heider, 2002; Leutwein & Heider, 2001; Leuthner & Heider, 2000).

The second purported method of benzene activation is methylation, which generates toluene. No benzene methylases have yet been documented, and although oxygenases have been observed in facultative benzene-toluene degraders such as *Pseudomonas veronii* (Morales, et al., 2016), such enzymes are less relevant to strict anaerobic metabolism. However, the downstream pathways of toluene degradation have been well-documented - *Thauera aromatica* for example has *bss* (benzylsuccinate synthase) genes (Heider, 2007; Meckenstock & Mouttaki, Anaerobic Degradation of Non-Substituted Aromatic Hydrocarbons, 2011), which add a

fumarate diester to the methyl group of toluene. The holoenzyme is composed of alpha, beta, and gamma subunits, and the operon that encodes them is highly conserved among anaerobic toluene degraders (Achong & Spormann, 2001). Benzyl-succinate is then oxidized to succinate-CoA with benzylsuccinate-CoA transferase, and benzylsuccinate-CoA dehydrogenase generates (E)-2-benzylidene-succinyl-CoA, which is subsequently converted by benzylidene-succinyl-CoA hydratase, alcohol dehydrogenase, and benzoyl-succinyl-CoA thiolase into benzoyl-CoA (Leuthner & Heider, 2000; Leutwein & Heider, 2001; Leutwein & Heider, 2002). Downstream beta-oxidation genes for benzylsuccinate are encoded on the *bbs* operon, which is co-activated with the *bss* operon by toluene exposure (Leuthner & Heider, 2000). The *bss* genes have seen use as biomarkers for BTEX-contaminated sites (Beller, Kane, Legler, & Alvarez, 2002; Winderl, Anneser, Griebler, Meckenstock, & Lueders, 2008), and hint at the potential of benzene-specific genes as monitoring tools for remediation programs that can indicate attenuation potential and set timelines for removal. Nevertheless, the enzyme that mediates the critical first methylation of benzene remains unknown.

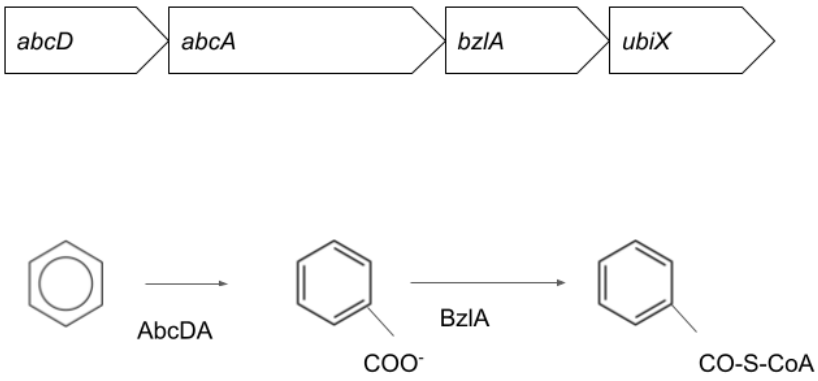

Figure 6-3. abc Operon (Peptococcaceae) and Proposed Pathway for Carboxylation-activated Benzene Degradation. Abc = anaerobic benzene carboxylase; Bzl = benzoyl-CoA ligase (Abu Laban et al. 2010; Luo et al. 2014).

The third purported method of benzene activation is carboxylation, which forms benzoate. Two candidate organisms have been identified that facilitate this reaction: *Peptococcaceae* (Abu Laban, Selesi, Rattei, Tischler, & Meckenstock, 2010) and *Ferroglobus placidus* (Holmes, Risso, Smith, & Lovley, 2012), although the latter is a hyperthermophilic archaeon with growth requirements that cause it to have limited relevance for *in situ* environmental bioremediation. The *Peptococcaceae* (F) are metabolically and morphologically diverse but obligately anaerobic, though proposals have been made to restrict the clade to *Peptococcus*-related genera (*Desulfonispora*, *Desulfitispora*, and *Desulfitibacter*) and uplift *Desulfitobacteriium*-type, *Desulfotomaculam*-type, and *Thermincola*-type taxa into novel families (Stackebrandt, 2014). The genes thought to be responsible for benzene oxidation in both these organisms are designated *abc* (anaerobic benzene carboxylase), and thought to include *abcD* and *abcA*

subunits. The *abcA* gene is homologous to *ppcD*, the delta subunit of phenyl-phosphate carboxylase (*ppc*) in *Thauera aromatica*, and is therefore a strong candidate for benzene activation. The *abc* operon also contains a *bzl* (benzoate-CoA ligase) gene, highly homologous to the benzoate-CoA ligase *bamY* in *Geobacter metallireducens* and used for the downstream catabolism of benzoate. The operon furthermore contains a *marR* (multiple antibiotic resistance) gene, which suggests a mechanism for regulatory activity based on the presence of organic solvents, and is functionally related to the putative properties of partner genes in the operon (Oh, Lee, & Kim, 2012; Silva, et al., 2018). AbcDA is the only gene product in all three proposed activation mechanisms that is both differentially expressed in the presence of benzene and homologous to known relevant carboxylase enzymes (Abu Laban, Selesi, Rattei, Tischler, & Meckenstock, 2010), making it a prime candidate for biochemical studies. Downstream of the *abcDA* genes on the operon are the *ubi* genes, which are carboxylases with homology to *abcA* that have been thoroughly studied (Marshall, et al., 2017; White, et al., 2015; Payer, et al., 2017). The *ubiD* gene product is a catechol decarboxylase which has been seen to require a prenylated flavin cofactor (Payer, et al., 2017) and the *ubiX* flavin prenyltransferase (White, et al., 2015). This can potentially complicate functional assays for AbcDA, which may have a quaternary structure that is more complex than simple heterodimers.

Other reports of benzene mineralization have been observed that have no links to any specific pathway. *Dechloromonas aromatica* RCB and *Azoarcus* DN11 have both exhibited degradative activity as isolated cultures, but neither of their genomes appear to host any canonical anaerobic benzene degradation genes, but rather oxygenases (Devanadera, et al., 2019; Salinero, et al., 2009). These organisms may therefore represent a novel mechanism of benzene oxidation that merits further study, and are especially unique due to their apparent ability to metabolize benzene as pure cultures, an uncommon property within the anaerobic benzene degradation scholarship. However, as no genes within their genomes have been

proposed as potential degradation mediators, there is little foothold for biochemical analyses of these two taxa at the current time.

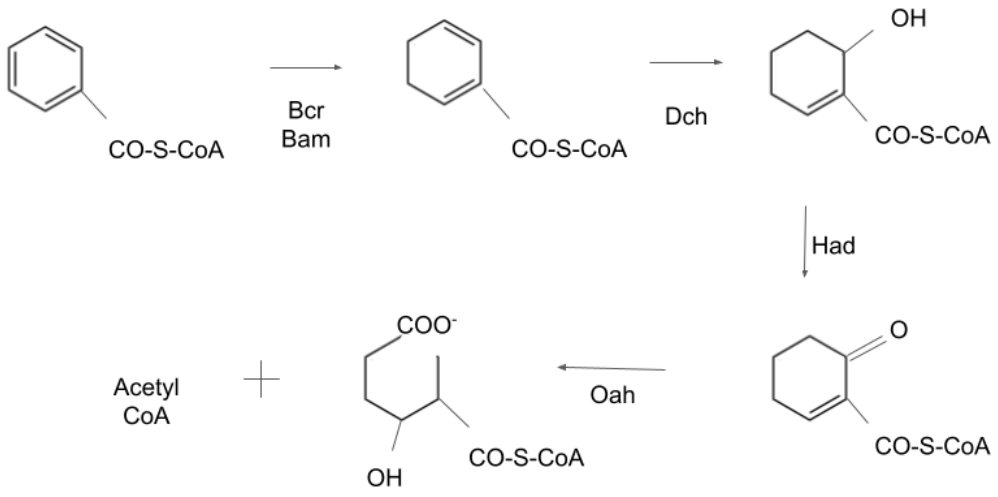

Figure 6-4. Beta-oxidation of central metabolite benzoyl-CoA (Pelotomaculum).

Bcr = benzoyl-CoA reductase; Dch = cyclohexa-1,5-diene-1-carboxyl-CoA hydratase; Had = 6-hydroxycyclohex-1-ene-1-carboxyl-CoA dehydrogenase; Oah = 6-oxo-cyclohex-1-ene-carbonyl-CoA hydrolase (Loffler, et al., 2011; Dong, et al., 2017).

Regardless of the initial benzene ring activation step, all three pathways (hydroxylation, methylation, and carboxylation) ultimately generate a central metabolite, benzoyl CoA (Vogt, Kleinsteuber, & Richnow, 2011; Meckenstock & Mouttaki, 2011). Benzoyl CoA is dearomatized by benzoyl CoA reductase (*bcr*) (Loffler, et al., 2011), and the resulting dienoyl CoA undergoes successive beta oxidation reactions with hydratases, dehydrogenases, and hydrogenases (Dong, et al., 2017) that generate acetyl CoA, a key input of biochemical energy cycles.

Although the downstream steps of benzene catabolism are relatively well-documented, it is nevertheless the initial activation of benzene that is most relevant to bioremediators; if it could be characterized and reconstituted *in vitro*, it would then be possible to bypass the slow and laborious process of cultivating mixed anaerobic culture for bioaugmentation. Of all three proposed activation mechanisms, therefore, it is carboxylation by the putative carboxylase enzyme AbcDA that shows the greatest apparent promise to be exploited as a mediator for benzene catabolism, as it could convert benzene into nontoxic benzoic acid in a single step. This study attempts to functionally characterize the putative benzene carboxylase AbcDA and confirm its proposed carboxylase activity in a biochemical context by synthesizing a recombinant fusion construct. Soluble expression of AbcA has not yet been accomplished in the literature, and is likely to require the use of genetic engineering techniques that promote hydrophilicity in the structure without compromising functional activity. If these sequence addendums could be established, AbcDA would be expected to be capable of soluble recombinant expression and purification from *Escherichia coli*. Biochemically, due to the homology with *ppc*, soluble fusion constructs were predicted to exhibit carboxylase activity and be able to convert benzene into benzoate in a cell-free system *in vitro*.

6.3 Methodology

6.3.1 Fusion Construct Creation

The *abcDA* genes (Abu Laban, Selesi, Rattei, Tischler, & Meckenstock, 2010), derived from the genome of *Peptococcaceae*, were fused with a hexaHis tag and cloned into a plasmid for transformation into *Escherichia coli*. Fusion constructs were generated with *abcD* and *abcA* genes with the tag in N and C terminal orientations. The tag consisted of a hexaHis sequence

implanted among a triple GGGGS linker sequence, based on the linkers present in major histocompatibility molecules and intended to promote solubility and flexibility (Chichili, Kumar, & Sivaraman, 2013; Chen, Zaro, & Shen, 2013).

Linker nucleic acid sequence 5'-3':

ggaggcgggggtagtcatcaccaccatcatcacggtgggggcggatctggtggcggagggtcg

Linker amino acid sequence N-C:

GGGGSHHHHHHGGGGSGGGGS

Primers were designed according to the parameters for gene-assembly extension PCR (polymerase chain reaction) and for generating cloning-competent ends (Wu, et al., 2006; Stemmer, Crameri, Ha, Brennan, & Heyneker, 1995; Polizzi & Kontroravdi, 2013; Xiong, et al., 2004). Melting temperatures were estimated by use of Thermofisher™ online cloning software ("Tm Calculator - CA" n.d.). Oligos were ordered from IDT™ via the MBSU core at the University of Alberta. p15TV-L was used as an expression vector, provided by the Edwards lab from the University of Toronto, and the restriction sites used were XbaI and XhoI on the 5' and 3' ends respectively. An *abc* operon cloned on p15TV-L was also provided by Edwards Lab from the University of Toronto for use as a template. Extension and assembly reactions were performed with Phusion© polymerase according to manufacturer instructions, and insertion into p15TV-L was performed with Infusion© polymerase. Early insertion attempts using FastDigest™ XbaI and XhoI enzymes did not result in transformants (data not shown). Transformations were performed with Invitrogen© DH5α and BL21 DE3 *E. coli*, and expression was executed in the latter strain within manufacturer-recommended parameters. Cloning success was confirmed by both colony-PCR (Costa & Weiner, 2006) and Sanger sequencing, the latter of which was executed by the DNA Core at the University of Alberta. Sequencing data and chromatograms

were analyzed by MEGA7 software (Kumar, Stecher, & Tamura, 2016). All molecular procedures were performed according to manufacturer protocols.

Oligo	Sequence
A Fi	GAT AAC AAT TCC CCT CTA GAA TGT ATC GTG ATT TAA GAG GAT ATA TTG
A Ri	TTA GCA GCC GGA TCC TCG AGA AAC CGG TAG TAA TCA AGA AAA AG
LA F	TCA CGG TGG GGG CGG ATC TGG TGG CGG AGG GTC GAT GTA TCG TGA TTT AAG AGG ATA TAT
AL R	GTG ATG ATG GTG GTG ATG CGA CCC TCC GCC ACC CTT TTT CTT GAT TAC TAC CGG TT
D Fi	GAT AAC AAT TCC CCT CTA GAA TGT ACG ATA AAC CGT CAA ACC
D Ri	TTA GCA GCC GGA TCC TCG AGG ATC ACA CCT TAG CAC GTT CT
LD F	CAT CAC CAC CAT CAT CAC GGT GGC GGA GGG TCG ATG TAC GAA AAA CCG TCA AAC
DL R	GTG ATG ATG GTG GTG ATG CGA CCC TCC GCC ACC AGA ACG TGC TAT GGT GTG ATC
L F	GAT AAC AAT TCC CCT CTA GAA TGT CAT CCT CGT CAT CCC ATC ACC ACC ATC ATC AC
L R	TTA GCA GCC GGA TCC TCG AGT CAA CTT GAC GAG GAT GAT GAG TGA TGA TGG TGG TGA TG

Table 6-1. Oligos used for Assembly of Fusion Constructs.

Letter designations represent, in 5'-3' order, the orientation of linker and gene or the forward and reverse infusion overhangs. L = linker; A = abcA; D = abcD; F = forward; R = reverse; i = Infusion overhang. Miscellaneous oligos used for unsuccessful attempts at amplicon generation are listed in Appendix A.

100 ng of individual amplicons were visualized by agarose gel electrophoresis with RedSafe™ stain, and 50 mg of protein lysates were visualized by acrylamide gels and Coomassie stain according to standard methods (Cold Spring Harbor Protocols). Generuler™ Plus and Prestained Pageruler™ were used as ladders for DNA and protein visualizations respectively. Nucleic acids were quantified by UV spectrophotometry via Nanodrop™ and amino acid concentrations were quantified by colorimetric Pierce™ BCA assay according to manufacturer protocols.

6.4 Results and Discussion

The majority of planned constructs were cloned successfully into p15TV-L vectors after multiple attempts at troubleshooting primer design and overlap extension PCR (Vallejo, Pogulis, & Pease, 2008) (Supplemental 6-1), but only AbcD constructs were successfully induced in BL21 DE3 strain *E. coli* (Figure 5-5). Because AbcA could not be expressed into the soluble fraction, enzymatic assays that required the holoenzyme could not be performed. Multiple iterations of induction and expression were attempted within manufacturer parameters and adapted from standard protocol recommendations (Sambrok & Russell, 2006). Cloning into pT7-7 vectors

using SalI and EcoRI restriction sites was also attempted using identical methods as well as manufacturer-recommended protocols with FastDigest™ restriction enzymes, but cloning into pT7-7 did not meet with success.

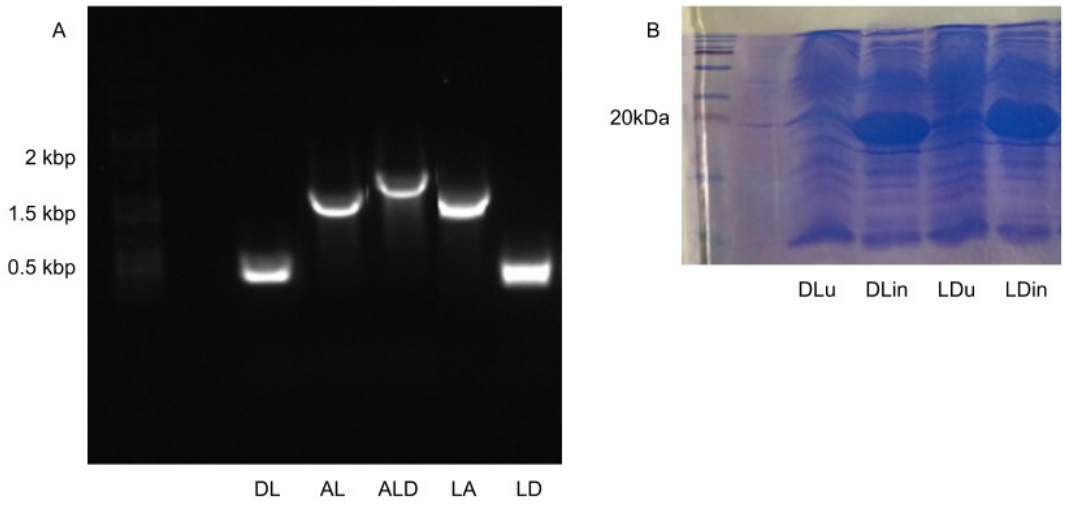

Figure 6-5. Fusion Constructs Visualized on Agarose and Acrylamide.

A: Agarose gel electrophoresis of fusion construct DNA. Fusion sequences were amplified from completed p15TV-L plasmids. Letter designations indicate order of sequence entities from 5'-3'. D = abcD; A = abcA; L = linker. DLA generation was unsuccessful. B: SDS-PAGE of fusion construct protein. Fusion constructs were induced for expression and visualized by acrylamide gel and Coomassie stain. D = abcD; L = linker; u = uninduced; in = induced (1 mM IPTG).

The failure of AbcA expression ultimately precluded all further biochemical experimentation, including planned enzymatic activity assays of purified AbcDA fusion construct enzymes immobilized on HisPur™ Ni^{2+}-coated beads, performed under anaerobic conditions in a similar

manner to previous enzymatic assays involving nitrite reductases (Harborne, Griffiths, Busby, & Cole, 1992). Further elucidation of the pathway and specific reaction mechanisms can be performed by using more technically-intensive enzymatic assays that can determine holoenzyme structures, small-molecule cofactors and substrate selectivity (Marshall, et al., 2017; White, et al., 2015; Payer, et al., 2017), based on previous studies that characterized the structure and function of UbiD and UbiX carboxylases. Importantly, these experiments required the use of overexpressed protein, which were not available for AbcA. Native protein capture of AbcA may potentially be possible using immobilized AbcD-bound bead beds co-incubated with cell lysates from anaerobic benzene-degrading microcosms, but this approach is necessarily destructive and requires a substantial volume of slow-growing, low-biomass cultures that have required years of careful anaerobic cultivation to be established; unfortunately, this investment of culture volume could not be justified for a preliminary assay in which the probability of a successful pulldown was unknown.

AbcA, the subunit of the AbcDA enzyme that exhibited the greatest homology to known carboxylase Ppc, could not be expressed in the soluble fraction as recombinant protein, despite multiple attempts at troubleshooting. Without this subunit, no downstream functional characterization assays were possible. Further attempts may try using different linker motifs to polarize the protein into the hydrophilic portion, including linkers based on humoral immunoglobulin sequences (Chichili, Kumar, & Sivaraman, 2013; Chen, Zaro, & Shen, 2013; Huston, et al., 1988), or attempt induction in bacteria that are specifically designed to accommodate *Clostridia* codons that are rarely seen in *E. coli* (Zdanovsky & Zdanovskaia, 2000) in order to promote more reliable expression of *Peptococcaceae* (*Bacteria-Firmicutes-Clostridia-Clostridiales*) proteins. Alternatively, the use of *Clostridium* expression toolkits (Joseph, Kim, & Sandoval, 2018) themselves, which have seen substantial recent advancements, may be more amenable to expression of AbcA due to greater phylogenetic

proximity relative to *E. coli*. Another complication may be that the AbcA enzyme required a multitude of cofactors from the operon to stabilize its protein structure. In this case, expression of multiple operon genes simultaneously would be necessary for the generation of AbcA. Regardless of the difficulties with expression, AbcDA continues to be the most promising putative enzyme for biochemical studies, and its potential merits further study. However, if soluble expression of AbcDA continues to elude researchers, they may instead attempt to functionally characterize Gmet 0231 and Gmet 0232 from *Geobacter metallireducens* (Zhang T. , et al., 2014) for recombinant expression, or perform studies that would determine the methylase responsible for toluene production.

Number	Genes, 5' 3'	Sequence	Notes
1	abcD-abcA	TACCGTGATCGTTTGCATGT	
2	abcD-abcA	TTTTCCTGACAGGGAGCATC	
3	abcA-bzlA	GGTTTGCTTTGACTGCACCT	
4	abcA-bzlA	GAATCCTGTCCTCCGTTTCA	(Luo, et al., 2014)
5	abcD F	ATGTACGATAAACCGTCAAACC	YP_158784/ GU357992.1 (Abu Laban, Selesi, Rattei, Tischler, & Meckenstock, 2010)
6	abcD R	AGAACGTGCTAAGGTGTGATC	
7	abcA F	ATGTATCGTGATTTAAGAGGATATATTG	
8	abcA R	CTTTTTCTTGATTACTACCGGTTT	
9	bssA F	ATGCCCTTTGTTGCCAGTAT	AF441130. (Fowler, Gutierrez-Zamora, Manefield, & Gieg, 2014; Kane, Beller, Legler,, & Anderson, 2002)
10	bssA R	GCTGCATTTCTTCGAAACCT	
11	Link F	GGTGGTGGTAGTCATCATCATCATCATCA TGGT	PCR assembly of linker for abcDA
12	Link R	ACTACCACCACCACTACCACCACCATGAT GATGATGATGATGA	PCR assembly of linker for abcDA
13	abcD R1	ATGACTACCACCACCAGAACGTGCTAAGG TGTGATC	Gene Assembly, overlap extension

14	Link F1	ACCTTAGCACGTTCTGGTGGTGGTAGTCATCATCAT	
15	Link R1	TAAATCACGATACATACTACCACCACCACTACCACC	
16	abcA F1	AGTGGTGGTGGTAGTATGTATCGTGATTTAAGAGGATATATTG	
17	abcA R1	ACTACCACCACCACCCTTTTTCTTGATTACTACCGGTTTAT	
18	Link F2	TAATCAAGAAAAAGGGTGGTGGTAGTCATCATCATCATCATCATGGT	
19	Link R2	CGGTTTATCGTACATACTACCACCACCACCACTACC	
20	abcD F1	GGTGGTGGTGGTAGTATGTACGATAAACCGTCAAACC	
21	abcA R1'	TGATGATGACTACCACCACCCTTTTTCTTGATTACTACCGGTTTAT	
22	Link F2'	CGGTAGTAATCAAGAAAAAGGGTGGTGGTAGTCATCATCAT	
23	DLA F	acgttctagaATGTACGATAAACCGTCAAACC	
24	DLA R	acgtctcgagctaCTTTTTCTTGATTACTACCGGTTT	
25	ALD F	acgttctagaATGTATCGTGATTTAAGAGGATATATTG	

26	ALD R	acgtctcgagctaAGAACGTGCTAAGGTGTGATC	
27	Link F3	actgtctagaatgGGTGGTGGTAGTCATCATCATC	
28	Link R3	acgtctcgagctaACTACCACCACCACTACCACC	
29	DLA F'	gctatctagaATGTACGATAAACCGTCAAACC	
30	abcD Ra	TGATGACTACCACCACCACCAGAACGTGCTAAGGTGTGAT	
31	abcD Rb	CACCACCATGATGATGATGATGATGACTACCACCACCACC	
32	abcD Rc	ACTACCACCACCACCACTACCACCACCACCATGATGATGATGA	
33	abcA F2	GTAGTGGTGGTGGTGGTAGTATGTATCGTGATTTAAGAGGATATAT	
34	Link R4	agcgaattcACTACCACCACCACCACTACCAC	
35	abcA F3	cctgaattcATGTATCGTGATTTAAGAGGATATAT	
36	abcD Fa	GTGGTAGTGGTGGTGGTGGTAGTATGTACGATAAACCGTCAAA	
37	abcD Fb	TCATCATCATCATGGTGGTGGTGGTAGTGGTGGTGGTGGTAGT	

38	abcD Fc	GGTGGTGGTGGTAGTCATCATCATCATCATCATGGTGGTG	
39	abcA R2	TGATGACTACCACCACCACCCTTTTTCTTGATTACTACCGGTT	
40	Link F4	cgtgaattcGGTGGTGGTGGTAGTCATCA	
41	abcA R3	acggaattcCTTTTTCTTGATTACTACCGGTT	
42	abcD Ra'	GGTGATGACTACCCCCGCCTCCAGAACGTGCTAAGGTGTGAT	
43	abcD Rb'	CGCCCCCACCGTGATGATGGTGGTGATGACTACCCCCG	
44	abcD Rc'	CGACCCTCCGCCACCAGATCCGCCCCCACCGTG	
45	abcA F2'	GTGGCGGAGGGTCGATGTATCGTGATTTAAGAGGATATAT	
46	abcD Fa'	GATCTGGTGGCGGAGGGTCGATGTACGATAAACCGTCAAA	
47	abcD Fb'	ACCATCATCACGGTGGGGATCTGGTGGCGGAGG	
48	abcD Fc'	GGAGGCGGGGGTAGTCATCACCACCATCATCACGGTGGG	
49	abcA R2'	GACTACCCCCGCCTCCCTTTTTCTTGATTACTACCGGTT	
50	Link F'	actgtctagaatgGGAGGCGGGGGTAGTC	

51	Link R'	cagtctcgagctaCGACCCTCCGCCAC	
52	abcA F4	GGAGGCGGGGGTAGTCATCACCACCATC ATCACGGTGGGG	
53	abcA R4	CGACCCTCCGCCACCAGATCCGCCCCCA CCGTGATGATGG	

Supplemental 6-1. Miscellaneous Primers used for Fusion Construct Assembly Attempts.

F = forward, R = reverse. For multiple subunit fusions, D = abcD, A = abcA, L = linker. Lowercase a/b/c indicate sets of gene assembly primers. Prime (') marks indicate alternative primers revised from originals. Lowercase sequence nucleotides indicate added restriction sites and overhangs, while capital nucleotides indicate template or gene sequences. bssA = benzyl-succinate synthase A; bssA primers were planned for biomarker monitoring purposes but ultimately not produced. All primers listed in Appendix A were ultimately unsuccessful at fusion construct generation.

7 Future Work

This thesis has focused primarily on iron-reducing cultures, which are relatively unique among anaerobic benzene degraders in Canada and deemed particularly worthy of experimental attention. However, many difficulties remain to be resolved in other redox conditions, particularly culturing complications from the generation of toxic metabolites, including the accumulation of sulfide in sulfate-reducing redox conditions (Reis, Almeida, Lemos, & Carrondo, 1992), and the accumulation of nitrite in nitrate-reducing redox conditions (Gitiafroz, 2012), both of which can be deleterious to the metabolic activity of anaerobic cultures.

7.1 Proposed Future Experiment: Eliminating Sulfide in Sulfate-reducing cultures with Powdered Activated Carbon

Anaerobic benzene degradation under sulfate-reducing conditions has previously been demonstrated in multiple cultures (Kleinsteuber, et al., 2008; Taubert, et al., 2012), including those sourced from Albertan sediments. Hydrogen sulfide is a toxic byproduct (Koster, Rinzema, Devegt, & Lettinga, 1986; Oleszkiewicz, Marstaller, & McCartney, 1989; Reis, Almeida, Lemos, & Carrondo, 1992) that results from sulfate-reduction processes (Okabe, Hielsen, & Charcklis, 1992; Reis, Almeida, Lemos, & Carrondo, 1992), and therefore negatively feedbacks against any continuous closed anaerobic system that utilizes sulfate as a TEA (terminal electron acceptor).

Both biotic and abiotic hydrogen sulfide removal techniques have been investigated in previous bioremediation studies. Biotic oxidation of sulfide using microbial fuel cells (Rakoczy, et al., 2013) and *Thiobacillus* cultures (Li & Khanal, 2016) have been reported, although the former showed relatively low removal rates, while the latter required the input of molecular oxygen. Abiotic sulfide-removal techniques have exhibited more efficacy, and have typically been achieved by precipitation by ferrous salts (Jin, Fallgren, Bilgin, Morris, & Barnes, 2007; Firer, Friedler, & Lahav, 2008) or adsorption (Ren et al. 2020) by carbonaceous materials (Zulkefli, et al., 2019) such as biochar (Oliveira, et al., 2020; Kanjanarong, et al., 2017; Sethupathi, et al., 2017). The effectiveness of carbon-based materials makes these amendments relevant to hydrogen sulfide removal in sulfate-reducing benzene-degrading cultures. This study evaluates the potential for one such adsorbent material, known as WPC PAC (WPC powdered activated carbon) (Calgon Carbon Corporation n.d.), derived from discarded plant material, to minimize

sulfide concentrations and propagate continued sulfate-reducing benzene degradation. Such processes have potential to be applied both *in situ* and *ex situ* to eliminate sulfide in growth media.

The mechanisms by which carbon-based materials remove sulfide have previously been documented (Oliveira, et al., 2020; Kanjanarong, et al., 2017; Sethupathi, et al., 2017), and are thought to involve chemisorption onto carboxyl and hydroxyl groups of the material surface. Previously-characterized biochars have achieved sulfide removal efficiencies of > 89% at initial sulfide concentrations of approximately 131 mg L^{-1} (Oliveira et al. 2020). According to the manufacturer, WPC PAC is composed of 18% ash and has an iodine number of 800, with a size profile of 99% < 0.150 mm and 90% < 0.045 mm (Calgon Carbon Corporation n.d.), but there are no metrics publicly available regarding pore size, pore volume, or BET (Brunauer–Emmett–Teller) surface area, of which 500-1500 m^2 g^{-1} is typical for carbonaceous materials (Menendez-Diaz & Martin-Gullon, 2006). The lack of these values makes the performance of WPC PAC difficult to predict, and complicates comparisons to previously reported biochars, so the chemical characterization of the WPC PAC is an additional priority for the study. Nevertheless, the WPC PAC is expected to sorb sulfide or provide growth substrates for microorganisms for biofilm formation (Carrel, et al., 2018), and promote benzene metabolism thereby. Hydrogen sulfide levels can be monitored using previously described standard methods for quantification of acid volatile sulfides (Rice, Bridgewater, American Public Health Association, American Water Works Association, & Water Environment Federation, 2012), with appropriate external standards.

7.2 Proposed Future Experiment: Eliminating Nitrite in Nitrate-reducing cultures with Recombinant NirBD Enzymes

Nitrite is a toxic byproduct that results from incomplete denitrification of nitrate (Vogt, Kleinsteuber, & Richnow, 2011). Although tolerance varies (Dou, Liu, & Hu, 2008), nitrite concentrations of 5-7 mM can be detrimental to the continued metabolic activity of previously reported benzene-degrading nitrate-reducing cultures (Gitiafroz, 2012), and is a common inhibitor of degradative ability in other anaerobic cultures (Musat, Wilkes, Behrends, Woebken, & Widdel, 2010; Jianlong, Horan, Stentiford, & Yi, 2001; Li, Vilcherrez, Carvajal-Arroyo, Sierra-Alvarez, & Field, 2016).

Nitrate-reducing benzene-degrading cultures have been described previously (Zaan, et al., 2012; Luo, et al., 2014; Coates, et al., 2001; Kasai, Takahata, Manefield, & Watanabe, 2006; Devanadera, et al., 2019), including microcosms sourced from Albertan clay and sand sediments. These microcosms had been cultivated using nitrate as a TEA and had exhibited steady nitrite accumulation over hundreds of days of maintenance. Continuously rising nitrite levels are detrimental to culture metabolism, and will ultimately require redress to counter activity inhibition. This phenomenon is conventionally countered by centrifugation and reconstitution with fresh mineral media, but this procedure may potentially be destructive to microbial populations due to the removal of soluble cofactors, infiltration of oxygen, and from the physical stress of centrifugation itself. Previous studies have attempted to pair nitrate-reducing benzene degradation to anammox processes (Peng S. , et al., 2017), but these cultures have also demonstrated inhibition of anammox by benzene at an IC50 of 18.2 mg/L i.e. 0.23 mM (Peng, et al., 2018). The sensitivity of anammox activity to the aromatic contaminant, and the

importance of avoiding introduction of non-native culture into the environment, makes coculture of anammox bacteria less ideal as a technique to complement bioaugmentation strategies.

The Albertan cultures referenced above did not contain endemic *Planctomycetes* anammox bacteria, although this does not preclude the presence of other Nir-expressing organisms. The continued presence of nitrite in these cultures suggests a lack of Nir-capable microorganism activity to fulfill complete denitrification. To maintain a completely Alberta-indigenous nitrate-reducing culture without coincubation with non-native culture, it may be necessary to pursue cell-free nitrite-removal methods.

One potential cell-free method is the use of enzymatic digestion. These processes have industrial scale precedents, and has been used in both batch and continuous processes for the removal of specific sugars from liquids (Grumezescu & Holban, 2019). The nitrite reductase of *Escherichia coli* K12 has previously been characterized, and enzymatic activity can be reconstituted *in vitro* by expression and translation of the *nirB* and *nirD* genes (Harborne, Griffiths, Busby, & Cole, 1992). NirBD is thus a well-characterized enzymatic system that can potentially be adapted for use in mixed culture. The NirB and NirD subunits, independently expressed as recombinant proteins and assembled *in vitro*, can function without incident between 4-30℃ (Harborne, Griffiths, Busby, & Cole, 1992) at a rate of approximately 250 nmol min^{-1} over 10 min with 2.4 mg enzyme i.e. 80 µL of 30 mg mL^{-1} enzyme extract. This is equivalent to a reduction in nitrite of 15 µM h^{-1} and 0.36 mM d^{-1} if the half-life of 4.8 mg of holoenzyme allowed for 24 h of persistence and activity. It is therefore reasonable to expect that purified, immobilized holoenzymes have the capacity to reduce nitrite load and toxicity in nitrate-reducing cultures. The impermanence of the enzymes further ensures that treated cultures are not contaminated by extraneous organisms or persistent biological materials.

8 Conclusions

The cultures described within this work are cultivars that have been painstakingly brought back to an active benzene-degrading state after multiple years of neglect. Within that timeframe, the cultures have been expanded in volume, diversified into new redox conditions, and investigated as to their degradation metrics, stoichiometries, and microbial communities (Figure 8-1).

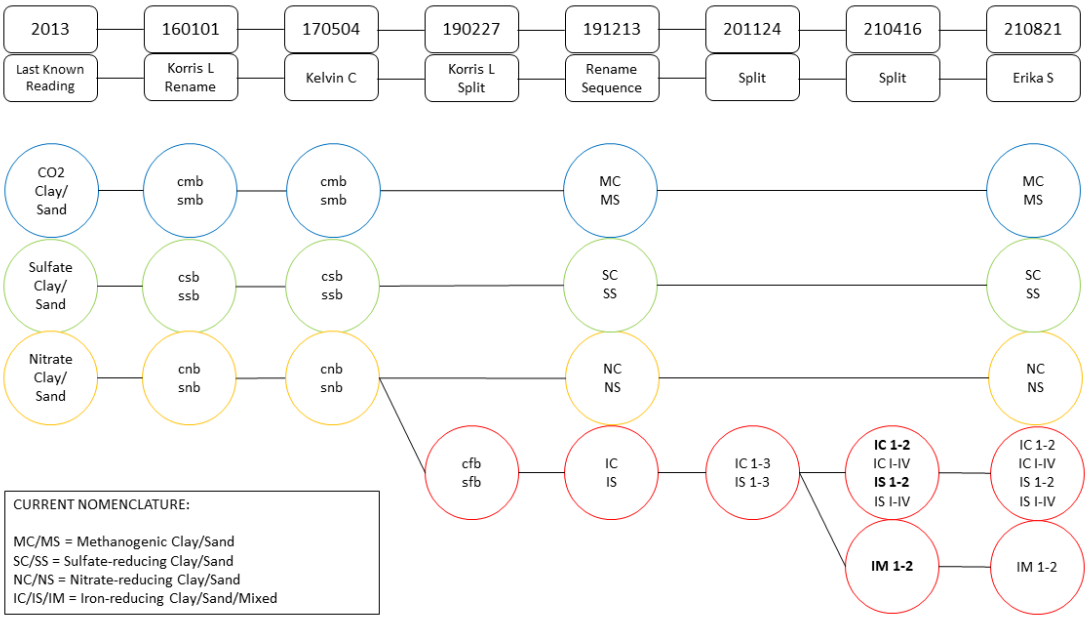

Figure 8-1. Pedigree of Anaerobic Benzene-degrading Cultures.

Timeline in yy/mm/dd format. Circles indicate microcosm subtypes, with numbers indicating replicates. Names (first name, last initial) indicate change in stewardship. 'Rename' indicates change in microcosm designation. 'Split' indicates a transfer of culture to new bottles or an establishment of a new redox condition. 'Sequence' indicates a 16S rRNA sequencing event.

The four main research questions presented in this thesis were as follows:

1. Can microbes native to Albertan sediments support anaerobic benzene degradation under methanogenic, sulfate-reducing, iron-reducing, and nitrate-reducing conditions?
2. What are the taxonomical details and genetic characteristics of Albertan iron-reducing benzene-degrading cultures?
3. Can Albertan iron-reducing benzene-degrading cultures be biostimulated with external chelators and magnetite subtypes?
4. What are the functional characteristics of the putative benzene carboxylase AbcDA?

This work has established that:

1. Microbes native to Albertan sediments have the capacity to degrade benzene under methanogenic, sulfate-reducing, nitrate-reducing, and iron-reducing conditions, with the latter two redox conditions yielding the highest rates of degradation. *Peptococcaceae/Thermincola* and *Geobacter* were identified in nitrate-reducing and iron-reducing cultures respectively.
2. *Geobacter metallireducens* was identified at a species level in active iron-reducing cultures as the most prominent taxon; however, putative hydroxylation genes *gmet 0231* and *gmet 0232* were not detected.
3. Iron-reducing cultures could be amended with chelators to improve benzene-degrading activity, although the specific mechanisms that underly this phenomenon remain unknown. The contribution of magnetite to iron-reducing processes remains an area of study with great potential.
4. Conventional dual-tag systems designed to promote protein solubility in the putative carboxylase AbcDA were insufficient for the task, and other avenues of genetic manipulation may be required to synthesize the construct for enzymatic assays.

The establishment and maintenance of benzene-degrading mixed anaerobic cultures is a highly technical, time-intensive process with a pervasive, polyfactorial *Nebel des Krieges* that complicates troubleshooting and optimization. The failures of multiple experiments detailed in this thesis are a testament to this crucial fact. This work is a six-year compilation of foundational studies representing a small portion of a major collaborative worldwide effort to defeat an infamously difficult and toxic environmental contaminant by biological means. Though the genesis of indigenous anaerobic benzene-degrading cultures with Albertan provenance has thus far been successful, much work remains with regards to their expansion and analysis; optimistically, the studies thus far will aid future researchers in their research initiatives and provide a solid basis for new benzene remediation strategies in Alberta.

BIBLIOGRAPHY

Abbasian, F., Lockington, R., Mallavarapu, M., & Naidu, R. (2015). A Comprehensive Review of Aliphatic Hydrocarbon Biodegradation by Bacteria. *Applied Biochemistry and Biotechnology, 176*(3), 670-99.

Abu Laban, N., Selesi, D., Jobelius, C., & Meckenstock, R. U. (2009). Anaerobic Benzene Degradation by Gram-Positive Sulfate-Reducing Bacteria. *FEMS Microbiology Ecology, 68*(3), 300-311.

Abu Laban, N., Selesi, D., Rattei, T., Tischler, P., & Meckenstock, R. (2010). Identification of Enzymes Involved in Anaerobic Benzene Degradation by a Strictly Anaerobic Iron-Reducing Enrichment Culture. *Environmental Microbiology, 12*(10), 2783-96.

Aburto-Medina, A., & Ball, A. S. (2015). Microorganism Involved in Anaerobic Benzene Degradation. *Annals of Microbiology*. doi:https://doi.org/10.1007/s13213-014-0926-8.

Achong, R., & Spormann, A. M. (2001). Benzylsuccinate Synthase of Azoarcus Sp. Strain T: Cloning, Sequencing, Transcriptional Organization, and Its Role in Anaerobic Toluene and M-Xylene Mineralization. *Journal of Bacteriology*. doi:https://doi.org/10.1128/jb.183.23.6763-6770.2001

Adams, G. O., Fufeyin, P. T., Okoro, S. E., & Ehinomen, I. (2020). Bioremediation, Biostimulation and Bioaugmention: A Review. *International Journal of Environmental Bioremediation & Biodegradation*. doi:https://doi.org/10.12691/ijebb-3-1-5

Akafia, M. M., Harrington, J. M., Bargar, J. R., & Duckworth, O. W. (2014). Metal Oxyhydroxide Dissolution as Promoted by Structurally Diverse Siderophores and Oxalate. *Geochimica et Cosmochimica Acta*. doi:https://doi.org/10.1016/j.gca.2014.06.024

Aklujkar, M., Krushkal, J., DiBartolo, G., Lapidus, A., Land, M., & Lovley, D. (2009). The genome sequence of Geobacter metallireducens: features of metabolism, physiology and regulation common and dissimilar to Geobacter sulfurreducens. *BMC Microbiology, 9*(109). doi:doi:10.1186/1471-2180-9-109

Alfreider, A., & Vogt, C. (2007). Bacterial Diversity and Aerobic Biodegradation Potential in a BTEX-Contaminated Aquifer. *Water, Air, and Soil Pollution*. doi:https://doi.org/10.1007/s11270-007-9390-4

Anderson, R. T., & Lovley, D. R. (1997). Ecology and Biogeochemistry of in Situ Groundwater Bioremediation. *Advances in Microbial Ecology*. doi:https://doi.org/10.1007/978-1-4757-9074-0_7

Austin, H., Delzelli, E., & Cole, P. (1989). Benzene and Leukemia: A Review of the Literature and a Risk Assessment. *Journal of Safety Research*. doi:https://doi.org/10.1016/0022-4375(89)90043-1

Azubuike, C. C., Chikere, C. B., & Okpokwasili, G. C. (2016). Bioremediation Techniques–classification Based on Site of Application: Principles, Advantages, Limitations and Prospects. *World Journal of Microbiology and Biotechnology*. doi:https://doi.org/10.1007/s11274-016-2137-x

Bae, J., & Jeon, B. (2013). Increased Emergence of Fluoroquinolone-Resistant Campylobacter Jejuni in Biofilm. *Antimicrobial Agents and Chemotherapy*. doi:https://doi.org/10.1128/aac.00995-13

Baek, G., Jung, H., Kim, J., & Lee, C. (2017). A Long-Term Study on the Effect of Magnetite Supplementation in Continuous Anaerobic Digestion of Dairy Effluent - Magnetic Separation and Recycling of Magnetite. *Bioresource Technology, 241*, 830-40.

Balch, W., Fox, G., Magrum, J., Woese, C., & Wolfe, R. (1979). Methanogens: Reevaluation of a Unique Biological Group. *Microbiological Reviews, 43*(2), 290-96.

Barona-Gomez, F., Lautru, S., Francou, F.-X., Leblond, P., Pernodet, J.-L., & Challis, G. (2006). Multiple Biosynthetic and Uptake Systems Mediate Siderophore-Dependent Iron Acquisition in Streptomyces Coelicolor A3(2) and Streptomyces Ambofaciens ATCC 23877. *Microbiology*(152 (11)), 3355-66.

Bedard, D. L., Ritalahti, K. M., & Loffler, F. E. (2007). The Dehalococcoides Population in Sediment-Free Mixed Cultures Metabolically Dechlorinates the Commercial Polychlorinated Biphenyl Mixture Aroclor 1260. *Applied and Environmental Microbiology, 73*(8), 2513-21.

Beer, D., Stoodley, P., Roe, F., & Lewandowski, Z. (1994). Effects of Biofilm Structures on Oxygen Distribution and Mass Transport. *Biotechnology and Bioengineering, 43*(11), 1131-38.

Beller, H. R., Kane, S. R., Legler, T. C., & Alvarez, P. J. (2002). A Real-Time Polymerase Chain Reaction Method for Monitoring Anaerobic, Hydrocarbon-Degrading Bacteria Based on a Catabolic Gene. *Environmental Science & Technology*(36), 3977-84.

Ben Hariz, I., Al Ayni, F., & Monser, L. (2014). Removal of Sulfur Compounds from Petroleum Refinery Wastewater through Adsorption on Modified Activated Carbon. *Water Science and Technology: A Journal of the International Association on Water Pollution Research, 70*(8), 1376-82.

Bertrand, J.-C., Caurnette, P., Lebaron, P., Matheron, R., Normand, P., & Sime-Ngando, T. (2015). *Environmental Microbiology: Fundamentals and Applications: Microbial Ecology.* Springer.

Bik, H. M., & Pitch Interactive. (2021). Phinch: An Interactive, Exploratory Data Visualization Framework for –Omic Datasets. doi:https://doi.org/10.1101/009944

Bork, P., & Zeller, G. (2021). From Microbiome Analysis Tools Developed at EMBL: https://microbiome-tools.embl.de/

Burland, S. M., & Edwards, E. A. (1999). Anaerobic Benzene Biodegradation Linked to Nitrate Reduction. *Applied and Environmental Microbiology*. doi:https://doi.org/10.1128/aem.65.2.529-533.1999

Byrne, J. M., Klueglein, N., Pearce, C., Rosso, K. M., Appel, E., & Kappler, A. (2015). Redox Cycling of Fe(II) and Fe(III) in Magnetite by Fe-Metabolizing Bacteria. *Science, 6229*, 1473-76.

Calgon Carbon Corporation. (2020). From WPC: https://www.calgoncarbon.com/products/wpc/

Canada Environment, & Canada Health and Welfare. (1993). *Benzene*. From https://www.canada.ca/content/dam/hc-sc/migration/hc-sc/ewh-semt/alt_formats/hecs-sesc/pdf/pubs/contaminants/psl1-lsp1/benzene/benzene-eng.pdf.

Carrel, M., Morales, V. L., Beltran, M. A., Derlon, N., Kaufmann, R., Morgenroth, E., & Holzner, M. (2018). Biofilms in 3D Porous Media: Delineating the Influence of the Pore Network Geometry, Flow and Mass Transfer on Biofilm Development. *Water Research, 134*, 280-91.

Cervini-Silva, J., & Sposito, G. (2002). Steady-State Dissolution Kinetics of Aluminum-Goethite in the Presence of Desferrioxamine-B and Oxalate Ligands. *Environmental Science & Technology, 36*(3), 337-42.

Cheah, S.-F., Kraemer, S. M., Cervini-Silva, J., & Sposito, G. (2003). Steady-State Dissolution Kinetics of Goethite in the Presence of Desferrioxamine B and Oxalate Ligands: Implications for the Microbial Acquisition of Iron. *Chemical Geology*. doi:https://doi.org/10.1016/s0009-2541(02)00421-7

Chen, S., Rotaru, A.-E., Liu, F., Philips, J., Woodard, T. L., Nevin, K. P., & Lovley, D. R. (2014). Carbon Cloth Stimulates Direct Interspecies Electron Transfer in Syntrophic Co-Cultures. *Bioresource Technology, 173*, 82-86.

Chen, S., Rotaru, A.-E., Shrestha, P. M., Malvankar, N. S., Liu, F., Fan, W., . . . Lovley, D. R. (2014). Promoting Interspecies Electron Transfer with Biochar. *Scientific Reports, 4*, 5019.

Chen, X., Zaro, J. L., & Shen, W.-C. (2013). usion Protein Linkers: Property, Design and Functionality. *Advanced Drug Delivery Reviews, 65*(10), 1357-69.

Chichili, V. P., Kumar, V., & Sivaraman, J. (2013). Linkers in the Structural Biology of Protein-Protein Interactions. *Protein Science*. doi:https://doi.org/10.1002/pro.2206

Childers, S. E., Ciugo, S., & Lovley, D. R. (2002). Geobacter Metallireducens Accesses Insoluble Fe(III) Oxide by Chemotaxis. *Nature, 6882*, 767-69.

Coates, J., Chakraborty, R., Lack, J., O'Connor, S., Cole, K., Bender, K., & Achenbach, L. (2001). Anaerobic Benzene Oxidation Coupled to Nitrate Reduction in Pure Culture by Two Strains of Dechloromonas. *Nature, 411*(6841), 1039-43.

Codd, R., Richardson-Sanchez, T., Teffer, T. J., & Gotsbacher, M. P. (2018). Advances in the Chemical Biology of Desferrioxamine B. *ACS Chemical Biology, 13*(1), 11-25.

Coelho, L., Alves, R., Monteiro, P., Huerta-Cepas, J., Freitas, A. T., & Bork, P. (2019). NG-meta-profiler: fast processing of metagenomes using NGLess, a domain-specific language. *Microbiome, 7*(84). doi:https://doi.org/10.1186/s40168-019-0684-8

Cold Spring Harbor Protocols. (n.d.). doi:https://doi.org/10.1101/pdb/.

Cook, L., & Dunny, G. (2013). ffects of Biofilm Growth on Plasmid Copy Number and Expression of Antibiotic Resistance Genes in Enterococcus Faecalis. *Antimicrobial Agents and Chemotherapy, 57*(4), 1850–56.

Corcoll, N., Osterlund, T., Sinclair, L., Eiler, A., Kristiansson, E., Backhaus, T., & Eriksson, M. (2017). Comparison of Four DNA Extraction Methods for Comprehensive Assessment of 16S rRNA Bacterial Diversity in Marine Biofilms Using High-Throughput Sequencing. *FEMS Microbiology Letters, 364*(14). doi:https://doi.org/10.1093/femsle/fnx139

Cornelis, P., Wei, Q., Andrews, S. C., & Vinckx, T. (2011). Iron Homeostasis and Management of Oxidative Stress Response in Bacteria. *Metallomics*. doi:https://doi.org/10.1039/c1mt00022e

Cornell, R. M., & Schwerfmann, U. (2003). *The Iron Oxides: Structure, Properties, Reactions, Occurrences and Uses.* John Wiley & Sons.

Costa, G. L., & Weiner, M. P. (2006). Colony PCR. *CSH Protocols, 1*. doi:https://doi.org/10.1101/pdb.prot4141

Costa, J. d., Cohen, D. R., Magalhaes, C. F., Hibbert, B., Archer, M., Myers, T. J., & Hand, S. J. (2020). Siderophore-Assisted Dissolution of Iron(III) Hydroxide Oxides from Iron-Rich Fossil Matrices. *ChemPlusChem, 85*(8), 1747-53.

Costea, P., Hildebrand, F., Arumugam, M., Backhed, F., Blaser, M., Bushman, F., . . . Bork, P. (2018). Enterotypes in the landscape of gut microbial community composition. *Nat Microbiol, 3*(1), 8-16. doi:10.1038/s41564-017-0072-8

Costerton, J. W., Cheng, K. J., Geesey, G. G., Ladd, T., Nickel, J. C., Dasgupta, M., & Marrie, T. J. (1987). Bacterial Biofilms in Nature and Disease. *Annual Review of Microbiology*. doi:https://doi.org/10.1146/annurev.mi.41.100187.002251

Crichton, R. R., & Charloteaux-Wauters, M. (1987). Iron Transport and Storage. *European Journal of Biochemistry*. doi:https://doi.org/10.1111/j.1432-1033.1987.tb11155.x

Crumbliss, A., & Harrington, J. M. (2009). Iron Sequestration by Small Molecules: Thermodynamic and Kinetic Studies of Natural Siderophores and Synthetic Model Compounds. *Advances in Inorganic Chemistry*. doi:https://doi.org/10.1016/s0898-8838(09)00204-9

Cruz Viggi, C., Rossetti, S., Fazi, S., Paiano, P., Majone, M., & Aulenta, F. (2014). Magnetite Particles Triggering a Faster and More Robust Syntrophic Pathway of Methanogenic Propionate Degradation. *Environmental Science & Technology, 48*(13), 7536-43.

Cunningham, J. A., Rahme, H., Hopkins, G. D., Lebron, C., & Reinhard, M. (2001). Enhanced in Situ Bioremediation of BTEX-Contaminated Groundwater by Combined Injection of Nitrate and Sulfate. *Environmental Science & Technology, 35*(8), 1663-70.

Cuss, C. W., Donner, M. W., Grant-Weaver, I., Noernberg, T., Pelletier, R., Sinnatamby, R. N., & Shotyk, W. (2018). Measuring the Distribution of Trace Elements amongst Dissolved Colloidal Species as a Fingerprint for the Contribution of Tributaries to Large Boreal Rivers. *The Science of the Total Environment*(642), 1242-51.

Da Silva, M., & Alvarez, P. J. (2007). Assessment of Anaerobic Benzene Degradation Potential Using 16S rRNA Gene-Targeted Real-Time PCR. *Environmental Microbiology, 9*(1), 72-80.

Dachis, B., Shaffer, B., & Thivierge, V. (n.d.). All's Well That Ends Well: Addressing End-of-Life Liabilities for Oil and Gas Wells. *SSRN Electronic Journal*. doi:https://doi.org/10.2139/ssrn.3044449

Dang, Y., Holmes, D. E., Zhao, Z., Woodard, T. L., Zhang, Y., Sun, D., . . . Lovley, D. R. (2016). Enhancing Anaerobic Digestion of Complex Organic Waste with Carbon-Based Conductive Materials. *Bioresource Technology*. doi:https://doi.org/10.1016/j.biortech.2016.08.114

Darzi, Y., Letunic, I., Bork, P., & Yamada, T. (2018). iPath3.0: interactive pathways explorer v3. *Nucleic Acids Res, 2*(46). doi:10.1093/nar/gky299

Decho, A. W., Visscher, P. T., & Reid, P. (2005). Production and Cycling of Natural Microbial Exopolymers (EPS) within a Marine Stromatolite. *Palaeogeography, Palaeoclimatology, Palaeoecology*. doi:https://doi.org/10.1016/j.palaeo.2004.10.015

Devanadera, A., Vejarano, F., Zhai, Y., Suzuki-Minakuchi, C., Ohtsubo, Y., Tsuda, M., . . . Nojiri, H. (2019). Complete Genome Sequence of an Anaerobic Benzene-Degrading Bacterium, Sp. Strain DN11. *Microbiology Resource Announcements, 8*(11). doi:https://doi.org/10.1128/MRA.01699-18

Dhungana, S., Anthony, C. R., & Hersman, L. E. (2007). Effect of Exogenous Reductant on Growth and Iron Mobilization from Ferrihydrite by the Pseudomonas Mendocina Ymp Strain. *Applied and Environmental Microbiology, 73*(10), 3428-30.

Dias, R., Silva, L., Eller, M., Oliveira, V., Paula, S., & Silva, C. (2014). Metagenomics: Library Construction and Screening Methods.

Dong, X., Droge, J., Toerne, C., Marozava, S., McHardy, A. C., & Meckenstock, R. U. (2017). Reconstructing Metabolic Pathways of a Member of the Genus Pelotomaculum Suggesting Its Potential to Oxidize Benzene to Carbon Dioxide with Direct Reduction of Sulfate. *FEMS Microbiology Ecology, 93*(3). doi:https://doi.org/10.1093/femsec/fiw254

D'Onofrio, A., Crawford, J. M., Stewart, E. J., Witt, K., Gabrish, E., Epstein, S., . . . Lewis, K. (2010). Siderophores from Neighboring Organisms Promote the Growth of Uncultured Bacteria. *Chemistry & Biology, 17*(3), 254-64.

Dou, J., Liu, X., & Hu, Z. (2008). Anaerobic BTEX Degradation in Soil Bioaugmented with Mixed Consortia under Nitrate Reducing Conditions. *Journal of Environmental Sciences, 20*(5), 585-92.

Economic Dashboard - Oil Production. (2019). From https://economicdashboard.alberta.ca/OilProduction

Edwards, E. A., & Grbic-Galic, D. (1994). Anaerobic Degradation of Toluene and O-Xylene by a Methanogenic Consortium. *Applied and Environmental Microbiology, 60*(1), 313-22.

Edwards, E., Wilis, E., Reinhard, M., & Grbic-Galic, D. (1992). Anaerobic Degradation of Toluene and Xylene by Aquifer Microorganisms under Sulfate-Reducing Conditions. *Applied and Environmental Microbiology, 58*(3), 794-800.

Endicott, N. P., Lee, E., & Wencewicz, T. A. (2017). Structural Basis for Xenosiderophore Utilization by the Human Pathogen Staphylococcus Aureus. *ACS Infectious Diseases, 3*(7), 542-53.

Farkas, E., Enyedy, E., Zekany, L., & Deak, G. (2001). Interaction between iron(II) and Hydroxamic Acids: Oxidation of iron(II) to iron(III) by Desferrioxamine B under Anaerobic Conditions. *Journal of Inorganic Biochemistry, 82*(2-3), 107-14.

Fassbinder, J. W., Staniek, H., & Vali, H. (1990). Occurrence of Magnetic Bacteria in Soil. *Nature, 6254*, 161-63.

Feinstein, L. M., Sul, W. J., & Blackwood, C. B. (2009). Assessment of Bias Associated with Incomplete Extraction of Microbial DNA from Soil. *Applied and Environmental Microbiology, 75*(16), 5428-33.

Feliciano, G. T., da Silva, A. J., Reguera, G., & Artacho, E. (2012). Molecular and Electronic Structure of the Peptide Subunit of Geobacter Sulfurreducens Conductive Pili from First Principles. *The Journal of Physical Chemistry, 116*(30), 8023–30.

Feliciano, G. T., Steidl, R. J., & Reguera, G. (2015). Structural and Functional Insights into the Conductive Pili of Geobacter Sulfurreducens Revealed in Molecular Dynamics Simulations. *Physical Chemistry Chemical Physics: PCCP, 17*(34), 22217-26.

Firer, D., Friedler, E., & Lahav, O. (2008). Control of Sulfide in Sewer Systems by Dosage of Iron Salts: Comparison between Theoretical and Experimental Results, and Practical Implications. *The Science of the Total Environment, 392*(1), 145–56.

Fishbein, L. (1985). An Overview of Environmental and Toxicological Aspects of Aromatic Hydrocarbons. IV. Ethylbenzene. *The Science of the Total Environment, 44*(3), 269-87.

Flemming, H.-C., & Wingender, J. (2010). The Biofilm Matrix. *Nature Reviews Microbiology, 8*(9), 623-33.

Fowler, J., Gutierrez-Zamora, M.-L., Manefield, M., & Gieg, L. M. (2014). Identification of Toluene Degraders in a Methanogenic Enrichment Culture. *FEMS Microbiology Ecology*. doi:https://doi.org/10.1111/1574-6941.12364

Fuchs, G., Boll, M., & Heider, J. (2011). Microbial Degradation of Aromatic Compounds - from One Strategy to Four. *Nature Reviews Microbiology, 9*(11), 803-16.

Gatesy, J. (2002). Molecular Evolution and Phylogenetics (M. Nei and S. Kumar). *Molecular Phylogenetics and Evolution*. doi:https://doi.org/10.1016/s1055-7903(02)00247-6

Gibson, J. J., Birks, S. J., Moncur, M., Yi, Y., Tattrie, K., Jasechko, S., . . . Eby, P. (2012). Isotopic and Geochemical Tracers for Fingerprinting Process-Affected Waters in the Oil Sands Industry: A Pilot Study. *CANM*.

Gieg, L., Fowler, J., & Berdugo-Clavijo, C. (2014). Syntrophic Biodegradation of Hydrocarbon Contaminants. *Current Opinion in Biotechnology, 27*, 21-29.

Gitiafroz, R. (2012). Microorganisms and Metabolic Pathways Involved in Anaerobic Benzene Biodegradation under Nitrate-Reducing Conditions.

Gorski, C. A., Nurmi, J. T., Tratnyek, P. G., Hofstetter, T. B., & Scherer, M. M. (2010). Redox Behavior of Magnetite: Implications for Contaminant Reduction. *Environmental Science & Technology, 44*(1), 55-60.

Government of Alberta. (2019). *Alberta Major Projects*. From https://majorprojects.alberta.ca/#/?sector=Oil-and-Gas&type=Oil-and-Gas_Distribution/Storage,Oil-and-Gas_Gas,Oil-and-Gas_Oil-Sands:-In-Situ,Oil-and-Gas_Oil-Sands:-Mining,Oil-and-Gas_Upgrader

Government of Canada. (1994). *Federal Contaminated Sites Inventory*. From https://www.tbs-sct.gc.ca/fcsi-rscf/home-accueil-eng.aspx

Government of Canada, Environment Canada, & Health Canada. (1993). *Benzene. Priority Substances List Assessment Report.*

Government of Canada, P. S. (2019). *Information Archivée Dans Le Web | Information Archived on the Web*. From http://publications.gc.ca/collections/collection_2013/bvg-oag/FA1-2-2002-0-eng.pdf

Grumezescu, A., & Holban, A.-M. (2019). *Milk-Based Beverages: Volume 9: The Science of Beverages.* Woodhead Publishing.

Guan, L., Kanoh, K., & Kamino, K. (2001). Effect of Exogenous Siderophores on Iron Uptake Activity of Marine Bacteria under Iron-Limited Conditions. *Applied and Environmental Microbiology, 67*(4), 1710-17.

Guan, L., Onuki, H., & Kamino, K. (2000). Bacterial Growth Stimulation with Exogenous Siderophore and Synthetic N-Acyl Homoserine Lactone Autoinducers under Iron-Limited and Low-Nutrient Conditions. *Applied and Environmental Microbiology, 66*(7), 2797-2803.

Gunter, K., Toupet, C., & Schupp, T. (1993). Characterization of an Iron-Regulated Promoter Involved in Desferrioxamine B Synthesis in Streptomyces Pilosus: Repressor-Binding Site and Homology to the Diphtheria Toxin Gene Promoter. *Journal of Bacteriology, 175*(11), 3295-3302.

Guo, F., & Zhang, T. (2013). Biases during DNA Extraction of Activated Sludge Samples Revealed by High Throughput Sequencing. *Applied Microbiology and Biotechnology, 97*(10), 4607-16.

Harborne, N. R., Griffiths, L., Busby, S. J., & Cole, J. A. (1992). Transcriptional Control, Translation and Function of the Products of the Five Open Reading Frames of the Escherichia Coli Nir Operon. *Molecular Microbiology*. doi:https://doi.org/10.1111/j.1365-2958.1992.tb01460.x

Harmsen, M., Yang, L., Pamp, S. J., & Tolker-Nielsen, T. (2010). An Update on Pseudomonas Aeruginosa Biofilm Formation, Tolerance, and Dispersal. *FEMS Immunology and Medical Microbiology, 59*(3), 253-68.

He, C., Lin, W., Zheng, X., Wang, C., Hu, Z., & Wang, W. (2019). Synergistic Effect of Magnetite and Zero-Valent Iron on Anaerobic Degradation and Methanogenesis of Phenol. *Bioresource Technology, 291*, 121874.

He, C.-S., He, P.-P., Yang, H.-Y., Li, L.-L., Lin, Y., Mu, Y., & Yu, H.-Q. (2017). Impact of Zero-Valent Iron Nanoparticles on the Activity of Anaerobic Granular Sludge: From Macroscopic to Microcosmic Investigation. *Water Research*, https://doi.org/10.1016/j.watres.2017.09.061.

Heider, J. (2007). Adding Handles to Unhandy Substrates: Anaerobic Hydrocarbon Activation Mechanisms. *Current Opinion in Chemical Biology, 11*(2), 188-94.

Heintz, D., Gallien, S., Wischgoll, S., Ullmann, A. K., Schaeffer, C., Kretzschmar, A. K., . . . Boll, M. (2009). Differential Membrane Proteome Analysis Reveals Novel Proteins Involved in the Degradation of Aromatic Compounds in Geobacter Metallireducens. *Molecular & Cellular Proteomics: MCP, 8*(9), 2159-69.

Hengge, R. (2009). Principles of c-Di-GMP Signalling in Bacteria. *Nature Reviews. Microbiology, 7*(4), 263-73.

Hermann, S., Kleinsteuber, S., Chatzinotas, A., Kuppardt, S., Lueders, T., Richnow, H.-H., & Vogt, C. (2010). Functional Characterization of an Anaerobic Benzene-Degrading Enrichment Culture by DNA Stable Isotope Probing. *Environmental Microbiology, 12*(2), 401-11.

Herrmann, S., Kleinsteuber, S., Neu, T. R., Richnow, H. H., & Vogt, C. (2008). Enrichment of Anaerobic Benzene-Degrading Microorganisms by in Situ Microcosms. *FEMS Microbiology Ecology, 63*(1), 94-106.

Hersman, L., Lloyd, T., & Sposito, G. (1995). Siderophore-Promoted. *Geochimica et Cosmochimica Acta*. doi:https://doi.org/10.1016/0016-7037(95)00221-k

Hider, R. C., & Kong, X. (2010). Chemistry and Biology of Siderophores. *Natural Product Reports*. doi:https://doi.org/10.1039/b906679a

Holden, A. A., Donahue, R. B., & Ulrich, A. C. (2011). Geochemical Interactions between Process-Affected Water from Oil Sands Tailings Ponds and North Alberta Surficial Sediments. *Journal of Contaminant Hydrology*. doi:https://doi.org/10.1016/j.jconhyd.2010.09.008

Holden, V. I., & Bachman, M. A. (2015). Diverging Roles of Bacterial Siderophores during Infection. *Metallomics*. doi:https://doi.org/10.1039/c4mt00333k

Holmen, B. A., Sison, J. D., Nelson, D. C., & Casey, W. H. (1999). Hydroxamate Siderophores, Cell Growth and Fe(III) Cycling in Two Anaerobic Iron Oxide Media Containing

Geobacter Metallireducens. *Geochimica et Cosmochimica Acta*. doi:https://doi.org/10.1016/s0016-7037(99)00023-x

Holmes, D. E., Risso, C., Smith, J. A., & Lovley, D. R. (2012). Genome-Scale Analysis of Anaerobic Benzoate and Phenol Metabolism in the Hyperthermophilic Archaeon Ferroglobus Placidus. *The ISME Journal, 6*(1), 146-57.

Holmes, D. E., Rotaru, A.-E., Ueki, T., Shrestha, P. M., Ferry, J. G., & Lovley, D. R. (2018). Electron and Proton Flux for Carbon Dioxide Reduction in Methanosarcina Barkeri During Direct Interspecies Electron Transfer. *Frontiers in Microbiology*. doi:https://doi.org/10.3389/fmicb.2018.03109

Huerta-Cepas, J., Szklarczyk, D., Heller, D., Hernandez-Plaza, A., Forslund, S., Cook, H., . . . Bork, P. (2019). eggNOG 5.0: a hierarchical, functionally and phylogenetically annotated orthology resource based on 5090 organisms and 2502 viruses. *Nucleic Acids Research*(47). doi:10.1093/nar/gky1085

Hurley, A., & Bassler, B. L. (2017). Asymmetric Regulation of Quorum-Sensing Receptors Drives Autoinducer-Specific Gene Expression Programs in Vibrio Cholerae. *PLoS Genetics, 13*(5), e1006826.

Huston, J., Levinson, D., Mudgett-Hunter, M., Tai, M. S., Novotny, J., Margolies, M. N., . . . Crea, R. (1988). Protein Engineering of Antibody Binding Sites: Recovery of Specific Activity in an Anti-Digoxin Single-Chain Fv Analogue Produced in Escherichia Coli. *Proceedings of the National Academy of Sciences of the United States of America, 85*(16), 5879-83.

Inhulsen, S., Aguilar, C., Schmid, N., Suppiger, A., Riedel, K., & Eberl, L. (2012). Identification of Functions Linking Quorum Sensing with Biofilm Formation in Burkholderia Cenocepacia H111. *MicrobiologyOpen, 1*(2), 225-42.

Irie, Y., Starkey, M., Edwards, A. N., Wozniak, D. J., Romeo, T., & Parsek, M. R. (2010). Pseudomonas Aeruginosa Biofilm Matrix Polysaccharide Psl Is Regulated Transcriptionally by RpoS and Post-Transcriptionally by RsmA. *Molecular Microbiology, 78*(1), 158-72.

Jackson, R. H., Cornish-Bowden, A., & Cole, J. A. (1981). Prosthetic Groups of the NADH-Dependent Nitrite Reductase from Escherichia Coli K12. *Biochemical Journal, 193*(3), 861-67.

Jansen, A. T., Sharma, J. S., Barbour, S. L., & Hendry, M. J. (n.d.). Effect of Strong Acid on Some Geotechnical Properties of Fine-Grained Soils. *In*, 891-95.

Ji, Z., Zhang, H., Liu, H., Yaghi, O., & Yang, P. (2018). Cytoprotective Metal-Organic Frameworks for Anaerobic Bacteria. *Proceedings of the National Academy of Sciences of the United States of America, 115*(42), 10582-87.

Jianlong, W., Horan, N., Stentiford, E. D., & Yi, Q. (2001). Anaerobic Degradation of 4-chlorophenol under Denitrifying Conditions with Nitrate as the Only Electron Acceptor. *Toxicological & Environmental Chemistry*. doi:https://doi.org/10.1080/02772240109359011

Jin, S., Fallgren, P. H., Bilgin, A., Morris, J. M., & Barnes, P. W. (2007). Bioremediation of Benzene, Ethylbenzene, and Xylenes in Groundwater under Iron-Amended, Sulfate-Reducing Conditions. *Environmental Toxicology and Chemistry / SETAC, 26*(2), 249-53.

Johann, H. (2007). Adding Handles to Unhandy Substrates: Anaerobic Hydrocarbon Activation Mechanisms. *Current Opinion in Chemical Biology, 11*(2), 188-94.

Johnstone, T. C., & Nolan, E. M. (2015). Beyond Iron: Non-Classical Biological Functions of Bacterial Siderophores. *Dalton Transactions, 44*(14), 6320-39.

Joseph, R. C., Kim, N. M., & Sandoval, N. R. (2018). Recent Developments of the Synthetic Biology Toolkit for Clostridium. *Frontiers in Microbiology*. doi:https://doi.org/10.3389/fmicb.2018.00154

Kane, S., Beller, H., L. T., & Anderson, R. (2002). Biochemical and genetic evidence of benzylsuccinate synthase in toluene-degrading, ferric iron-reducing Geobacter metallireducens. *Biodegradation, 13*(2), 149-154.

Kang, K., Schenkeveld, W. D., Biswakarma, J., Borowski, S. C., Hug, S. J., Hering, J. G., & Kraemer, S. M. (2019). Low Fe(II) Concentrations Catalyze the Dissolution of Various Fe(III) (hydr)oxide Minerals in the Presence of Diverse Ligands and over a Broad pH Range. *Environmental Science & Technology*. doi:https://doi.org/10.1021/acs.est.8b03909

Kang, Y. S., Risbud, S., Rabolt, J. F., & Stroeve, P. (1998). Synthesis and Characterization of Nanometer-Size Fe3O4and γ-Fe2O3Particles. *Chemistry of Materials*. doi:https://doi.org/10.1021/cm970904s

Kanjanarong, J., Giri, B. S., Jaisi, D. P., Oliveira, F. R., Boonsawang, P., Chaiprapat, S., . . . Khanal, S. K. (2017). Removal of Hydrogen Sulfide Generated during Anaerobic Treatment of Sulfate-Laden Wastewater Using Biochar: Evaluation of Efficiency and Mechanisms. *Bioresource Technology*. doi:https://doi.org/10.1016/j.biortech.2017.03.009

Kasai, Y., Takahata, Y., Manefield, M., & Watanabe, K. (2006). RNA-Based Stable Isotope Probing and Isolation of Anaerobic Benzene-Degrading Bacteria from Gasoline-Contaminated Groundwater. *Applied and Environmental Microbiology, 72*(5), 3586-92.

Kato, S., Hashimoto, K., & Watanabe, K. (2012). Methanogenesis Facilitated by Electric Syntrophy via (semi)conductive Iron-Oxide Minerals. *Environmental Microbiology, 14*(7), 1646-54.

Kato, S., Hashimoto, K., & Watanabe, K. (2012). Microbial Interspecies Electron Transfer via Electric Currents through Conductive Minerals. *Proceedings of the National Academy of Sciences of the United States of America, 109*(25), 10042-46.

Keller, A. H., Kleinsteuber, S., & Vogt, C. (2018). Anaerobic Benzene Mineralization by Nitrate-Reducing and Sulfate-Reducing Microbial Consortia Enriched From the Same Site: Comparison of Community Composition and Degradation Characteristics. *Microbial Ecology, 75*(4), 941-53.

Khan, A., Singh, P., & Srivastava, A. (2018). Synthesis, Nature and Utility of Universal Iron Chelator – Siderophore: A Review. *Microbiological Research*. doi:https://doi.org/10.1016/j.micres.2017.10.012

Kim, D., Duckworth, O. W., & Strathmann, T. J. (2009). Hydroxamate Siderophore-Promoted Reactions between iron(II) and Nitroaromatic Groundwater Contaminants. *Geochimica et Cosmochimica Acta.* doi:https://doi.org/10.1016/j.gca.2008.11.039

Kirschling, T. L., Gregory, K. B., Minkley, E. G., Lowry, G. V., & Tilton, R. D. (2010). Impact of Nanoscale Zero Valent Iron on Geochemistry and Microbial Populations in

Trichloroethylene Contaminated Aquifer Materials. *Environmental Science & Technology*. doi:https://doi.org/10.1021/es903744f

Klausen, M., Heydorn, A., Ragas, P., Lambertsen, L., Aaes-Jorgensen, A., Molin, S., & Tolker-Nielsen, T. (2003). Biofilm Formation by Pseudomonas Aeruginosa Wild Type, Flagella and Type IV Pili Mutants. *Molecular Microbiology, 48*(6), 1511-24.

Kleber, M., Eusterhues, K., Keiluweit, M., Mikutta, C., Mikutta, R., & Nico, P. S. (2015). Mineral–Organic Associations: Formation, Properties, and Relevance in Soil Environments. *Advances in Agronomy*. doi:https://doi.org/10.1016/bs.agron.2014.10.005

Kleinsteuber, S., Schleinitz, K. M., Breitfeld, J., Harms, H., RIchnow, H. H., & Vogt, C. (2008). Molecular Characterization of Bacterial Communities Mineralizing Benzene under Sulfate-Reducing Conditions. *FEMS Microbiology Ecology, 66*(1), 143-57.

Koster, I., Rinzema, A., Devegt, A., & Lettinga, G. (1986). Sulfide Inhibition of the Methanogenic Activity of Granular Sludge at Various pH-Levels. *Water Research*. doi:https://doi.org/10.1016/0043-1354(86)90121-1

Kraemer, S. M. (2004). Iron Oxide Dissolution and Solubility in the Presence of Siderophores. *Aquatic Sciences - Research Across Boundaries*. doi:https://doi.org/10.1007/s00027-003-0690-5

Kuhn, K. M., Maurice, P. A., Neubauer, E., Hofmann, T., & von der Kammer, F. (2014). Accessibility of Humic-Associated Fe to a Microbial Siderophore: Implications for Bioavailability. *Environmental Science & Technology, 48*(2), 1015-22.

Kumar, S., Stecher, G., & Tamura, K. (2016). MEGA7: Molecular Evolutionary Genetics Analysis Version 7.0 for Bigger Datasets. *Molecular Biology and Evolution, 33*(7), 1870-74.

Kunapuli, U., Lueders, T., & Meckenstock, R. U. (2007). The Use of Stable Isotope Probing to Identify Key Iron-Reducing Microorganisms Involved in Anaerobic Benzene Degradation. *The ISME Journal, 1*(7), 643-53.

Le, K., Villaruz, A. E., Zheng, Y., He, L., Fisher, E. L., Nguyen, T. H., & Ho, T. V. (2019). Role of Phenol-Soluble Modulins in Staphylococcus Epidermidis Biofilm Formation and Infection of Indwelling Medical Devices. *Journal of Molecular Biology, 431*(16), 3015-27.

Leang, C., Malvankar, N. S., Franks, A. E., Nevin, K. P., & Lovley, D. R. (2013). Engineering Geobacter Sulfurreducens to Produce a Highly Cohesive Conductive Matrix with Enhanced Capacity for Current Production. *Energy & Environmental Science*. doi:https://doi.org/10.1039/c3ee40441b

Lee, K., & Ulrich, A. (2021). Indigenous Microbial Communities in Albertan Sediments Are Capable of Anaerobic Benzene Biodegradation under Methanogenic, Sulfate-Reducing, Nitrate-Reducing, and Iron-Reducing Redox Conditions. *Water Environment Research: A Research Publication of the Water Environment Federation, 93*(4), 524-34.

Letunic, I., & Bork, P. (2019). Interactive Tree Of Life (iTOL) v4: recent updates and new developments. *Nucleic Acids Res, 2*(47). doi:10.1093/nar/gkz239

Leuthner, B., & Heider, J. (2000). Anaerobic Toluene Catabolism of Thauera Aromatica: The Bbs Operon Codes for Enzymes of β Oxidation of the Intermediate Benzylsuccinate. *Journal of Bacteriology*. doi:https://doi.org/10.1128/jb.182.2.272-277.2000

Leutwein, C., & Heider, J. (2001). Succinyl-CoA:(R)-Benzylsuccinate CoA-Transferase: An Enzyme of the Anaerobic Toluene Catabolic Pathway in Denitrifying Bacteria. *Journal of Bacteriology, 183*(14), 4288-95.

Leutwein, C., & Heider, J. (2002). (R)-Benzylsuccinyl-CoA Dehydrogenase of Thauera Aromatica, an Enzyme of the Anaerobic Toluene Catabolic Pathway. *Archives of Microbiology, 178*(6), 517-24.

Levar, C. E., Chan, C. H., Mehta-Kolte, M. G., & Bond, D. R. (2014). An Inner Membrane Cytochrome Required Only for Reduction of High Redox Potential Extracellular Electron Acceptors. *mBio, 5*(6), e02034.

Levar, C., Hoffman, C., Dunshee, A., & Toner, B. (2017). Redox potential as a master variable controlling pathways of metal reduction by Geobacter sulfurreducens. *ISME, 11*, 741–752. doi:doi:10.1038/ismej.2016.146

Li, G., Vilcherrez, D., Carvajal-Arroyo, J. M., Sierra-Alvarez, R., & Field, J. A. (2016). Exogenous Nitrate Attenuates Nitrite Toxicity to Anaerobic Ammonium Oxidizing (anammox) Bacteria. *Chemosphere, 144*, 2360-67.

Li, H., Chang, J., Liu, P., Fu, L., Ding, D., & Lu, Y. (2015). Direct Interspecies Electron Transfer Accelerates Syntrophic Oxidation of Butyrate in Paddy Soil Enrichments. *Environmental Microbiology, 17*(5), 1533-47.

Li, Y., & Khanal, S. K. (2016). *Bioenergy: Principles and Applications.* John Wiley & Sons.

Liermann, L. J., Kalinowski, B. E., Brantley, S. L., & Ferry, J. G. (2000). Role of Bacterial Siderophores in Dissolution of Hornblende. *Geochimica et Cosmochimica Acta*. doi:https://doi.org/10.1016/s0016-7037(99)00288-4

Lin, Q., Wang, Y., Yang, X., Ruan, D., Wang, S., Wei, X., & Qiu, R. (2018). Effect of Low-Molecular-Weight Organic Acids on Hematite Dissolution Promoted by Desferrioxamine B. *Environmental Science and Pollution Research International, 25*(1), 163-73.

Lin, R., Cheng, J., Zhang, J., Zhou, J., Cen, K., & Murphy, J. D. (2017). Boosting Biomethane Yield and Production Rate with Graphene: The Potential of Direct Interspecies Electron Transfer in Anaerobic Digestion. *Bioresource Technology*. doi:https://doi.org/10.1016/j.biortech.2017.05.017

Lindsay, W. L. (1988). Solubility and Redox Equilibria of Iron Compounds in Soils. *Iron in Soils and Clay Minerals*. doi:https://doi.org/10.1007/978-94-009-4007-9_3

Liu, F., Rotaru, A., Shrestha, P., Malvankar, N., Nevin, K., & Lovley, D. (2012). Promoting Direct Interspecies Electron Transfer with Activated Carbon. *Energy & Environmental Science*. doi:https://doi.org/10.1039/c2ee22459c

Liu, F., Rotaru, A.-E., Shrestha, P. M., Malvankar, N. S., Nevin, K. P., & Lovley, D. R. (2015). Magnetite Compensates for the Lack of a Pilin-Associated c-Type Cytochrome in Extracellular Electron Exchange. *Environmental Microbiology, 17*(3), 648-55.

Liu, X., Wang, S., Xu, A., Zhang, L., Liu, H., & Ma, L. Z. (2019). Biological Synthesis of High-Conductive Pili in Aerobic Bacterium Pseudomonas Aeruginosa. *Applied Microbiology and Biotechnology, 103*(3), 1535-44.

Liu, X., Zhuo, S., Rensing, C., & Zhou, S. (2018). Syntrophic Growth with Direct Interspecies Electron Transfer between Pili-Free Geobacter Species. *The ISME Journal, 12*(9), 2142-51.

Liu, Y., Wang, Z., Liu, J., Levar, C., Edwards, M. J., Babauta, J. T., & Kennedy, D. W. (2014). A Trans-Outer Membrane Porin-Cytochrome Protein Complex for Extracellular Electron Transfer by Geobacter Sulfurreducens PCA. *Environmental Microbiology Reports, 6*(6), 776-85.

Lloyd, J. R., Leang, C., Hodges-Myerson, A. L., Coppi, M. V., Cuifo, S., Methe, B., . . . Lovley, D. R. (2003). Biochemical and Genetic Characterization of PpcA, a Periplasmic c-Type Cytochrome in Geobacter Sulfurreducens. *Biochemical Journal*. doi:https://doi.org/10.1042/bj20020597

Loffler, C., Kuntze, K., Vazquez, J. R., Rugor, A., Kung, J. W., Bottcher, A., & Boll, M. (2011). Occurrence, Genes and Expression of the W/Se-Containing Class II Benzoyl-Coenzyme A Reductases in Anaerobic Bacteria. *Environmental Microbiology, 13*(3), 696-709.

Loring, J. S., Simanova, A. A., & Persson, P. (2008). Highly Mobile Iron Pool from a Dissolution-Readsorption Process. *Langmuir: The ACS Journal of Surfaces and Colloids, 24*(14), 7054-57.

Lovley, D. R. (1997). Potential for Anaerobic Bioremediation of BTEX in Petroleum-Contaminated Aquifers. *Journal of Industrial Microbiology and Biotechnology*. doi:https://doi.org/10.1038/sj.jim.2900246

Lovley, D. R. (2017). Syntrophy Goes Electric: Direct Interspecies Electron Transfer. *Annual Review of Microbiology, 71*, 643-64.

Lovley, D. R., & Phillips, E. J. (1988). Novel Mode of Microbial Energy Metabolism: Organic Carbon Oxidation Coupled to Dissimilatory Reduction of Iron or Manganese. *Applied and Environmental Microbiology, 54*(6), 1472-80.

Lovley, D. R., & Woodward, J. C. (1996). Mechanisms for Chelator Stimulation of Microbial Fe(III)-Oxide Reduction. *Chemical Geology*. doi:https://doi.org/10.1016/s0009-2541(96)00037-x

Lovley, D. R., Baedecker, M. J., Lonergan, D. J., Cozzarelli, I. M., Phillips, E. J., & Siegel, D. I. (1989). Oxidation of Aromatic Contaminants Coupled to Microbial Iron Reduction. *Nature*. doi:https://doi.org/10.1038/339297a0

Lovley, D. R., Coates, J. D., Blunt-Harris, E. L., Phillips, E. J., & Woodward, J. C. (1996). Humic Substances as Electron Acceptors for Microbial Respiration. *Nature*. doi:https://doi.org/10.1038/382445a0

Lovley, D. R., Coates, J. D., Woodward, J. C., & Phillips, E. (1995). Benzene Oxidation Coupled to Sulfate Reduction. *Applied and Environmental Microbiology, 61*(3), 953-58.

Lovley, D. R., Giovannoni, S. J., White, C., Champine, J. E., Phillips, E. J., Gorby, Y. A., & Goodwin, S. (1993). Geobacter Metallireducens Gen. Nov. Sp. Nov., a Microorganism Capable of Coupling the Complete Oxidation of Organic Compounds to the Reduction of Iron and Other Metals. *Archives of Microbiology, 159*(4), 336-44.

Lovley, D. R., Giovannoni, S. J., White, D. C., Champine, J. E., Phillips, J. P., Gorby, Y. A., & Goodwin, S. (1993). Geobacter Metallireducens Gen. Nov. Sp. Nov., a Microorganism Capable of Coupling the Complete Oxidation of Organic Compounds to the Reduction of Iron and Other Metals. *Archives of Microbiology*. doi:https://doi.org/10.1007/bf00290916

Lovley, D. R., Greening, R. C., & Ferry, J. G. (1984). Rapidly Growing Rumen Methanogenic Organism That Synthesizes Coenzyme M and Has a High Affinity for Formate. *Applied and Environmental Microbiology, 48*(1), 81-87.

Lovley, D. R., Woodward, J. C., & Chapelle, F. H. (1996). Rapid Anaerobic Benzene Oxidation with a Variety of Chelated Fe(III) Forms. *Applied and Environmental Microbiology, 62*(1), 288-91.

Lovley, D., & Phillips, E. (1986). Organic Matter Mineralization with Reduction of Ferric Iron in Anaerobic Sediments. *Applied and Environmental Microbiology, 51*(4), 683-89.

Lovley, D., & Walker, D. (n.d.). Geobacter Protein Nanowires. doi:https://doi.org/10.7287/peerj.preprints.27773

Lovley, D., Woodward, J., & Chapelle, F. (1994). Stimulated Anoxic Biodegradation of Aromatic Hydrocarbons using Fe(III) Ligands. *Nature, 370*(6485), 128-31.

Lovley, D., Woodward, J., & Chapelle, F. (1994). Stimulated Anoxic Biodegradation of Aromatic Hydrocarbons Using Fe(III) Ligands. *Nature*. doi:https://doi.org/10.1038/370128a0

Lu, F., Luo, C., Shao, L., & He, P. (2016). Biochar Alleviates Combined Stress of Ammonium and Acids by Firstly Enriching Methanosaeta and Then Methanosarcina. *Water Research*. doi:https://doi.org/10.1016/j.watres.2015.12.029

Lueders, T. (2017). The Ecology of Anaerobic Degraders of BTEX Hydrocarbons in Aquifers. *FEMS Microbiology Ecology*. doi:https://doi.org/10.1093/femsec/fiw220

Luo, F., Devine, C., & Edwards, E. (2016). Cultivating Microbial Dark Matter in Benzene-Degrading Methanogenic Consortia. *Environmental Microbiology, 18*(9), 2923-36.

Luo, F., Gitiafroz, R., Devine, C. E., Gong, Y., Hug, L. A., Raskin, L., & Edwards, E. A. (2014). Metatranscriptome of an Anaerobic Benzene-Degrading, Nitrate-Reducing Enrichment Culture Reveals Involvement of Carboxylation in Benzene Ring Activation. *Applied and Environmental Microbiology, 80*(14), 4095-4107.

Ma, L., Conover, M., Lu, H., Parsek, M. R., Bayles, K., & Wozniak, D. J. (2009). “Assembly and Development of the Pseudomonas Aeruginosa Biofilm Matrix. *PLoS Pathogens, 5*(3), e1000354.

Malvankar, N. S., Vargas, M., Nevin, K., Tremblay, P.-L., Evans-Lutterodt, K., Nykpanchuk, D., . . . Lovley, D. R. (2015). Structural Basis for Metallic-like Conductivity in Microbial Nanowires. *mBio, 6*(2), e00084.

Marshall, S. A., Fisher, K., Cheallaigh, A. N., White, M. D., Payne, K. A., Parker, D. A., . . . Leys, D. (2017). Oxidative Maturation and Structural Characterization of Prenylated FMN Binding by UbiD, a Decarboxylase Involved in Bacterial Ubiquinone Biosynthesis. *The Journal of Biological Chemistry, 292*(11), 4623-37.

Martins, M. C., Romao, C. V., Folgosa, F., Borges, P. T., Frazao, C., & Teixeira, M. (2019). How Superoxide Reductases and Flavodiiron Proteins Combat Oxidative Stress in Anaerobes. *Free Radical Biology & Medicine, 140*, 36-60.

McGlynn, S. E., Chadwick, G. L., Kempes, C. P., & Orphan, V. J. (2015). Single Cell Activity Reveals Direct Electron Transfer in Methanotrophic Consortia. *Nature, 526*(7574), 531-35.

McHale, C. M., Zhang, L., & Smith, M. T. (2012). Current Understanding of the Mechanism of Benzene-Induced Leukemia in Humans: Implications for Risk Assessment. *Carcinogenesis, 33*(2), 240-52.

Meckenstock, R. U., & Mouttaki, H. (2011). Anaerobic Degradation of Non-Substituted Aromatic Hydrocarbons. *Current Opinion in Biotechnology, 22*(3), 406-14.

Meckenstock, R. U., Boll, M., Mouttaki, H., Koelschbach, J. S., Tarouco, P. C., Weyrauch, P., . . . Himmelberg, A. M. (2016). Anaerobic Degradation of Benzene and Polycyclic Aromatic Hydrocarbons. *Journal of Molecular Microbiology and Biotechnology, 26*(1-3), 92-118.

Meckenstock, R. U., Elsner, M., Griebler, C., Lueders, T., Stumpp, C., Aamand, J., & Agathos, S. N. (2015). Biodegradation: Updating the Concepts of Control for Microbial Cleanup in Contaminated Aquifers. *Environmental Science & Technology, 49*(12), 7073-81.

Mehta, T. M., Coppi, V., Childers, S. E., & Lovley, D. R. (2005). Outer Membrane c-Type Cytochromes Required for Fe(III) and Mn(IV) Oxide Reduction in Geobacter Sulfurreducens. *Applied and Environmental Microbiology, 71*(12), 8634-41.

Melzer, S., Winter, G., Jager, K., Hubschmann, T., Hause, G., Syrowatka, F., . . . Muller, S. (2015). Cytometric Patterns Reveal Growth States of Shewanella Putrefaciens. *Microbial Biotechnology, 8*(3), 379-91.

Mende, D., Letunic, I., Huerta-Cepas, J., Li, S., Forslund, K., Sunagawa, S., & Bork, P. (2017). proGenomes: a resource for consistent functional and taxonomic annotations of prokaryotic genomes. *Nucleic Acids Res*(45). doi:10.1093/nar/gkw989

Menendez-Diaz, J. A., & Martin-Gullon, I. (2006). Chapter 1 Types of Carbon Adsorbents and Their Production. *Interface Science and Technology*. doi:https://doi.org/10.1016/s1573-4285(06)80010-4

Mikutta, C., & Kretzschmar, R. (2008). Synthetic Coprecipitates of Exopolysaccharides and Ferrihydrite. Part II: Siderophore-Promoted Dissolution. *Geochimica et Cosmochimica Acta*. doi:https://doi.org/10.1016/j.gca.2007.11.034

Milanese, A., Mende, D., Paoli, L., Salazar, G., Ruscheweyh, H.-J., Cuenca, M., . . . Sunagawa, S. (2019). Microbial abundance, activity and population genomic profiling with mOTUs2. *Nature Communications, 10*(1014).

Monds, R. D., Newell, P. D., Gross, R. H., & O'Toole, G. A. (2007). Phosphate-Dependent Modulation of c-Di-GMP Levels Regulates Pseudomonas Fluorescens Pf0-1 Biofilm Formation by Controlling Secretion of the Adhesin LapA. *Molecular Microbiology*. doi:https://doi.org/10.1111/j.1365-2958.2006.05539.x

Morales, M., Sentchilo, V., Bertelli, C., Komljenovic, A., Kryuchkova-Mostacci, N., Bourdiloud, A., & Linke, B. (2016). The Genome of the Toluene-Degrading Pseudomonas Veronii Strain 1YdBTEX2 and Its Differential Gene Expression in Contaminated Sand. *PloS One, 11*(11), e0165850.

Morris, B. E., Henneberger, R., Huber, H., & Moissl-Eichinger, C. (2013). Microbial Syntrophy: Interaction for the Common Good. *FEMS Microbiology Reviews, 37*(3), 384-406.

Musat, F., & Widdel, F. (2008). Anaerobic Degradation of Benzene by a Marine Sulfate-Reducing Enrichment Culture, and Cell Hybridization of the Dominant Phylotype. *Environmental Microbiology, 10*(1), 10-19.

Musat, F., Wilkes, H., Behrends, A., Woebken, D., & Widdel, F. (2010). Microbial Nitrate-Dependent Cyclohexane Degradation Coupled with Anaerobic Ammonium Oxidation. *The ISME Journal, 4*(10), 1290-1301.

Nales, M., Butler, B. J., & Edwards, E. A. (1998). Anaerobic Benzene Biodegradation: A Microcosm Survey. *Bioremediation Journal*. doi:https://doi.org/10.1080/10889869891214268

Natural Resources Canada. (2020). *Orphan and Abandoned Well Research Needs Assessment*. From https://www.nrcan.gc.ca/maps-tools-publications/publications/energy-publications/publications/orphan-and-abandoned-well-research-needs-assessment/22764

Neilands, J. B. (1995). Siderophores: Structure and Function of Microbial Iron Transport Compounds. *The Journal of Biological Chemistry, 270*(45), 26723-26.

Nevin, K. P., & Lovley, D. R. (2000). Lack of Production of Electron-Shuttling Compounds or Solubilization of Fe(III) during Reduction of Insoluble Fe(III) Oxide by Geobacter Metallireducens. *Applied and Environmental Microbiology, 66*(5), 2248-51.

Ngara, T., & Zhang, H. (2018). Recent Advances in Function-based Metagenomics Screening. *Genomics Proteomics Bioinformatics, 16*, 405-415.

Nielsen, A. T., Tolker-Nielsen, T., Barken, K. B., & Molin, S. (2000). Role of Commensal Relationships on the Spatial Structure of a Surface-Attached Microbial Consortium. *Environmental Microbiology, 2*(1), 59-68.

Noguchi, M., Kurisu, F., Kasuga, I., & Furumai, H. (2014). Time-Resolved DNA Stable Isotope Probing Links Desulfobacterales- and Coriobacteriaceae-Related Bacteria to Anaerobic Degradation of Benzene under Methanogenic Conditions. *Microbes and Environments / JSME, 29*(2), 191-99.

Novick, R. P., & Geisinger, E. (2008). Quorum Sensing in Staphylococci. *Annual Review of Genetics*. doi:https://doi.org/10.1146/annurev.genet.42.110807.091640

O'Connor, J. R., Kuwada, N. J., Huangyutitham, V., Wiggins, P. A., & Harwood, C. S. (2012). Surface Sensing and Lateral Subcellular Localization of WspA, the Receptor in a Chemosensory-like System Leading to c-Di-GMP Production. *Molecular Microbiology*. doi:https://doi.org/10.1111/mmi.12013

Oh, H. Y., Lee, J. O., & Kim, O. B. (2012). Increase of Organic Solvent Tolerance of Escherichia Coli by the Deletion of Two Regulator Genes, fadR and marR. *Applied Microbiology and Biotechnology, 96*(6), 1619-27.

Oka, A. R., Phelps, C. D., McGuinness, L. M., Mumford, A., Young, L. Y., & Kerkhof, L. J. (2008). Identification of Critical Members in a Sulfidogenic Benzene-Degrading Consortium by DNA Stable Isotope Probing. *Applied and Environmental Microbiology*. doi:https://doi.org/10.1128/aem.01082-08

Okabe, S. P., Hielsen, P. H., & Charcklis, W. G. (1992). Factors Affecting Microbial Sulfate Reduction by Desulfovibrio Desulfuricans in Continuous Culture: Limiting Nutrients and Sulfide Concentration. *Biotechnology and Bioengineering, 40*(6), 725-34.

Oleszkiewicz, J. A., Marstaller, T., & McCartney, D. M. (1989). Effects of pH on Sulfide Toxicity to Anaerobic Processes. *Environmental Technology Letters*. doi:https://doi.org/10.1080/09593338909384801

Oliveira, F. R., Surendra, K. C., Jiasi, D. P., Lu, H., Unal-Tosun, G., Sung, S., & Khanal, S. K. (2020). Alleviating Sulfide Toxicity Using Biochar during Anaerobic Treatment of Sulfate-Laden Wastewater. *Bioresource Technology, 301*, 122711.

Ondov, B. D., Bergman, N. H., & Phillippy, A. M. (2013). Krona: Interactive Metagenomic Visualization in a Web Browser. *Encyclopedia of Metagenomics*. doi:https://doi.org/10.1007/978-1-4614-6418-1_802-1

Orphan Inventory. (2021). From https://www.orphanwell.ca/about/orphan-inventory/.

Page, R. D., & Holmes, E. C. (2009). *Molecular Evolution: A Phylogenetic Approach.* John Wiley & Sons.

Pantaleon, V., Monot, M., Eckert, C., Hoys, S., Collignon, A., Janoir, C., & Candela, T. (2018). Clostridium Difficile Forms Variable Biofilms on Abiotic Surface. *Anaerobe, 53*, 34-37.

Park, A. J., Murphy, K., Krieger, J. R., Brewer, D., Taylor, P., Habash, M., & Khursigara, C. M. (2014). A Temporal Examination of the Planktonic and Biofilm Proteome of Whole Cell Pseudomonas Aeruginosa PAO1 Using Quantitative Mass Spectrometry. *Molecular & Cellular Proteomics, 13*(4), 1095-1105.

Payer, S. E., Marshall, S. A., Barland, N., Sheng, X., Reiter, T., Dordic, A., & Steinkellner, G. (2017). Regioselective Para-Carboxylation of Catechols with a Prenylated Flavin Dependent Decarboxylase. *Angewandte Chemie, 56*(44), 13893-97.

Peng, H., Zhang, Y., Tan, D., Zhao, Z., Zhao, H., & Xie, Q. (2018). Roles of Magnetite and Granular Activated Carbon in Improvement of Anaerobic Sludge Digestion. *Bioresource Technology*. doi:https://doi.org/10.1016/j.biortech.2017.10.047

Peng, J., & Wan, A. (1997). Measurement of Henry's Constants of High-Volatility Organic Compounds Using a Headspace Autosampler. *Environmental Science & Technology*. doi:https://doi.org/10.1021/es970240n

Peng, S., Han, X., Song, F., Zhang, L., Wei, C., Lu, P., & Zhang, D. (2018). Inhibition of Benzene, Toluene, Phenol and Benzoate in Single and Combination on Anammox Activity: Implication to the denitrification–Anammox Synergy. *Biodegradation*. doi:https://doi.org/10.1007/s10532-018-9853-x

Peng, S., Zhang, L., Zhang, D., Lu, P., Zhang, X., & He, Q. (2017). Denitrification Synergized with ANAMMOX for the Anaerobic Degradation of Benzene: Performance and Microbial Community Structure. *Applied Microbiology and Biotechnology, 101*(10), 4315-25.

Peralta, D. R., Adler, C., Corbalan, N. S., Garcia, E. C., Pomares, M. F., & Vincent, P. A. (2016). "Enterobactin as Part of the Oxidative Stress Response Repertoire. *PLOS ONE*. doi:https://doi.org/10.1371/journal.pone.0157799

Petrova, O. E., & Sauer, K. (2016). Escaping the Biofilm in More than One Way: Desorption, Detachment or Dispersion. *Current Opinion in Microbiology*. doi:https://doi.org/10.1016/j.mib.2016.01.004

Philipp, B., & Schink, B. (2012). Different Strategies in Anaerobic Biodegradation of Aromatic Compounds: Nitrate Reducers versus Strict Anaerobes. *Environmental Microbiology Reports, 4*(5), 469-78.

Poggenburg, C., Mikutta, R., Liebmann, P., Koch, M., & Guggenberger, G. (2018). Siderophore-Promoted Dissolution of Ferrihydrite Associated with Adsorbed and Coprecipitated Natural Organic Matter. *Organic Geochemistry*. doi:https://doi.org/10.1016/j.orggeochem.2018.09.004

Polizzi, K. M., & Kontroravdi, C. (2013). *Synthetic Biology.*

Powers, S. E., Hunt, C. S., Heermann, S. E., Corseuil, H. X., Rice, D., & Alvarez, P. J. (2001). *The Transport and Fate of Ethanol and BTEX in Groundwater Contaminated by Gasohol.* Critical Reviews in Environmental Science and Technology. doi:https://doi.org/10.1080/20016491089181

Qian, X., Mester, T., Morgado, L., Arakawa, T., Sharma, M. L., Inoue, K., . . . Lovley, D. R. (2011). Biochemical Characterization of Purified OmcS, a c-Type Cytochrome Required

for Insoluble Fe(III) Reduction in Geobacter Sulfurreducens. *Biochimica et Biophysica Acta, 1807*(4), 404-12.

Rabus, R., Boll, M., Heider, J., Meckenstock, R. U., Buckel, W., Einsle, O., & Ermler, U. (2016). Anaerobic Microbial Degradation of Hydrocarbons: From Enzymatic Reactions to the Environment. *Journal of Molecular Microbiology and Biotechnology, 26*(1-3), 5-28.

Rakoczy, J., Feisthauer, S., Wasmund, K., Bombach, P., Neu, T. R., Vogt, C., & Richnow, H. H. (2013). Benzene and Sulfide Removal from Groundwater Treated in a Microbial Fuel Cell. *Biotechnology and Bioengineering*. doi:https://doi.org/10.1002/bit.24979

Reardon, P. N., & Mueller, K. T. (2013). Structure of the Type IVa Major Pilin from the Electrically Conductive Bacterial Nanowires of Geobacter Sulfurreducens. *The Journal of Biological Chemistry, 288*(41), 29260-66.

Reguera, G., McCarthy, K. D., Mehta, T., Nicoll, J. S., Tuominen, M. T., & Lovley, D. R. (2005). Extracellular Electron Transfer via Microbial Nanowires. *Nature, 435*(7045), 1098-1101.

Reichard, P. U., Kretzschmar, R., & Kraemar, S. M. (2007). Dissolution Mechanisms of Goethite in the Presence of Siderophores and Organic Acids. *Geochimica et Cosmochimica Acta*. doi:https://doi.org/10.1016/j.gca.2006.12.022

Reis, M. A., Almeida, J. S., Lemos, P. C., & Carrondo, M. J. (1992). Effect of Hydrogen Sulfide on Growth of Sulfate Reducing Bacteria. *Biotechnology and Bioengineering*. doi:https://doi.org/10.1002/bit.260400506

Ren, B., Lyczko, N., Zhao, Y., & Nizihou, A. (2020). Alum Sludge as an Efficient Sorbent for Hydrogen Sulfide Removal: Experimental, Mechanisms and Modeling Studies. *Chemosphere, 248*, 126010.

Rice, E. W., Bridgewater, L., American Public Health Association, American Water Works Association, & Water Environment Federation. (2012). *Standard Methods for the Examination of Water and Wastewater.* Amer. Public Health Assn.

Ronan, J. >., Kadi, N., McMahon, S. A., Naismith, J. H., Alkhalaf, L. M., & Challis, G. L. (2018). "Desferrioxamine Biosynthesis: Diverse Hydroxamate Assembly by Substrate-Tolerant Acyl Transferase DesC. *Philosophical Transactions of the Royal Society of London. Series B, Biological Sciences*. doi:https://doi.org/10.1098/rstb.2017.0068

Rotaru, A., Shrestha, P., Liu, F., Markovaite, B., Chen, S., Nevin, K., & Lovley, D. (2014). Direct Interspecies Electron Transfer between Geobacter Metallireducens and Methanosarcina Barkeri. *Applied and Environmental Microbiology, 80*(15), 1599-4605.

Rotaru, A.-E., Shrestha, P., Liu, F., Shrestha, M., Shrestha, D., Embree, M., . . . Lovley, D. (2014). A New Model for Electron Flow during Anaerobic Digestion: Direct Interspecies Electron Transfer to Methanosaeta for the Reduction of Carbon Dioxide to Methane. *Energy Environ. Sci*. doi:https://doi.org/10.1039/c3ee42189a

Ruiz-Aguilar, G. M., Fernandez-Sanchez, J. M., Kane, S. R., Kim, D., & Alvarez, P. J. (2002). Effect of Ethanol and Methyl-Tert-Butyl Ether on Monoaromatic Hydrocarbon Biodegradation: Response Variability for Different Aquifer Materials under Various Electron-Accepting Conditions. *Environmental Toxicology and Chemistry / SETAC, 21*(12), 2631-39.

Saad, E. M., Sun, J., Chen, S., Borkiewicz, O. J., Zhu, M., Duckworth, O. W., & Tang, Y. (2017). Siderophore and Organic Acid Promoted Dissolution and Transformation of Cr(III)-Fe(III)-(oxy)hydroxides. *Environmental Science & Technology, 51*(6), 3223-32.

Sakai, N., Kurisu, F., Yagi, O., Nakajima, F., & Yamamoto, K. (2009). Identification of Putative Benzene-Degrading Bacteria in Methanogenic Enrichment Cultures. *Journal of Bioscience and Bioengineering, 108*(6), 501-7.

Salinero, K. K., Keller, K., Feil, W. S., Feil, H., Trong, S., Di Bartolo, G., & Lapidus, A. (2009). Metabolic Analysis of the Soil Microbe Dechloromonas Aromatica Str. RCB: Indications of a Surprisingly Complex Life-Style and Cryptic Anaerobic Pathways for Aromatic Degradation. *BMC Genomics, 10*, 351.

Sambrok, J., & Russell, D. W. (2006). Expression of Cloned Genes inE. coli Using IPTG-Inducible Promoters. *Cold Spring Harbor Protocols*. doi:https://doi.org/10.1101/pdb.prot4085

Sand, W., & Gehrke, T. (2006). Extracellular Polymeric Substances Mediate Bioleaching/biocorrosion via Interfacial Processes Involving iron(III) Ions and Acidophilic Bacteria. *Research in Microbiology, 157*(1), 49-56.

Sandy, M., & Butler, A. (2009). Microbial Iron Acquisition: Marine and Terrestrial Siderophores. *Chemical Reviews, 109*(10), 4580-95.

Savage, V. J., Chopra, I., & O'Neill, A. J. (2013). Staphylococcus Aureus Biofilms Promote Horizontal Transfer of Antibiotic Resistance. *Antimicrobial Agents and Chemotherapy, 57*(4), 1968-70.

Schauder, S., Shokat, K., Surette, M. G., & Bassler, B. L. (2001). The LuxS Family of Bacterial Autoinducers: Biosynthesis of a Novel Quorum-Sensing Signal Molecule. *Molecular Microbiology, 41*(2), 463-76.

Schie, P. M., & Fletcher, M. (1999). Adhesion of Biodegradative Anaerobic Bacteria to Solid Surfaces. *Applied and Environmental Microbiology, 65*(11), 5082-88.

Schloss, P. D., Westcott, S. L., Ryabin, T., Hall, J. R., Hartmann, M., Hollister, E. B., & Lesniewski, R. A. (2009). Introducing Mothur: Open-Source, Platform-Independent, Community-Supported Software for Describing and Comparing Microbial Communities. *Applied and Environmental Microbiology*. doi:https://doi.org/10.1128/aem.01541-09

Schwabe, R., Anke, M. K., Szymanska, K., Wiche, O., & Tischler, D. (2018). Analysis of Desferrioxamine-like Siderophores and Their Capability to Selectively Bind Metals and Metalloids: Development of a Robust Analytical RP-HPLC Method. *Research in Microbiology, 169*(10), 598-607.

Schwertmann, U. (1988). Some Properties of Soil and Synthetic Iron Oxides. *Iron in Soils and Clay Minerals*. doi:https://doi.org/10.1007/978-94-009-4007-9_9

Schwertmann, U., & Cornell, R. M. (2008). *Iron Oxides in the Laboratory: Preparation and Characterization.* John Wiley & Sons.

Sethupathi, S., Zhang, M., Rajapaksha, A., Lee, S., Nor, N. M., Mohamed, A., . . . Ok, Y. (2017). Biochars as Potential Adsorbers of CH4, CO2 and H2S. *Sustainability*. doi:https://doi.org/10.3390/su9010121

Shi, L., Dong, H., Reguera, G., Beyenal, H., Lu, A., Liu, J., . . . Fredrickson, J. K. (2016). Extracellular Electron Transfer Mechanisms between Microorganisms and Minerals. *Nature Reviews. Microbiology, 14*(10), 651-62.

Shrestha, P. M., Rotaru, A.-E., Summers, Z. M., Shrestha, M., Liu, F., & Lovley, D. R. (2013). Transcriptomic and Genetic Analysis of Direct Interspecies Electron Transfer. *Applied and Environmental Microbiology, 79*(7), 2397-2404.

Siddique, A., Suraksa, B., Horprathum, M., Oaew, S., & Cheunkar, S. (2019). Wastewater Biofilm Formation on Self-Assembled Monolayer Surfaces Using Elastomeric Flow Cells. *Anaerobe, 57*, 11-18.

Silva, C. M., Silva, D. N., da Costa, S. B., de Sa Almeida, J. S., Boente, R. F., Teixeira, F. L., . . . Lobo, L. A. (2018). Inactivation of MarR Gene Homologs Increases Susceptibility to Antimicrobials in Bacteroides Fragilis. *Brazilian Journal of Microbiology: [publication of the Brazilian Society for Microbiology], 49*(1), 200-206.

Silva, M. L., Da Silva, M., & Alvarez, P. (2002). Effects of Ethanol versus MTBE on Benzene, Toluene, Ethylbenzene, and Xylene Natural Attenuation in Aquifer Columns. *Journal of Environmental Engineering*. doi:https://doi.org/10.1061/(asce)0733-9372(2002)128:9(862)

Silva, M., Ruiz-Aguilar, G., & Alvarez, P. (2005). Enhanced Anaerobic Biodegradation of BTEX-Ethanol Mixtures in Aquifer Columns Amended with Sulfate, Chelated Ferric Iron or Nitrate. *Biodegradation*. doi:https://doi.org/10.1007/s10532-004-4897-5

Singh, I. (2020). *Alberta's Looming Multibillion-Dollar Orphan Wells Problem Prompts Auditor General Probe*. From https://www.cbc.ca/news/business/alberta-orphan-wells-liability-audit-review-1.5433603

Small, C., Ulrich, A., & Hashisho, Z. (2012). Adsorption of Acid Extractable Oil Sands Tailings Organics onto Raw and Activated Oil Sands Coke. *Journal of Environmental Engineering*. doi:https://doi.org/10.1061/(asce)ee.1943-7870.0000543

Stackebrandt, E. (2014). The Emended Family Peptococcaceae and Description of the Families Desulfitobacteriaceae, Desulfotomaculaceae, and Thermincolaceae. *The Prokaryotes*. doi:https://doi.org/10.1007/978-3-642-30120-9_364

Stemmer, W. P., Crameri, A., Ha, D., Brennan, T. M., & Heyneker, H. L. (1995). Single-Step Assembly of a Gene and Entire Plasmid from Large Numbers of Oligodeoxyribonucleotides. *Gene, 164*(1), 49-56.

Stoodley, P., Cargo, R., Rupp, C. J., Wilson, S., & Klapper, I. (2002). Biofilm Material Properties as Related to Shear-Induced Deformation and Detachment Phenomena. *Journal of Industrial Microbiology & Biotechnology, 29*(6), 361-67.

Stucki, J. W., Lee, K., Zhang, L., & Larson, R. A. (2002). Effects of Iron Oxidation States on the Surface and Structural Properties of Smectites. *Pure and Applied Chemistry*. doi:https://doi.org/10.1351/pac200274112145

Summers, Z. M., Fogarty, H. E., Leang, C., Franks, A. E., Malvankar, N. S., & Lovley, D. R. (2010). Direct Exchange of Electrons within Aggregates of an Evolved Syntrophic Coculture of Anaerobic Bacteria. *Science, 330*(6009), 1413-15.

Sunyoto, N. M., Zhu, M., Zhang, Z., & Zhang, D. (2016). Effect of Biochar Addition on Hydrogen and Methane Production in Two-Phase Anaerobic Digestion of Aqueous Carbohydrates Food Waste. *Bioresource Technology*. doi:https://doi.org/10.1016/j.biortech.2016.07.089

Suri, N., Gassara, F., Stanislav, P., & Voordouw, G. (2019). Microbially Enhanced Oil Recovery by Alkylbenzene-Oxidizing Nitrate-Reducing Bacteria. *Frontiers in Microbiology*. doi:https://doi.org/10.3389/fmicb.2019.01243

Swofford, D., Olsen, G., Waddell, P., & Hillis, D. (2021). Phylogenetic Inference. In *Molecular Systematics* (pp. 407-514). Sunderland: Sinauer Associates.

Tang, H.-Y., Holmes, D. E., Ueki, T., Palacios, P. A., & Lovley, D. R. (2019). Iron Corrosion via Direct Metal-Microbe Electron Transfer. *mBio*. doi:https://doi.org/10.1128/mBio.00303-19

Taubert, M., Vogt, C., Wubet, T., Kleinsteuber, S., Tarkka, M. T., Harms, H., . . . Seifert, J. (2012). Protein-SIP Enables Time-Resolved Analysis of the Carbon Flux in a Sulfate-Reducing, Benzene-Degrading Microbial Consortium. *The ISME Journal*. doi:https://doi.org/10.1038/ismej.2012.68

Tm Calculator. (2020). From https://www.thermofisher.com/ca/en/home/brands/thermo-scientific/molecular-biology/molecular-biology-learning-center/molecular-biology-resource-library/thermo-scientific-web-tools/tm-calculator.htm

Toth, C. R., Luo, F., Bawa, N., Webb, J., Guo, S., Dworatzek, S., & Edwards, E. A. (2021). Anaerobic Benzene Biodegradation Linked to the Growth of Highly Specific Bacterial Clades. *Environmental Science & Technology, 55*(12), 7970-80.

Ueki, T., Nevin, K. P., Rotaru, A.-E., Wang, L.-Y., Ward, J. E., Woodard, T. L., & Lovley, D. R. (2018). Geobacter Strains Expressing Poorly Conductive Pili Reveal Constraints on Direct Interspecies Electron Transfer Mechanisms. *mBio*. doi:https://doi.org/10.1128/mbio.01273-18

Ulrich, A. C., Donahue, R., & Biggar, K. (2007). *Suncor South Tailings Pond Research Project: 2006 Groundwater Monitoring and Soil Program Annual Report.* Suncor Energy Inc.

Ulrich, A., & Edwards, E. (2003). “Physiological and Molecular Characterization of Anaerobic Benzene-Degrading Mixed Cultures. *Environmental Microbiology*. doi:https://doi.org/10.1046/j.1462-2920.2003.00390.x

United States International Trade Commission, & United States Tariff Commission. (1984). *Synthetic Organic Chemicals: United States Production and Sales.*

Vallejo, A. N., Pogulis, R. J., & Pease, L. R. (2008). Microbiological Evidence for Fe(III) Reduction on Early Earth. *Nature, 395*(6697), 65-67.

Vargas, M., Kashefi, K., Blunt-Harris, E., & Lovley, D. (1998). Microbiological Evidence for Fe(III) Reduction on Early Earth. *Nature, 6697*, 65-97.

Vasquez-Cardenas, D., van de Vossenberg, J., Polerecky, L., Malkin, S. Y., Schauer, R., Hidalgo-Martinez, S., . . . Boschker, H. T. (2015). Microbial Carbon Metabolism Associated with Electrogenic Sulphur Oxidation in Coastal Sediments. *The ISME Journal, 9*(9), 1966-78.

Vestby, L. K., Gronseth, T., Simm, R., & Nesse, L. L. (2020). Bacterial Biofilm and Its Role in the Pathogenesis of Disease. *Antibiotics (Basel, Switzerland)*. doi:https://doi.org/10.3390/antibiotics9020059

Villatoro-Monzon, W. R., Morales-Ibarria, M. G., Velazquez, E. K., Ramirez-Saad, H., & Razo-Flores, E. (2008). Benzene Biodegradation under Anaerobic Conditions Coupled with Metal Oxides Reduction. *Water, Air, and Soil Pollution*. doi:https://doi.org/10.1007/s11270-008-9643-x

Vishnivetskaya, T. A., Layton, A. C., Lau, M. C., Chauhan, A., Cheng, K. R., Meyers, A. J., & Murphy, J. R. (2014). Commercial DNA Extraction Kits Impact Observed Microbial Community Composition in Permafrost Samples. *FEMS Microbiology Ecology, 87*(1), 217-30.

Vogel, M., Kopinke, F.-D., & Mackenzie, K. (2019). Acceleration of Microiron-Based Dechlorination in Water by Contact with Fibrous Activated Carbon. *The Science of the Total Environment, 660*, 1274-82.

Vogt, C., Kleinsteuber, S., & Richnow, H.-H. (2011). Anaerobic Benzene Degradation by Bacteria. *Microbial Biotechnology, 4*(6), 710-24.

Walker, D. J., Nevin, K. P., Holmes, D. E., Rotaru, A.-E., Ward, J. E., Woodard, T. L., & Zhu, J. (2020). Syntrophus Conductive Pili Demonstrate That Common Hydrogen-Donating Syntrophs Can Have a Direct Electron Transfer Option. *The ISME Journal, 14*(3), 837-46.

Wang, F., Gu, Y., O'Brien, P., Yi, S. M., Yalcin, S. E., Srikanth, V., & Shen, C. (2019). Structure of Microbial Nanowires Reveals Stacked Hemes That Transport Electrons over Micrometers. *Cell, 177*(2), 361-69.e10.

Wang, G., Li, Q., Gao, X., & Wang, X. C. (2018). Synergetic Promotion of Syntrophic Methane Production from Anaerobic Digestion of Complex Organic Wastes by Biochar: Performance and Associated Mechanisms. *Bioresource Technology*. doi:https://doi.org/10.1016/j.biortech.2017.12.004

Wang, Z., Schenkeveld, W. D., Kraemer, S. M., & Giammar, D. E. (2015). Synergistic Effect of Reductive and Ligand-Promoted Dissolution of Goethite. *Environmental Science & Technology, 49*(12), 7236-44.

Weelink, S. A., van Eekert, M. H., & Stams, A. J. (2010). Degradation of BTEX by Anaerobic Bacteria: Physiology and Application. *Reviews in Environmental Science and Bio/Technology*. doi:https://doi.org/10.1007/s11157-010-9219-2

White, A. F., Peterson, M. L., & Hochella, M. F. (1994). Electrochemistry and Dissolution Kinetics of Magnetite and Ilmenite. *Geochimica et Cosmochimica Acta*. doi:https://doi.org/10.1016/0016-7037(94)90420-0

White, M. D., Payne, K. A., Fisher, K., Marshall, S. A., Parker, D., Rattray, N. J., & Trivedi, D. K. (2015). UbiX Is a Flavin Prenyltransferase Required for Bacterial Ubiquinone Biosynthesis. *Nature*. doi:https://doi.org/10.1038/nature14559

Wibowo, N., Wibowo, S. D., Setiawan, J., & Ismadji, S. (2007). Adsorption of Benzene and Toluene from Aqueous Solutions onto Activated Carbon and Its Acid and Heat Treated Forms: Influence of Surface Chemistry on Adsorption. *Journal of Hazardous Materials, 146*(1-2), 237-42.

Wilkinson, K., & Lead, J. (2007). *Environmental Colloids and Particles: Behaviour, Separation and Characterisation.* Chemistry International -- Newsmagazine for IUPAC. doi:https://doi.org/10.1515/ci.2007.29.2.21a

Winderl, C., Anneser, B., Griebler, C., Meckenstock, R. U., & Lueders, T. (2008). Depth-Resolved Quantification of Anaerobic Toluene Degraders and Aquifer Microbial Community Patterns in Distinct Redox Zones of a Tar Oil Contaminant Plume. *Applied and Environmental Microbiology, 74*(3), 792-801.

Wingender, J., Neu, T. R., & Flemming, H.-C. (1999). What Are Bacterial Extracellular Polymeric Substances? *Microbial Extracellular Polymeric Substances*. doi:https://doi.org/10.1007/978-3-642-60147-7_1

Winkelmann, F. (1991). *Handbook of Microbial Iron Chelates.* CRC Press.

Wirbel, J., Zych, K., Essex, M., Karcher, N., Kartal, E., Salazar, G., . . . Zeller, G. (2020). Microbiome meta-analysis and cross-disease comparison enabled by the SIAMCAT machine-learning toolbox. *bioRXiv*. doi:https://doi.org/10.1101/2020.02.06.931808

Wolfaardt, G., Lawrence, J., Robarts, R., Caldwell, S., & Caldwell, D. (1994). Multicellular Organization in a Degradative Biofilm Community. *Applied and Environmental Microbiology*. doi:https://doi.org/10.1128/aem.60.2.434-446.1994

Wu, G., Wolf, J. B., Ibrahim, A. F., Vadasz, S., Gunasinghe, M., & Freeland, S. J. (2006). Simplified Gene Synthesis: A One-Step Approach to PCR-Based Gene Construction. *Journal of Biotechnology, 124*(3), 496-503.

Xiong, A.-S., Yao, Q.-H., Peng, R.-H., Li, X., Fan, H.-Q., Cheng, Z.-M., & Li, Y. (2004). A Simple, Rapid, High-Fidelity and Cost-Effective PCR-Based Two-Step DNA Synthesis Method for Long Gene Sequences. *Nucleic Acids Research, 32*(12), e98.

Xu, N., & Gao, Y. (2008). Characterization of Hematite Dissolution Affected by Oxalate Coating, Kinetics and pH. *Applied Geochemistry*. doi:https://doi.org/10.1016/j.apgeochem.2007.12.026

Yamada, C., Kato, S., Ueno, Y., Ishii, M., & Igarashi, Y. (2015). Conductive Iron Oxides Accelerate Thermophilic Methanogenesis from Acetate and Propionate. *Journal of Bioscience and Bioengineering, 119*(6), 678-82.

Yan, W., Shen, N., Xiao, Y., Chen, Y., Sun, F., Tyagi, V. K., & Zhou, Y. (2017). The Role of Conductive Materials in the Start-up Period of Thermophilic Anaerobic System. *Bioresource Technology*. doi:https://doi.org/10.1016/j.biortech.2017.05.046

Yang, L., Nilsson, M., Gjermansen, M., Givskov, M., & Tolker-Nielsen, T. (2009). Pyoverdine and PQS Mediated Subpopulation Interactions Involved in Pseudomonas Aeruginosa Biofilm Formation. *Molecular Microbiology, 74*(6), 1380-92.

Yang, Y., Zhang, Y., Li, Z., Zhao, Z., Quan, X., & Zhao, Z. (2017). “Adding Granular Activated Carbon into Anaerobic Sludge Digestion to Promote Methane Production and Sludge Decomposition. *Journal of Cleaner Production*. doi:https://doi.org/10.1016/j.jclepro.2017.02.156

Yang, Z., Guo, R., Shi, X., Wang, C., Wang, L., & Dai, M. (2016). Magnetite Nanoparticles Enable a Rapid Conversion of Volatile Fatty Acids to Methane. *RSC Advances*. doi:https://doi.org/10.1039/c6ra02280d

Yonezawa, H., Osaki, T., Hanawa, T., Kurata, S., Ochiai, K., & Kamiya, S. (2013). Impact of Helicobacter Pylori Biofilm Formation on Clarithromycin Susceptibility and Generation of Resistance Mutations. *PloS One, 8*(9), e73301.

Yue, J. C., & Clayton, M. K. (2005). A Similarity Measure Based on Species Proportions. *Communications in Statistics - Theory and Methods*. doi:https://doi.org/10.1080/sta-200066418

Zaan, B., Saia, F. T., Stams, A. J., Plugge, C. M., de Vos, W. M., Smidt, H., . . . Gerritse, J. (2012). Anaerobic Benzene Degradation under Denitrifying Conditions: Peptococcaceae as Dominant Benzene Degraders and Evidence for a Syntrophic Process. *Environmental Microbiology, 14*(5), 1171-81.

Zacharoff, L., Chan, C., & Bond, D. R. (2016). Reduction of Low Potential Electron Acceptors Requires the CbcL Inner Membrane Cytochrome of Geobacter Sulfurreducens. *Bioelectrochemistry, 107*, 7-13.

Zdanovsky, A., & Zdanovskaia, M. (2000). Simple and Efficient Method for Heterologous Expression of Clostridial Proteins. *Applied and Environmental Microbiology, 66*(8), 3166-73.

Zhang, J., & Lu, Y. (2016). Conductive Fe3O4 Nanoparticles Accelerate Syntrophic Methane Production from Butyrate Oxidation in Two Different Lake Sediments. *Frontiers in Microbiology*. doi:https://doi.org/10.3389/fmicb.2016.01316

Zhang, J., Zhao, W., Zhang, H., Wang, Z., Fan, C., & Zang, L. (2018). Recent Achievements in Enhancing Anaerobic Digestion with Carbon- Based Functional Materials. *Bioresource Technology, 266*, 555-67.

Zhang, T., Bain, T. S., Nevin, K. P., Barlett, M. A., & Lovley, D. R. (2012). Anaerobic Benzene Oxidation by Geobacter Species. *Applied and Environmental Microbiology, 78*(23), 8304-10.

Zhang, T., Tremblay, P.-L., Chaurasia, A. K., Smith, J. A., Bain, T. S., & Lovley, D. R. (2013). Anaerobic Benzene Oxidation via Phenol in Geobacter Metallireducens. *Applied and Environmental Microbiology, 79*(24), 7800-7806.

Zhang, T., Tremblay, P.-L., Chaurasia, A. K., Smith, J. A., Bain, T. S., & Lovley, D. R. (2014). Identification of Genes Specifically Required for the Anaerobic Metabolism of Benzene in Geobacter Metallireducens. *Frontiers in Microbiology*. doi:https://doi.org/10.3389/fmicb.2014.00245

Zhao, Z., Li, Y., Quan, X., & Zhang, Y. (2017). Towards Engineering Application: Potential Mechanism for Enhancing Anaerobic Digestion of Complex Organic Waste with Different Types of Conductive Materials. *Water Research, 115*, 266-77.

Zhao, Z., Zhang, Y., Woodard, T., Nevin, P., & Lovley, D. (2015). Enhancing Syntrophic Metabolism in up-Flow Anaerobic Sludge Blanket Reactors with Conductive Carbon Materials. *Bioresource Technology*. doi:https://doi.org/10.1016/j.biortech.2015.05.007

Zhou, S., Xu, J., Yang, G., & Zhuang, L. (2014). Methanogenesis Affected by the Co-Occurrence of iron(III) Oxides and Humic Substances. *FEMS Microbiology Ecology, 88*(1), 107-20.

Zhuang, L., Tang, J., Wang, Y., Hu, M., & Zhou, S. (2015). Conductive Iron Oxide Minerals Accelerate Syntrophic Cooperation in Methanogenic Benzoate Degradation. *Journal of Hazardous Materials, 293*, 37-45.

Zogai, X., Nimtz, M., Rohde, M., Bokranz, W., & Romling, U. (2001). “The Multicellular Morphotypes of Salmonella Typhimurium and Escherichia Coli Produce Cellulose as the Second Component of the Extracellular Matrix. *Molecular Microbiology, 39*(6), 1452-63.

Zulkefli, N., Masdar, M. S., Isahak, W., Jahim, J., Rejab, S., & Lye, C. (2019). Removal of Hydrogen Sulfide from a Biogas Mimic by Using Impregnated Activated Carbon Adsorbent. *PloS One, 14*(2), e0211713.